Wavelet Techniques for Solving Proportional Delay Differential Equations

Thesis submitted for the award of the Degree of
Doctor of Philosophy

in

MATHEMATICS

by

BASHARAT HUSSAIN

ENROLLMENT No: A181337

Under the supervision of:

Dr. Afroz

Associate Professor & Head
Department of Mathematics
School of Sciences

Maulana Azad National Urdu University
Hyderabad, India-500032

2022

मौलाना आज़ाद नेशनल उर्दू यूनिवर्सिटी مولانا آزاد نیشنل اُردو یونیورسٹی

MAULANA AZAD NATIONAL URDU UNIVERSITY

(A Central University, Ministry of Education, Govt. of India)

(Accredited Grade "A" by NAAC)

Declaration

I, **BASHARAT HUSSAIN**, declare that this Ph.D. thesis entitled, "***Wavelet Techniques for Solving Proportional Delay Differential Equations***" is original research carried out by me. No part of this thesis was published, or submitted to any other university/institution for the award of any degree/diploma.

Place: Hyderabad.
Date:

Signature of Research Scholar
Basharat Hussain

मौलाना आज़ाद नेशनल उर्दू यूनिवर्सिटी مولانا آزاد نیشنل اُردو یونیورسٹی
MAULANA AZAD NATIONAL URDU UNIVERSITY
(A Central University, Ministry of Education, Govt. of India)
(Accredited Grade "A" by NAAC)

Department of Mathematics, School of Sciences

Certificate

This is to certify that the thesis entitled, "***Wavelet Techniques for Solving Proportional Delay Differential Equations***", submitted for the award of the Degree of Doctor of Philosophy in Mathematics, School of Sciences, Maulana Azad National Urdu University, Hyderabad, is the result of the original research work carried out by Mr.**BASHARAT HUSSAIN** ENROLLMENT No. **A181337** under my supervision, and to the best of my knowledge and belief, the work embodied in this thesis does not form part of any thesis/dissertation already submitted to any university/institution for the award of any degree/diploma.

Supervisor
Dr. Afroz
Associate Proffesor & Head
Department of Mathematics
MANUU, Hyderabad, India

Head, Department of Mathematics,
Scool of Sciences,
MANUU, Hyderabad, India

Dean
Scool of Sciences,
MANUU, Hyderabad, India

Place: Hyderabad.
Date:

मौलाना आज़ाद नेशनल उर्दू यूनिवर्सिटी مولانا آزاد نیشنل اُردو یونیورسٹی
MAULANA AZAD NATIONAL URDU UNIVERSITY
(A Central University established by an Act of Parliament in 1998)

Synopsis Authenticity Certificate & Metadata

Name of the Research Scholar	Basharat Hussain
Enrolment No.	A181337
Degree (M. Phil / Ph. D.)	Ph.D.
Department / Centre / Institution	Department of Mathematics
Guide/Supervisor	Dr. Afroz (Associate Professor)
Thesis / Dissertation Title approved in DRC held on:	Wavelet Techniques for Solving Proportional Delay Differential Equations Date: 20-Apr-2022
Registration Date	24-Jul-2018
Submission Date	10-Oct-2022
Keywords	Proportional Delay Differential Equations, Fractional Differential Equations, Simultaneous Proportional Delay Differential Equations, Collocation Method, Haar wavelet, Numerical Solution.
Language of Thesis	Bilingual: English, Urdu
Title	Wavelet Techniques for Solving Proportional Delay Differential Equations
Format of accompanying material (PDF file, Image file, Text file, etc.)	PDF file

I hereby certify that the Synopsis contained in this CD/DVD is complete in all respect and is same as submitted in print.

Signature of the Scholar **Signature of the Guide** **Signature of the Librarian**

मौलाना आज़ाद नेशनल उर्दू यूनिवर्सिटी مولانا آزاد نیشنل اُردو یونیورسٹی

MAULANA AZAD NATIONAL URDU UNIVERSITY

(A Central University established by an Act of Parliament in 1998)

Consent Form for Digital Archiving

Name of the Research Scholar	Basharat Hussain
Degree (M. Phil / Ph.D.)	Ph.D.
Department / Centre / Institution	Department of Mathematics
Guide / Supervisor	Dr. Afroz (Associate Professor)
Thesis / Dissertation Title	Wavelet Techniques for Solving Proportional Delay Differential Equations

1. I do hereby authorize Maulana Azad National Urdu University and its relevant Departments to archive and to make available my thesis or dissertation in whole or in part in the University's Electronic Thesis and Dissertations (ETD) Archive, University's Intranet or University's website or any other electronic repository for Research Theses setup by other Departments of Govt. of India and to make it accessible worldwide in all forms of media, now or hereafter known.

2. I retain all other ownership rights to the copyright of the thesis/dissertation. I also retain the right to use in future works (such as articles or books) all or part of this thesis or dissertation.

Signature of Scholar **Signature & Seal of Guide** **Signature of Librarian**

CERTIFICATE OF PLAGIARISM CHECK

The following certificate of plagiarism check is issued with certification for the bonafide work carried out by him/her under my supervision and guidance. This thesis is free from plagiarism and has not been submitted previously in part or in full to this or any other University or institution for the award of any degree or diploma.

1.	Name of the Research Scholar	Basharat Hussain
2.	Research Programme	Ph.D.
3.	Title of the Thesis / Dissertation	Wavelet Techniques for Solving Proportional Delay Differential Equations
4.	Name of the Supervisor	Dr. Afroz (Associate Professor)
5.	Department / Research Centre	Department of Mathematics
6.	Acceptable Maximum Limit	10%
7.	% of Similarity of content Identified	9%
8.	Software Used	Turnitin
9.	Date of verification	03-Oct-2022

Signature of the Scholar **(Signature of the Supervisor)**

(Head of the Department) **(University Librarian)**

Digital Receipt

This receipt acknowledges that Turnitin received your paper. Below you will find the receipt information regarding your submission.

The first page of your submissions is displayed below.

Submission author:	Basharat Hussain
Assignment title:	Central Library
Submission title:	Wavelet Techniques for Solving Proportional Delay Differenti...
File name:	031022_Thesis_Basharat.pdf
File size:	2.69M
Page count:	125
Word count:	27,999
Character count:	134,603
Submission date:	03-Oct-2022 01:22PM (UTC+0530)
Submission ID:	1915242147

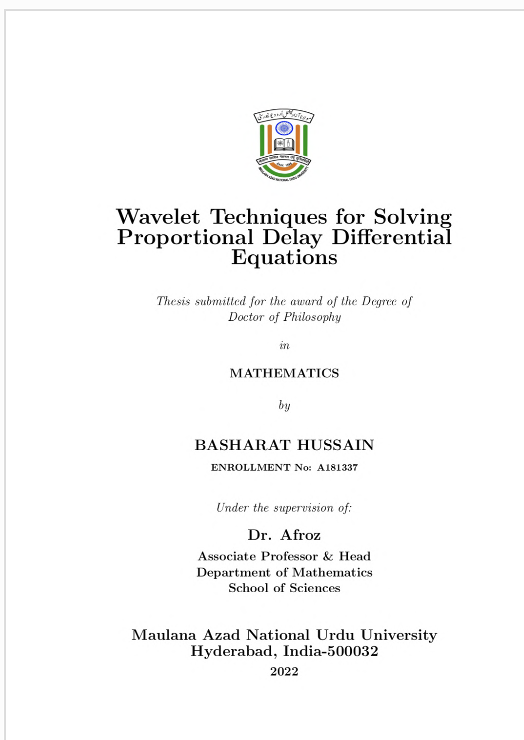

Wavelet Techniques for Solving Proportional Delay Differential Equations

Thesis submitted for the award of the Degree of Doctor of Philosophy

in

MATHEMATICS

by

BASHARAT HUSSAIN

ENROLLMENT No: A181337

Under the supervision of:

Dr. Afroz

Associate Professor & Head

Department of Mathematics

School of Sciences

Maulana Azad National Urdu University

Hyderabad, India-500032

2022

Wavelet Techniques for Solving Proportional Delay Differential Equations

ORIGINALITY REPORT

9%	6%	6%	3%
SIMILARITY INDEX	INTERNET SOURCES	PUBLICATIONS	STUDENT PAPERS

PRIMARY SOURCES

1	cyberleninka.org Internet Source	<1%
2	Submitted to Higher Education Commission Pakistan Student Paper	<1%
3	Submitted to Universiti Kebangsaan Malaysia Student Paper	<1%
4	Submitted to University of Witwatersrand Student Paper	<1%
5	www.bdigital.unal.edu.co Internet Source	<1%
6	d.researchbib.com Internet Source	<1%
7	Saedeh Foadian, Reza Pourgholi, S. Hashem Tabasi, Javad Damirchi. "The inverse solution of the coupled nonlinear reaction–diffusion equations by the Haar wavelets", International Journal of Computer Mathematics, 2017	<1%

63 Submitted to University of Melbourne
Student Paper <1%

64 library2.smu.ca
Internet Source <1%

65 SAKAR, Mehmet Giyas. "Numerical solution of neutral functional-differential equations with proportional delays", Balıkesir Üniversitesi, Endüstri Mühendisliği Bölümü, 2017.
Publication <1%

66 A.H. Bhrawy, E. Tohidi, F. Soleymani. "A new Bernoulli matrix method for solving high-order linear and nonlinear Fredholm integro-differential equations with piecewise intervals", Applied Mathematics and Computation, 2012
Publication <1%

67 www.hindawi.com
Internet Source <1%

Exclude quotes	On	Exclude matches	< 14 words
Exclude bibliography	On		

Acknowledgements

"Alhamdulillah, praise be to Allah, the most High the most Merciful, Lord of all worlds, the Sustainer and Master in the Day of Judgment, praise be upon to His messenger Mohammad (SAW) and those that follow him until the end of time." I thank you Allah for sustaining my life throughout this endeavor.
I owe a huge debt of gratitude to a number of people for their guidance and support throughout my Ph.D. journey. My deepest gratitude to my supervisor, Dr. Afroz, for having shared his deep knowledge, invaluable advice, and kind support. I am greatly thankful for his devoted time and all the trust that he has endowed me with through these years. It has been my honour to work with Dr. Afroz & Head, Associate Professor, Department of Mathematics, Maulana Azad National Urdu University, Hyderabad, whose rigorous training and constant encouragement were solely instrumental in completing the work.

I would like to express my sincere thanks to Prof. Salman Ahmad Khan, Dean, School of Sciences, and Prof. Akther Parvez, University Librarian, MANUU, Hyderabad, for providing a friendly and stimulating working environment.

I am extremely grateful to Prof. S.N. Hasan for sharing insightful ideas, constructive criticism, and unwavering support in all possible ways during my doctoral study. I must thank the esteemed and dynamic faculty members, Prof. S. Maqbool Ahmed, Dr. S. Salahuddin, Dr. Khaja Moinuddin, Dr. Subash Alha, Dr. Majid A. Chaudhary, and Dr. S. Wasim Raja for their valuable suggestions, proper guidance, and timely assistance in one or the other way.

I would also like to thank Ishfaq Ahmad, Farooq Hussain, Tahir Manzoor, and all my colleagues in the department, for their support and motivation during my research work. Also, thanks to Mr. Rupak, Mr. Sohail, Mr. Danim, and other non-teaching staff for being kind and assistive.

I would also like to extend my gratitude to Dr. Abdullah, Dr. Shah Jahan, Dr. Akmal Raza, Miss. Anshika Tanwar, and Mr. Faiz Imam for sharing their deep knowledge, experience, tireless instructions, and support throughout the duration of my Ph.D.

I am very thankful to the various institutes and centres such as the National Center for Mathematics, Central University of Karnataka, University of Hyderabad, IIT(BHU), JECRC University (Jaipur), University College of Engineering (Osmania University), BITS-Pilani(Hyderabad) for my selection and organising the workshop, instructional school, faculty development programme, and conferences, which really helped me to understand and learn the various concepts and aspects of different research fields. Let me also express my special thanks to the Department of Mathematics, BITS-Pilani (Hyderabad) for awarding me the best paper presentation award during the international webinar CPMV-2021.

I will always be grateful to my friends Dr. Hamza Mutaher, Dr. Abdul Mannan, Mr. Zubair Alsam, Mr. Asad and all the well-wishers for their love and support.

My special thanks to my uncle, Dr. Basharat Hussain(KAS), my elder brother, Mr. Shafqat Hussain, and Mr. Rafi for assisting me in all possible ways throughout my academic career.

I wish to use this medium to thank my loving mother and father for their motivations and encouragement in my life, I can not thank you enough, you are indeed my first teacher and a shining light in my life. My sincerest regards to my brothers and sisters, thank you for your support and patience.

Basharat

Contents

List of Figures

List of Tables

Abbreviations

BVPs	**B**oundary **V**alue **P**roblems
DDEs	**D**elay **D**ifferential **E**quations
FDEs	**F**ractional **D**ifferential **E**quations
FT	**F**ourier **T**ransform
HWSM	**H**aar **W**avelet **S**eries **M**ethod
IVPs	**I**nitial **V**alue **P**roblems
IRKHSM	**I**terative **R**eproducing **K**ernel **H**ilbert **S**pace **M**ethod
MAEs	**M**aximum **A**bsolute **E**rrors
RMS	**R**oot **M**ean **S**quare
STFT	**S**hort **T**ime **F**ourier **T**ransform
MRA	**M**ultiresolution **A**nalysis
PDRDEs	**P**roportional **D**elay **R**iccati **D**ifferential **E**quations
R-L	**R**iemann **L**iouville
RDEs	**R**iccati **D**ifferential **E**quations
VIM	**V**aritional **I**teration **M**ethod

Chapter 1

Introduction

1.1 Historical background of Wavelet

Wavelet theory appeared with independent discoveries from Morlet in the context of signal processing of seismic data and Calderon [21] in mathematical analysis. The first proper formulation of wavelet started to appear more frequently in the 1980s; however similar ideas can be traced back to the work of Hungarian mathematician Alfred Haar in 1910. The first wavelet transformation was born in 1910 and named the Haar function. It was defined as a short negative pulse followed by a short positive pulse. A few decades later, in 1946, D. Gabor invented a wavelet, whose method is very similar to the Fourier transformation, where the principle is to apply a window defined by a Gaussian function. Until the 1980s, it was not a question of talking about wavelet transformation for the functions of A. Haar and by D. Gabor[105, 31]. But it was in 1982 that the wavelet method was for first time introduced by J. Morlet, and two years later, Grossman and Morlet [43] introduced the concept of decomposition of any arbitrary square-integrable function into square integrable wavelets of constant shape and laid the foundation of wavelet methods in mathematics. Another significant development in the context of wavelet theory is multi-resolution analysis (MRA); this remarkable technique is proposed by Mallat and Meyer [70] and explains the general formalism for the construction of an orthogonal wavelet basis. In 1987, I. Daubechies created orthogonal wavelets, identified under the name of Daubechies wavelets [28]. They are characterized by their number of zero moments. Moreover, different fields can easily use this family of wavelets. The wavelet method is a potent tool in its original domain (seismology); this technique's performance has aroused the interest of different researchers to extrapolate the theory to other fields such as image compression, medical imaging, video telephony, and finite element modelling. This work sheds light on the wavelet method in numerical analysis. In this context, this thesis is mainly devoted to solve a special class of delay differential equations known as the pantograph equation. Haar wavelet series and delayed Haar wavelet series have been used to solve linear and nonlinear initial value problems of Integer and fractional order, Boundary value problems, and system of differential equations. But before looking specifically at this technique, it is essential to understand the wavelet method with its particularities, projection spaces and definition, and existing wavelet families.

The term "wavelet" is translated from the French word "Ondelette", meaning "small wave". Wavelet functions are known to serve as the bases for square integrable functions and hence are used to decompose square-integrable functions at multiple scales. Therefore, wavelets make it possible to analyze a signal in the time-frequency domain. This precise analysis makes it possible to extract distinctive elements to attenuate parasitic noises and thus represent a signal broken down into several spaces. Whereas Fourier transform decomposes a function(signal) in terms of trigonometric series. The standard Fourier transform defines the representation of a function(signal) as the sum or integral of the periodic sine and cosine functions.

Fourier transform of a function gives us the frequency spectrum of that function which shows what frequencies exist in the function(signal). The Fourier transform of a function is also called the Fourier spectrum of that function [4, 26, 28, 31, 105].

1.2 Short Time Fourier Transform

Fourier transform is a useful tool to determine the frequency characteristics of a function(signal), but it is not suitable if the function(signal) has a time-varying frequency. It has been known for some time, nevertheless, that the global Fourier transform is not appropriate for computing the spectrum information of a function (signal), as it requires all past and present information of the signal to determine its spectral density at a single frequency. Window Fourier Transform (WFT) or short-time Fourier Transform (STFT) have both been developed to address this issue. To localise the time-frequency of a non-stationary function(signal), a window function is defined. The window function's width must match the portion of the signal that can be considered stationary. Segments of the function's spectral information can be ascertained by moving the window function along the time axis. Again, the problem arises due to the fixed width of the window function, and hence wavelet transform comes into play. Before going into the technicalities of wavelets, we will provide some mathematical definitions related to STFT [4, 105].

Definition 1.1. [105, 4] A non trivial function $g \in L^2(\mathbb{R})$ is called a **window function** if $t * g(t) \in L^2(\mathbb{R})$. That is the function decays to zero rapidly.

The two most important parameters for a window functions are its radius and center.

Definition 1.2. [4] The center t^* and root mean square (RMS) radius, Δg of window function g are defined by

$$t^* = \frac{1}{\|g\|_2^2}\int_{-\infty}^{\infty} t|g(t)|^2 dt, \tag{1.2.1}$$

and

$$\Delta g = \frac{1}{\|g\|_2^2}\left(\int_{-\infty}^{\infty}(t-t^*)|g(t)|^2 dt\right)^{1/2}, \tag{1.2.2}$$

respectively. The width of the window function g will be $2\Delta g$.

Similarly, we can have as frequency window $\hat{g}(\omega)$ with center ω^* and RMS radius $\Delta\hat{g}$ defined analogous to (1.2.1), (1.2.2). D. Gabor was the first who realised the drawback of Fourier analysis and brought up the idea of window function and short-time Fourier transform (STFT). He combines the Fourier transform and Gaussian distribution function to produce a spectrogram that plots frequency against time. Gabor transform, also known as STFT, is nothing but a Fourier transform of a function weighted by the Gaussian window, which is sliding across in time. Unlike Fourier transform, Gabor transform tells about the location of a certain frequency component.

Definition 1.3. [4] The Gabor transform of a function f in the time-frequency domain (s,ω) is denoted by $G(f)(s,\omega)$, and is defined as

$$G(f)(s,\omega) \;= \hat{f}_g(s,\omega) = \textstyle\int_{-\infty}^{\infty} f(t)\overline{g(t-s)}dte^{-i\omega t} \tag{1.2.3}$$

where $g(t) = e^{-(t-s)^2/a^2}$ is Gaussian distribution function. The sliding process of g is controlled by the parameter s (s is the center of g), and the parameter a determine the spread of the short-time window for the Fourier transform[18].

If we look closely, the Gabor transform is effectively a convolution of the function (signal) $f(t)e^{-i\omega t}$ with the function $g(t)$.

Definition 1.4. [4] If a function $f \in L^2(\mathbb{R})$, then inversion formula

$$f(t) = G^{-1}(\hat{f}_g(s,\omega)) = \frac{1}{2\pi\|g\|_2^2}\int_{-\infty}^{\infty}\int_{-\infty}^{\infty} \hat{f}_g(s,\omega)\overline{g(t-s)}e^{i\omega t}d\omega dt.$$

Properties of Gabor Transform: Let $f, g, h \in L^2(\mathbb{R})$ and c, d be any two arbitrary constants. Then

a. Linearity:

$$G_g[cf + dh](s,\omega) = cG_g f(s,\omega) + dG_g h(s,\omega).$$

b. Time shift:

$$\begin{aligned} G_g[Tdf](s,\omega) &= G_g[f(t-d)](s,\omega), \\ &= e^{-id\omega}G_g f(s-d,\omega). \end{aligned}$$

c. Exponential Modulation:

$$\begin{aligned} G_g[M_d f](s,\omega) &= G_g[e^{id\omega}f(t)](s,\omega), \\ &= G_g f(t)(s,\omega-d), \\ &= T_d G_f(s,\omega). \end{aligned}$$

d. Conjugation:

$$G_g f(s,\omega) = \overline{G_g f(s,-\omega)}.$$

1.3 Uncertainty Principle

There is a fundamental uncertainty principle in time-frequency analysis that limits the capacity to achieve high resolution in both the time and frequency domains at the same time. The degree of detail we can see in each area is intuitively recognized as resolution. The resolution depends upon the width of the window function.

A small window produces a good resolution in time but gives poor frequency resolution, while a large window shows opposite behaviours; that is, if we want high resolution of the frequency content of function(signal), we have to compromise with the time at which the frequency component occurs. Hence, there is always a trade-off between simultaneous time and frequency localisation.

Definition 1.5. Let $f \in L^2(\mathbb{R})$, the dispersion of f about the point $d \in \mathbb{R}$ is the quantity

$$\Delta_d f = \frac{\int_{-\infty}^{\infty} (t-d)^2 \|f(t)\|^2 dt}{\int_{-\infty}^{\infty} \|f(t)\|^2 dt} \tag{1.3.1}$$

The dispersion about a point "d" is the measure of deviation or spread of its graph from $t = d$. This dispersion will be small if the graph of f is concentrated near $t = d$ and is spread out away from $t = d$. In frequency domain,

$$\Delta_r \hat{f} = \frac{\int_{-\infty}^{\infty} (t-d)^2 \|f(t)\|^2 dt}{\int_{-\infty}^{\infty} \|f(t)\|^2 dt}. \tag{1.3.2}$$

Theorem 1.6. *[4]* ***(Uncertainty principle)*** *Suppose f is a function in $L^2(\mathbb{R})$ which vanishes at $\pm\infty$. Then*

$$\Delta_d f . \Delta_r \hat{f} \geq \frac{1}{4}$$

for all points $d, r \in \mathbb{R}$.

The statement implies that $\Delta_d f, \Delta_r \hat{f}$ cannot simultaneously be small. In other words, when the time-frequency cell is narrow in time it is wider in frequency and vice-versa. In case of Gaussian function f(t)=$\frac{e^{\frac{-t^2}{2\sigma^2}}}{\sqrt{2\pi\sigma}}$ equality is achieved.

1.4 Axioms of Multiresolution Analysis and Wavelet Transform

[105] Multiresolution analysis (MRA) is a new and remarkable concept of wavelet theory. It provides a general framework using which one can construct their own families of orthogonal wavelet basis. Mallat's idea of MRA is to approximate a function at different resolutions by projecting them into different spaces.

Definition 1.7. MRA of $L^2(\mathbb{R})$ consists of a sequence $\{V_j\}_{j\in\mathbb{Z}}$ of nested closed subspaces of $L^2(\mathbb{R})$ satisfying,

$$V_j \subset V_{j+1} \ \forall j \in \mathbb{Z}.$$

$$\overline{\cup_{j=0}^{\infty} V_j} = L^2(\mathbb{R}), \cap_{j\in\mathbb{Z}} V_j = \{0\}.$$

Furthermore, for a function $f \in L^2(\mathbb{R})$, it is required that

$$f(t) \in V_0 \Longleftrightarrow f(2^j t) \in V_j \forall j \in \mathbb{N}, \text{(invariance to dilation)}$$

$$\{\phi(t-k) : k \in \mathbb{Z}\} \text{ is an orthonoraml basis for } V_0 \text{(invariance to translation)},$$

where $\phi(t) \in V_0$ is called scaling function.

This definition has the consequence that at each degree of resolution j, the family of functions$\{\phi_{j,k} : t \longrightarrow 2^j \phi(2^j t - k)\}_{k\in\mathbb{Z}}$ forms an orthonormal basis of the space V_j with respect to L^2-norm. As ϕ belongs to V_0, which is included in V_1, it follows that ϕ can be expressed as a linear combination of $\{\phi_{1,k}\}_{k\in\mathbb{Z}}$. In other words, there exists a sequence of reals $(h_k)_{k\in\mathbb{Z}}$ such that

$$\forall t \in \mathbb{R}, \phi(t) = \sum_{k\in Z} h_k \phi(2t-k).$$

The principle of this relation, called two-scale relation, allows us to develop fast decomposition or reconstruction algorithms in the context of a multiresolution analysis. It is, therefore, interesting to be able to refine the knowledge of a function by increasing the level of resolution without recalculating all of the associated coefficients. In V_{j+1} there exist a detail space W_j serves as the orthogonal complement of V_j in V_{j+1}. i.e.

$$V_{j+1} = V_j \oplus W_j. \tag{1.4.1}$$

The space W_j includes all the functions in V_{j+1} that are orthogonal to all those in V_j under some chosen norm. The set of functions which forms the basis for W_j are called wavelets. An immediate consequence of definition 1.7 and equation (1.4.1) for any $j_0 \in \mathbb{Z}$, the space $L^2(\mathbb{R})$ verifies:

$$L^2(\mathbb{R}) = \overline{V_{j_0} \oplus \oplus_{j=j_0}^{\infty} W_j} \tag{1.4.2}$$

There exists a function ψ such that $\{t \longrightarrow \psi(t-k)\}_{k\in\mathbb{Z}}$ is an orthonormal basis of W_0. The function ψ is called a wavelet. Again, for different level of resolution $j \in \mathbb{Z}$, the family $\{\psi_{j,k} : t \longrightarrow 2^{j/2}\psi(2^j t - k)\}_{k\in\mathbb{Z}}$ forms an orthonormal basis of the W_j space. Moreover, from the fact that space W_0 is included in V_1, the following two-scale relation can be established:

$$\forall t \in \mathbb{R}, \psi(t) = \sum_{k\in\mathbb{Z}} g_k \phi(2t-k) \tag{1.4.3}$$

where $(g_k)_{k\in\mathbb{Z}}$ is sequence of real numbers. A simple example of multiresolution analysis is that of Haar, generated by the scale function $\phi = \mathbb{I}[0,1)$ and the wavelet $\psi = \mathbb{I}_{[1/2,1)} - \mathbb{I}_{[0,1/2)}$, where $\mathbb{I}$ is characteristics or indicator function. Using the decomposition of the $L^2(\mathbb{R})$ space given in MRA definition (1.7) one can deduce that any function f belonging to $L^2(\mathbb{R})$ is written as:

$$f = \sum_{k\in\mathbb{Z}} \alpha_{j_0,k}\phi_{j_0,k} + \sum_{j=j_0}^{\infty}\sum_{k\in\mathbb{Z}} \beta_{j,k}\psi_{j,k},$$

where $\alpha_{j_0,k} = \int f\phi_{j_0,k}$ and $\beta_{j_0,k} = \int f\psi_{j,k}$.

In signal analysis, wavelet decomposition is a frequently used technique. Its key benefit is the ability to track the temporal evolution of a signal's frequency content. The analysis of non-stationary signals can therefore be done using it instead of the Fourier transform. In mathematics, a wavelet ψ is a summable square function of the Hilbert space $L^2(\mathbb{R})$, with an oscillating evolution most of the time and a zero average. This function is often chosen as a multiscale analysis, and reconstruction tool and many problems have been solved using the wavelet method. This function ψ is called wavelet if it satisfies the following admissibility condition in the frequency domain:

$$\int_{\mathbb{R}^+} \frac{|\hat{\psi}(\omega)|^2}{|\omega|} d\omega = \int_{\mathbb{R}^-} \frac{|\hat{\psi}(\omega)|^2}{|\omega|} d\omega < +\infty.$$

Note that $\hat{\psi}$ denotes the Fourier transform of ψ. This leads to the condition that the wavelet has zero integral:

$$\int_R \psi(t)dt = 0.$$

This condition invoked that the ψ has its zeroth moment vanishing. Also,ψ admits k zero moment if :

$$\int_R t^k\psi(t)dt = 0, \ where\ k = 0, 1, \ldots k.$$

Definition 1.8. [105] A double index family of wavelets generated by translation and dilation of ψ is:

$$\psi_{a,b}(t) = \frac{1}{\sqrt{|a|}}\psi\left(\frac{t-b}{b}\right), \; a, b \in \mathbb{R}, a \neq 0. \tag{1.4.4}$$

Definition 1.9. [105] The **continuous wavelet transform** of a function(signal) f can be written as:

$$\mathfrak{C}_{\psi}(a,b) = \frac{1}{\sqrt{|a|}}\int_{-\infty}^{\infty} f(t)\overline{\psi\left(\frac{t-b}{a}\right)}dt, \tag{1.4.5}$$

where "a" is called the scale factor and represents the inverse of the signal frequency, "b" is a time translation term. The mother wavelet function ϕ is continuous and differentiable with compact support. On discretizing the parameters a and b presented in above formula one can also define the discrete wavelet transform. For that let $a = a_0^j$ where $a_0 > 1$ and $j \in \mathbb{N}$ and let $b = kb_0a_0^j$, where $k \in \mathbb{N}$ and $b_0 > 0$. In particular, $a_0 = 2$ and $b_0 = 1$ gives the following family of wavelet indexed in $\mathbb{Z}$ commonly known as dyadic wavelet transform,

$$\psi_{j,k} = 2^{-j/2}\psi\left(2^{-j}t - k\right).$$

In this case, $j = 1, 2, \dots n$, where n is the base 2 logarithm of the number of the points forming the signal and $k = 1, 2 \dots 2^{j-1}$. $\{\psi_{j,k}(t)\}$ forms orthonormal basis for $L^2(\mathbb{R})$, i.e. Any function f belonging to $L^2(\mathbb{R})$ is written as:

$$f(t) = \sum_{j,k} a_{j,k}\psi_{j,k}(t),$$

where $a_{jk} = \langle f, \psi_{j,k}\rangle$.

Definition 1.10. [105] The dyadic discrete wavelet transform is written as:

$$C_{j,k} = 2^{-j/2} \int_{-\infty}^{\infty} f(t)\psi\left(2^{-j}t - k\right) dt, \tag{1.4.6}$$

where j is the decomposition level (or scale) and k is the time lag. The discrete wavelet transform is faster than the continuous variant and still permits an accurate reconstruction of the input signal by inverse transformation .

Definition 1.11. [105] " The inverse wavelet transform is given by

$$f(t) = \frac{1}{C_\psi} \int_{-\infty}^{\infty} \int_{-\infty}^{\infty} \mathfrak{C}_\psi(a,b)\psi_{a,b}(t)\frac{dadb}{a^2}, \tag{1.4.7}$$

where

$$C_\psi = \int_0^\infty \frac{|\hat{\psi}(\omega)|^2}{|\omega|} d\omega."$$

Various properties of wavelet transform

Let ψ_1 and ψ_2 be wavelets and let $f_1, f_2 \in L^2(\mathbb{R})$. Then:

a. **Linearity:**

$$\mathfrak{C}_\psi(a,b)[\alpha_1 f_1(t) + \alpha_2 f_2(t)] = \alpha_1 \mathfrak{C}_\psi(a,b)[f_1(t)] + \alpha_2 \mathfrak{C}_\psi(a,b)[f_2(t)],$$

where $\alpha_1, \alpha_2 \in \mathbb{R}$.

b. **Time shift:**

$$\mathfrak{C}_\psi(a,b)(T_\beta f(t)) = \mathfrak{C}_\psi(a, b-\beta)f(t),$$

where T_β is translation operator defined by $T_\beta f(t) = f(t-c)$.

c. Scaling/Dilation:

$$\mathfrak{C}_\psi(a,b)(D_d f(t)) = \frac{1}{\sqrt{d}}\mathfrak{C}_\psi\left(\frac{a}{d},\frac{b}{d}\right), d > 0,$$

where D_d is a dilation operator defined by $D_c f(t) = \frac{1}{d} f(\frac{t}{d}), d > 0$.

d. Symmetry

$$\mathfrak{C}_\psi(a,b)f(t) = \overline{\mathfrak{C}_\psi(\frac{1}{a},\frac{-b}{a})}, a \neq 0.$$

e. Parity:

$$C_{P\psi}(a,b)pf(t) = \mathfrak{C}(a,-b)f(t),$$

where P is the parity operator defined as $Pf(t) = f(-t)$.

f. Anti-linearity

$$\mathfrak{C}_{(\alpha_1\psi+\alpha_2\phi)}(a,b)f(t) = \overline{\alpha_1}\mathfrak{C}_\psi(a,b)f(t) + \overline{\alpha_2}\mathfrak{C}_\phi(a,b)f(t).$$

g.

$$\mathfrak{C}_{T_\beta\psi}(a,b)f(t) = \mathfrak{C}_\psi(a,b+\beta a)f(t).$$

h.

$$\mathfrak{C}_{D_d\psi}(a,b)f(t) = \tfrac{1}{\sqrt{d}}\mathfrak{C}_\psi(ad,b)f(t), d > 0.$$

1.5 Some Examples of Wavelets

The best known and most used families of wavelets are the wavelets of Daubechies, Haar, Morlet, Meyer, Symlets and Coiflets. Here we discuss some properties of these wavelet families. The comprehensive detail about some standard wavelets can be found in [52, 74, 28].

a. Daubechies Wavelet: I. Daubechies holds the distinction of having developed the most elegant wavelet function, which is now the basis for wavelet applications. Wavelets belonging to the Daubechies families are continuously differentiable and have compact support. These wavelets are particularly used as basis functions in signal and image processing and make it possible to represent functions at different levels of resolution. Daubechies wavelets donot have a closed analytic form, only the coefficients at the definition points are known. The compact domain of the definition of Daubechies wavelet scaling function ϕ is $[0, 2N-1]$ i.e ϕ is zero outside the domain while that of the corresponding wavelet function ψ is $[1-N, N]$, where N denotes the number of vanishing moments and $2N$ is the order of Daubechies wavelet or number of Daubechies filter coefficient. Two notations D_{2N} or Db_{2N} are used to refer to Daubechies wavelets. These wavelets are not symmetric except for $N = 1$, which is the Haar wavelet. The smoothness of these wavelets increases with the value of N. The father and mother wavelets of the first few Daubechies wavelet are shown in the Figure 1.2-1.4.

b. Haar Wavelet: A Haar wavelet is the simplest type of wavelet. The Haar wavelet transform serves as the prototype for all other wavelet transforms. In discrete form, Haar wavelets are related to a mathematical operation called the Haar wavelet transform. It decomposes a discrete signal into sub-signals of half its length. It is conceptually simple, computationally fast, and is memory efficient. Another advantage is that it is exactly reversible without the edge effects. Haar wavelet has certain mathematical properties such as compact support, orthogonality, and form basis for $L^2(\mathbb{R}) - space$. The basis is formed by translation and dilation of a scaling function and a mother wavelet. Haar wavelet is Daubechies wavelet of order 1, which admits zero vanishing moment and has a discontinuity. The graph of the scaling function and mother wavelet are shown in Figure 1.1. Also, rigorous mathematical detail is given in the section 2.2.

c. Morlet Wavelet: The mother wavelet for the Morlet wavelets family exists in both real and complex forms. Among them the most widely used complex Morlet wavelet is:

$$\psi_M(t) = e^{i\omega_0 t} e^{\frac{-t^2}{2\sigma_0^2}} + \epsilon(t),$$

and the Fourier transform of $\psi_M(t)$ is :

$$\hat{\psi}_M(t) = \sigma_0 e^{\frac{[(\omega-\omega_0)\sigma_0]^2}{2}} + \hat{\epsilon}(t),$$

where ω_0 represent the modulation frequency, and σ_0 denotes the width of the Gaussian. The first term alone in function $\psi_M(t)$ defined above does not satisfy the admissibility condition therefore, an additional term $\epsilon(t)$ has been added. However for large ω_0 (i.e. $\omega_0 > 5$), this additional term, which is also of Gaussian type, is numerically negligible (less than 10^{-5}) and will therefore, can be ignored in practice. Unlike the Haar wavelets family, the Morlet wavelet family is not orthogonal and does not have compact support. Also, their maximum energy lies within a narrow band around the origin. Two salient properties of Morlet wavelets are their symmetric nature and has a closed explicit mathematical expression. This wavelet is used in signal analysis, mechanical fault diagnosis, and ecological pattern detection.

d. Meyer Wavelet: This wavelet was first introduced by a French mathematician, Yves Meyer. It produced an orthogonal wavelet family with infinite support, and infinitely differentiable. The closed form expressions of Meyer scaling function $M(\omega)$ in the Fourier domain is:

$$\hat{M}(\omega) = \begin{cases} \frac{1}{\sqrt{2\pi}} & if \ |\omega| \leq \frac{2\pi}{3}, \\ \frac{1}{\sqrt{2\pi}} cos(\frac{\pi}{2}\nu(\frac{2|\omega|}{2\pi} - 1)) & if \ \frac{2\pi}{3} \leq |\omega| \leq \frac{4\pi}{3}, \\ 0 & otherwise. \end{cases} \tag{1.5.1}$$

Consequently, the closed from expression for Meyer wavelet function in Fourier domain is

$$\hat{\mathcal{W}}(\omega) = \begin{cases} 0 & if \ 0 < |\omega| \leq \frac{2\pi}{3}, \\ \frac{1}{\sqrt{2\pi}} sin(\frac{\pi}{2}\nu(\frac{3|\omega|}{2\pi} - 1))e^{-i\frac{\omega}{2}} & if \ \frac{2\pi}{3} < |\omega| \leq \frac{4\pi}{3}, \\ \frac{1}{\sqrt{2\pi}} cos(\frac{\pi}{2}\nu(\frac{\pi}{2}(\frac{3|\omega|}{2\pi} - 1))e^{-i\frac{\omega}{2}} & if \ \frac{4\pi}{3} < |\omega| \leq \frac{8\pi}{3}, \\ 0 & otherwise, \end{cases} \tag{1.5.2}$$

where auxiliary function ν is smooth function given by

$$\nu(x) = \begin{cases} 0 & if \ x < 0, \\ x & if \ 0 < x < 1, \\ 1 & if \ x > 1. \end{cases} \tag{1.5.3}$$

By choosing different auxiliary functions we can have variants of Meyer wavelet. Furthermore, $\hat{M}$ and $\hat{W}$ are compactly supported continuous functions in the frequency domain.

e. **Symlets Wavelet:** Symlets are a modified version of Daubechies wavelet proposed by the Daubechies and are more symmetric than Daubechies wavelet. Its symmetric property is useful in reducing edge effects. The family of symlets are compactly supported and from an orthogonal set. A symlet father wavelet and corresponding mother wavelet are shown in Figure 1.7.

f. **Coiflets Wavelet:** On request of the Coifman, Daubechies designed Coifman wavelet and hence it is named as Coiflet. Coiflets are also orthogonal like Daubechies but their mother wavelets have the additional property of vanishing moments. This property makes the Coiflets very attractive for quadrature formulas. Coiflets are near symmetric wavelets and are mostly used in image processing. A scaling and mother Coiflet is shown in Figure 1.8.

g. **Wavelet generated by using orthogonal polynomials:** Several orthogonal polynomials have also been used to construct wavelets families such as Chebyshev, Hermite, Lagender, Bernoulli, Laguerre, Jacobi, Gegenbauer, Lucas, Tylor, Chelyshkov, Genocchi wavelet.

1.6 Some Applications of wavelets

The wavelet method was created in the 19th century to improve signal analysis and processing. The main objective of this technique is to describe signals produced in the real world to characterize, identify, compress, filter, transmit, and predict. Long

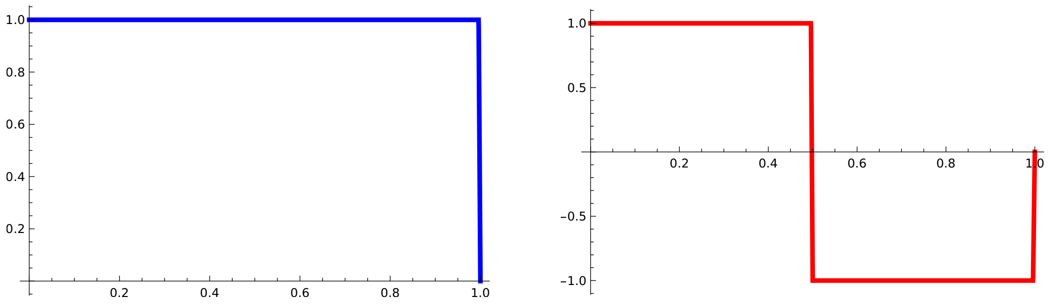

a b

FIGURE 1.1: (a) Haar scaling function, (b) Haar Mother wavelet.

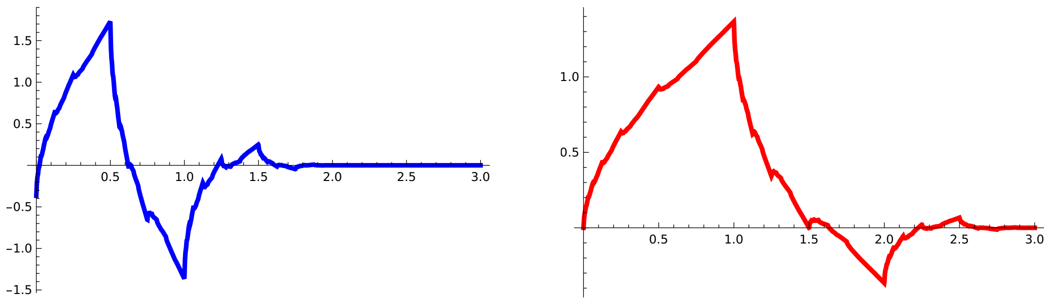

a b

FIGURE 1.2: (a) Daubechies(Db2) father wavelet, (b) Daubechies(Db2) Mother wavelet.

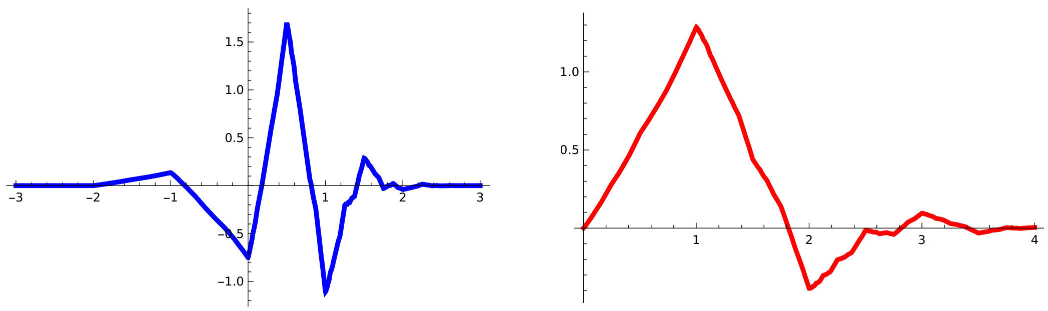

a b

FIGURE 1.3: (a) Daubechies(Db3) father wavelet, (b) Daubechies(Db3) Mother wavelet.

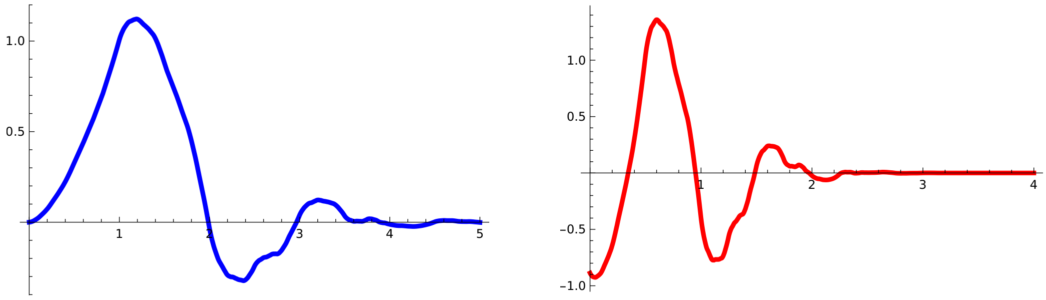

a b

FIGURE 1.4: (a) Daubechies(Db4) father wavelet, (b) Daubechies(Db4) Mother wavelet.

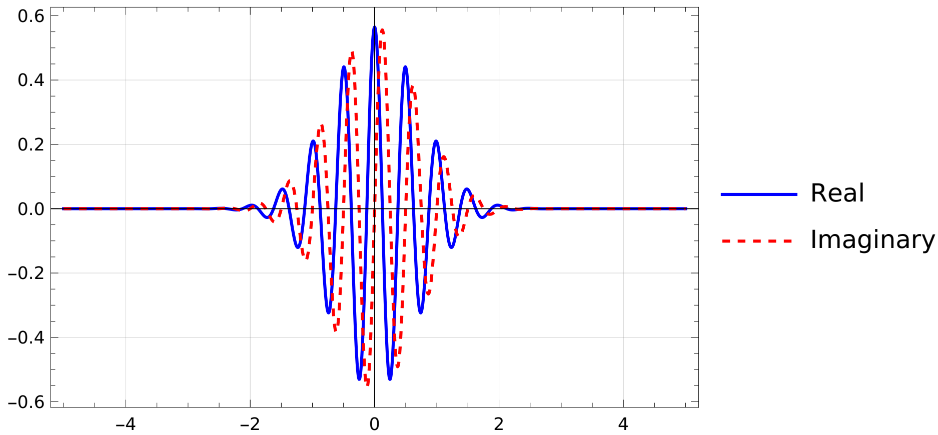

FIGURE 1.5: Real and Imaginary part of complex Morlet wavelet

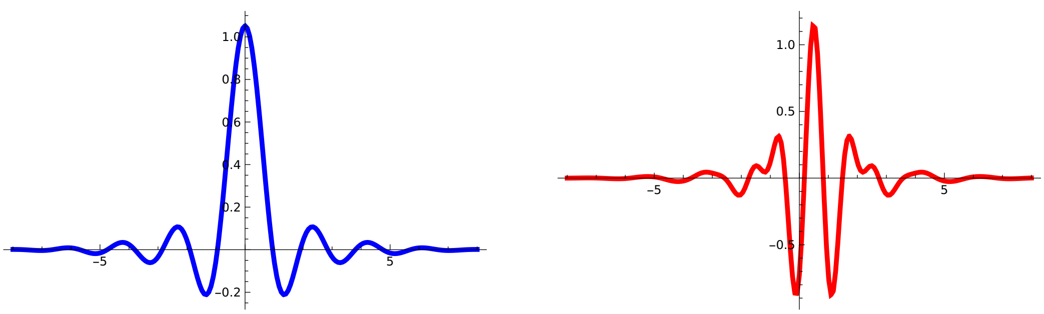

a b

FIGURE 1.6: (a) Meyer father wavelet, (b) Meyer Mother wavelet.

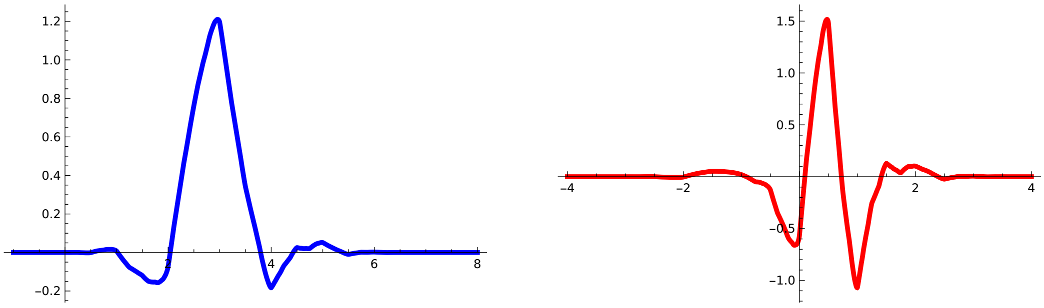

a b

Figure 1.7: (a) Symlet father wavelet, (b) Symlet Mother wavelet.

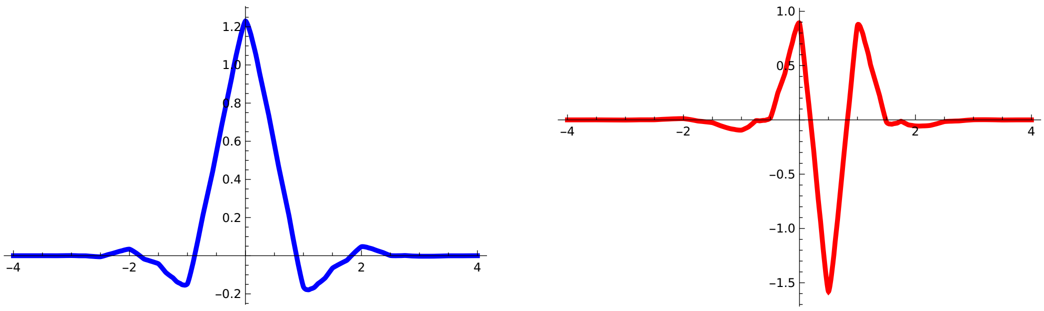

a b

Figure 1.8: (a) Coiflet father wavelet, (b) Coiflet Mother wavelet.

before this technique, the Fourier transformation (FT) (1822) was used for this action. FT decomposes the signal into a set of so-called “base” signals, cosine, and sine. However, it turned out that this method did not allow to have decomposition satisfactory. Wavelet has many applications in physics, engineering, mathematics, and other applied sciences. In this section, we have discussed a few applications of wavelet transform in several fields.

a. Applications in physics: Applications in physics: Wavelet has been widely used in developing new generation music synthesisers, detecting formants in speech analysis, and studying an underwater acoustic wave train. Geophysics and astrophysics: It has been applied in the detection and analysis of micro-earthquakes in oil exploration, analysis of local gravitational field in gravimetry, seismology, geomagnetism, astronomy, paleo-climatology etc. It has been used to identify coherent structures in turbulent fluids, diffusion-limited aggregates, and tree growth phenomena. It has applications in atomic physics where wavelet transforms are applied to analyse the higher order harmonics generated during laser-atom interactions. Wavelet transform has been used as an efficient tool in NMR spectroscopy for noise filtering and spectral line subtraction. A spectacular recent application of wavelet was the detection of gravitational waves by the LIGO and VIRGO experiments. The LIGO setup comprises two interferometers located in Hanford,WA, and Livingstone, LA, respectively, while the VIRGO interferometer located in Santo Stefano a Macerata, Pisa, Italy. Each captured a signal that represented the gravitational waves generated during the last femtosecond of the coalescence of two black holes. Though anticipated, but no one has ever observed the collision of two black holes. The presence of these gravitational waves is verified by applying non-stationary data analysis via the Morlet wavelet. This development in physics has confirmed various predictions of general relativity. More recently, the LIGO-VIRGO detector observed simultaneous emission of gravitational waves and electromagnetic waves from the two neutron stars of the spiral rotating binary system. This makes it possible to locate the source and estimate its distance. Here too, the detection and modelling of the phenomena are obtained by wavelet analysis. According to the experts, these results are fundamental and open a new era in astrophysics and cosmology.

b. Applications in medicine and biology: Among the medical and biological applications, wavelet has been utilized to analyze electrocardiograms (for example, in predicting, detecting, and classifying atrial fibrillation), electroencephalograms, brain tumour detection, and detection of precursors of abnormalities (for example, epilepsy). Long-range correlations in DNA sequences are also studied using the wavelet transform. In Nuclear Magnetic Resonance Spectroscopy (NMR) and wavelet transforms are commonly employed to estimate spectral lines.

c. Industrial applications: In industrial applications, wavelet has been used to monitor nuclear and electrical power plants. A nuclear power plant (NPP) is a complicated system consisting of large number of components with different physical behaviour. NPP emits different signals under continuously varying operational conditions. These signals carry valuable information which has to be analyzed for the safety of the plant. In order to extract information from these signals, wavelet theory is applied for signal processing. Another application of wavelet is the object shape recognition system, which plays a crucial role in robotics and automobile industry.

d. Applications in mathematics: Wavelet transform is considered an efficient mathematical tool to detect and analyze the singularities and irregular structure, estimating the effective Holder exponent in solving differential and integral equations of integer and fractional order, approximation theory, operator theory and inverse problems. Numerical methods based on wavelet theory has progressed in a variety of areas over the last two decades. Based on the construction algorithm, some wavelet-based techniques are; the wavelet weighted residual method, wavelet finite element method, wavelet boundary element, wavelet mesh-less method etc.

e. **Applications in crop science and vegetation:** The wavelet technique has been widely utilised to examine the time series of vegetation. Several techniques have been developed to improve forecasting quality and detecting land change as well as crop phenology. Wavelet transform plays an efficient role in the processing of remotely sensed data. Remote sensing is a technique which uses sensors to collect information about objects (mostly the Earth's surface) without making physical contact with them. This data is contaminated and is very difficult to analyse directly. Therefore, processing the data, which includes compression, noise reduction, classification, and feature extraction, is needed and could be efficiently done using wavelet transform.

f. **Applications in artificial intelligence:** Many artificial intelligence techniques are coupled with wavelet transform to build hybrid AI models to predict essential processes in hydrology such as; estimation and prediction of precipitation, forecasting of stream-flow caused by rainfall-runoff process, rainfall-runoff modelling, prediction of suspended sediment load due to turbulence in water bodies and many more hydro-climatologic applications. Wavelet has also been used in many artificial techniques for the texture identification of machine surfaces. Texture analysis models play a very important role in manufacturing industries. It is used to study the texture and evaluate the component's roughness without touching it. The role of the wavelet in this modelling is to pre-process the subdivided images by converting them into grey scale using continuous 2D wavelet transform. Several statistical features (Mean, Median, Maximum, Minimum, Range, Standard Deviation, Permutation Entropy, Energy, Shannon Entropy, L1 norm, L2 norm, Maximum norm, Maximum Energy to Entropy Ratio, Log Energy Entropy, Sure Entropy, Threshold Entropy and Maximum relative Energy) are calculated from wavelet coefficients. Wavelet transform has been coupled with an artificial neural network to develop an intelligent model for electricity demand predictions. The theory of wavelet has its application in structural health monitoring techniques. In this technique, non-destructive sensor technology is used to detect defects and degradation in the structure. The signal received by the sensor is processed efficiently using a wavelet from which the health status of the structure can be viewed.

1.7 Delay Differential Equations

Generally, researchers construct mathematical models which are governed by differential equations in which the present state of the system depends only on the current value of the dependent variable and/or its derivative. Sometimes these models show severe inconsistency with reality, especially in real-time modelling, economics model, cell growth model and analysis of stock marketing. In order to improve the dynamics of such a mathematical model, researchers incorporated delay terms in the governing differential equation, which results in a delay differential equation. Delay differential equations (DDEs) form a special class of differential equations in which the rate of the solution, depends on the present as well as some previous value of the dependent variable and/or their derivative. DDEs are widely used to model physical sciences, biosciences, engineering, electrodynamics and economics processes. In the monograph [92], F.A Rihan analyses the qualitative and quantitative features of DDEs along with their applications in biosciences, [48] studies the human neural balance control model using DDEs, [110] produced some results on the convergence of Nicholson's blowflies delay model. [109] used the DDEs model to study the influence of rainfall on cocoa yield at the farm level. Karatza & Karahis [54] actively use the DDEs to develop a population pharmacokinetic model, which is an appropriate approach to describe dual peaks in irbesartan's concentration-time profiles. Another important application of DDEs is in electrohydraulic servomechanisms (EHS); this mechanism is widely used in control systems as actuators [44]. The detailed analysis and applications of DDEs can be found in [13, 35, 56, 101] and the following chapters.

Depending upon the nature of delay/lag τ, DDEs have various formats such as

- DDEs with constant delay

$$\begin{cases} y'(t) = f(t, y(t), y(t-\tau)), t_0 \leq t \leq t_f, \\ y(t) = \phi_0(t), t \leq t_0. \end{cases} \tag{1.7.1}$$

- DDEs with time dependent delay $\tau(t)$

$$\begin{cases} y'(t) = f(t, y(t), y(t-\tau(t))), t_0 \leq t \leq t_f, \\ y(t) = \phi_0(t), t \leq t_0. \end{cases} \tag{1.7.2}$$

- DDEs with state dependent delay $\tau(t, y)$

$$\begin{cases} y'(t) = f(t, y(t), y(t - \tau(t, y))), t_0 \leq t \leq t_f, \\ y(t) = \phi_0(t), t \leq t_0. \end{cases} \tag{1.7.3}$$

- Neutral DDEs

$$\begin{cases} y'(t) = f(t, y(t), y(t - \tau_1(t, y)), y'(t - \tau_2(t, y))), t_0 \leq t \leq t_f, \\ y(t) = \phi_0(t), t \leq t_0. \end{cases} \tag{1.7.4}$$

- Proportional DDEs or Pantograph equations

$$\begin{cases} y'(t) = f(t, y(t), y(qt)), t_0 \leq t \leq t_f, \\ y(t) = \phi_0(t), t \leq t_0. \end{cases} \tag{1.7.5}$$

In the above equations, unlike the ordinary differential equations where we required an initial condition to solve the initial value problem here, we need an initial function $\phi_0(t)$ which is called a history function for obtaining the unique solution. The dynamical structure of DDEs is much richer than ordinary differential equations, i.e., the oscillatory and even chaotic behaviours can occur in the scalar case. Due to the involvement of delays term, the computational complexities of these equations increase; thus, it becomes too complicated to solve these equations analytically. Also, in some cases, the analytical solution of these equations does not exist; therefore, an efficient numerical technique is necessary to find the approximate solution. Basic numerical techniques for solving DDEs originates from the techniques available for ordinary differential equations, where additional operations like the inclusion of delay term are required.

1.8 Existence and Uniqueness

Here we state some results on the existence and uniqueness of the solution of DDEs. These results are obtained as particular instances of theorems proved in [45, 78],and [35]

Theorem 1.12. *[13]* ***(Local existence)*** *Let $f(t,u,v)$ be a continuous fucntion on $A \subseteq [t_0, t_f) \times \mathbb{R}^d \times \mathbb{R}^d$ and has locally bounded first derivative w.r.t u and v. Moreover, let $\tau(t) \geq 0$ be a delay function which is continuous in $[t_0, t_f), \tau(t_0) = 0$ &, for some $\xi > 0,\ t - \tau(t) > t_0$ in the interval $(t_0, t_0 + \xi]$. Then equation*

$$\begin{cases} y'(t) = f(t, y(t), y(t-\tau(t))), t_0 \leq t \leq t_f, \\ y(t_0) = y_0, \end{cases} \tag{1.8.1}$$

has unique solution in $[t_0, t_0 + \delta)$ for some $\delta > 0$ which depends continuously on the initial data.

Theorem 1.13. *[13]* ***(Global existence)*** *Let $f(t,u,v)$ be a continuous fucntion on $A \subseteq [t_0, t_f) \times \mathbb{R}^d \times \mathbb{R}^d$ and has locally bounded first derivative w.r.t u and v. Moreover, let $\tau(t) \geq 0$ be a delay function which is continuous in $[t_0, t_f), \tau(t_0) = 0$ &, for some $\xi > 0,\ t - \tau(t) > t_0$ in the interval $(t_0, t_0 + \xi]$. If the unique maximal solution of equation*

$$\begin{cases} y'(t) = f(t, y(t), y(t-\tau(t))), t_0 \leq t \leq t_f, \\ y(t_0) = y_0, \end{cases} \tag{1.8.2}$$

defined in the interval $[t_0, b)$, with $t_0 < b \leq t_f$ is bounded, then it exists on the entire interval $[t_0, t_f)$.

In [35], Driver has proved the Theorem 1.12, and some more general cases of state-dependent delay. For further developments and more general cases, we refer interested readers to [27, 45], and the references therein.

1.9 Methods for Solving DDEs

Here we have highlighted some analytical methods for solving delay differential equations.

1.9.1 Method of Steps for Solving DDEs

Delay differential equation may be solved as ordinary differential equations over successive intervals $[t_l, t_{l+1}]$ by the method of steps. The scalar DDE

$$y'(t) = f(t, y(t), y(t-\tau)), t > 0, \tag{1.9.1}$$

with initial function $\phi_0(t)$ defined on $t \in [-\tau, 0)$ and initial condition $y(0) = y_0$ is solved as a chain of differential equation.

$$\begin{aligned}
y_1'(t) &= f(t, y_1(t), \phi_0(t-\tau)), \quad 0 \le t \le \tau, \\
y_2'(t) &= f(t, y_2(t), y_1(t-\tau)), \quad \tau \le t \le 2\tau, \\
&\vdots \\
y_n'(t) &= f(t, y_n(t), y_{n-1}(t-\tau)), \quad (n-1)\tau \le t \le n\tau,
\end{aligned} \tag{1.9.2}$$

where $n \in \mathbb{Z}^+$.

Example 1.1. *consider a simple DDEs with constant delay*

$$y'(t) = y(t-1) \tag{1.9.3}$$

with initial function $y(t) = 1, \forall \;\; t \in [-1, 0]$ *and initial condition* $y(0) = 1$.

Using basic idea of method of steps, first we reduce the given DDEs on the interval $[0, 1]$ to a non autonomous ODE as

$$y_1'(t) = \phi_0(t-1)$$

where $\phi_0(t) = 1, \quad t \in [-1, 0]$. Now by using integral form of the solutions, we have $\forall \;\; t \in [0, 1]$

$$y_1'(t) = y(0) + \int_0^t \phi_0(s-1)ds$$

$$= y(0) + \int_0^t 1ds$$

$$= y(0) + t$$

$$= 1 + t$$

Now $y(t)$ (denoted by $y_1(t)$) is known in [0,1], proceeding as before we can reduce the DDE (1.9.3) on the interval [1,2] to a non-autonomous ODE as

$$y_2'(t) = y_1(t-1)$$

where $y_1(t) = 1 + t, \quad t \in [0, 1]$. Again by using integral form of the solution for $t \in [1, 2]$, we have

$$y_2'(t) = y_1(1) + \int_1^t y_1(s-1)ds$$

$$= y_1(1) + \int_0^t (1+t)ds$$

$$= y_1(1) + t + \frac{t^2}{2}$$

$$= 2 + t + \frac{t^2}{2}$$

Therefore, for $t \in [1, 2]$

$$y_2(t) = 2 + t + \frac{t^2}{2}.$$

One can continue the procedure until the desired solution is obtained. But most of the time the resulting integrals quickly become very cumbersome and it is very difficult to draw any conclusion about the solution from this exact procedure.

1.9.2 Laplace Transformation Method

Consider the equation

$$y'(t) = cy(t-1) + f(t) \quad t > 1, \tag{1.9.4}$$

with initial function $y(t) = g(t), \quad 0 \leq t \leq 1$. Taking the Laplace transforms on both side leads to

$$\begin{aligned} \int_1^\infty y'(t)e^{-st}dt &= \int_1^\infty y'(t-1)e^{-st}dt + \int_1^\infty f(t)e^{-st}dt \\ y(t)e^{-st}dt - \int_1^\infty y'(t)(-s)e^{-st}dt &= c\int_0^\infty y'(u)e^{-s(u+1)}du. \end{aligned}$$

Assume that $y(t)e^{-st} \to 0 \ as \ t \to \infty$, this leads to

$$-e^{-s}y(1) + s\int_1^\infty y(t)e^{-st}dt = ce^{-s}\int_0^1 y(u)e^{-su}du + ce^{-s}\int_1^\infty y(u)e^{-su}du.$$

Also assume that $s - ce^{-s} \neq 0$, then we have

$$\int_1^\infty y(t)e^{-st}dt = \frac{ce^{-s}\int_0^1 y(u)e^{-su}du + e^{-s}y(1) + \int_1^\infty f(t)e^{-st}dt}{s - ce^{-s}}. \tag{1.9.5}$$

Assume that the inversion of the Laplace transform can be applied to have

$$y(t) = \int_{(b)} \left(\frac{ce^{-s}\int_0^1 y(u)e^{-su}du + e^{-s}y(1) + \int_1^\infty f(t)e^{-st}dt}{s - ce^{-s}} \right) e^{st}ds, \tag{1.9.6}$$

where the integral is carried out over a vertical line $Re(s) = b$, with b sufficiently large. It turns out to be the case that all zeros of $s - ce^{-s}$ lie in a left half-plane, and that the relation in (1.9.6) is valid if all these zeros satisfy $Re(s) < b$. In [27], other methods such as solution by definite integrals, series expansions, distribution of characteristics Roots along with the asymptotic behaviour of the solution and problem stability are discussed.

The purpose of this thesis is to present a reliable numerical approximation of a special class of delay differential equations known as Pantograph equation. The simplest form of proportional delay differential equation is

$$y'(t) = ry(t) + sy(qt), \ 0 < q < 1, \ t \geq 0, \tag{1.9.7}$$

where $r, s, \in \mathbb{C}$.

In some literature, these equations are mentioned as proportional delay differential equations. These equations explain many physical and mathematical phenomena, such as the dynamics of an overhead current collection system for an electric locomotive, light absorption in the galaxy, queuing theory, partition problems in number theory, cell growth model, and probability theory. Numerical solutions of IVPs, BVPs, a systems of differential equations, and fractional-order differential equations, along with their applications have been discussed in the following chapters.

1.10 Objective

This research formulates new numerical techniques for solving proportional delay differential equations. The Haar wavelet series method and the modified Haar wavelet series method are constructed to solve linear and nonlinear initial value problems (IVPs), boundary value problems, systems of differential equations , and fractional order IVPs. These schemes are capable of producing results with high accuracy and with less computational cost. All computer simulations are carried out in MATLAB on a 16GB RAM 64 bit machine carrying an Intel i5 processor. These methods involve fewer cumbersome manual calculations as compared to other numerical schemes.

1.11 Thesis Outline

The thesis discussed Haar wavelet techniques to solve different types of proportional delay differential equations. In Chapter 2, we introduced some preliminaries and definitions of Haar wavelets and their integrals which will be used throughout the thesis and developed a numerical technique to solve the proportional delay Riccati differential equation using Haar wavelets. Chapter 3 of the thesis deals with the Haar wavelet-based numerical technique for solving the proportional delay variants of Dirichlet boundary value problems. We have applied the Haar wavelet series method for solving simultaneous proportional delay differential equations in Chapter 4. Chapter 5 presents the modified Haar wavelet series method to solve higher-order multi-pantograph equations arising in electrodynamics. In Chapter 6, we discussed some concepts of fractional calculus and developed a reliable collocation numerical technique to solve proportional delay Riccati differential equations of Fractional Order.

Chapter 2

Approximate solution for proportional delay Riccati differential equations by Haar wavelet method

2.1 Riccati Differential Equations

The Riccati differential equations (RDEs) come under the class of nonlinear differential equations. These equations are widely studied for numerous problems of contemporary analysis and their applications and are not easy to solve explicitly. This makes it interesting to investigate the solutions of these equations. Here, we have considered the following Riccati differential equations:

$$y'(t) = q_1(t) + y(t)\left(q_2(t) + q_3(t)y(t)\right), \quad t_0 \leq t \leq t_f, \quad y(t_0) = y_0, \tag{2.1.1}$$

where $q_1(t), q_2(t)$ and $q_3(t)(\neq 0)$ are continuous, t_0, t_f and $y(t_0)$ are arbitrary constant and $y(t)$ is unknown function.

Its proportional-delay variant can be written as

$$y'(t) = \psi(t) + by(t) + cy(\alpha t)(d - y(\alpha t)), \quad t_0 \leq t \leq t_f, \quad y(t_0) = y_0, \tag{2.1.2}$$

where $c \neq 0,\ b,\ d,\ y_0 \in C$, and $\alpha > 0$, $\psi(t)$ is a continuous and $\alpha \neq 1$. When $0 < \alpha < 1$ equation (2.1.2) yields a retarded equation, whereas $\alpha > 1$ produces advanced equation. It follows from Picard-Lindelöf theorem that the solutions of equation (2.1.1) and equation (2.1.2) exists and it is unique. For further studies related to Riccati differential equations see [14, 75, 90, 91].

RDEs widely appear in random processes, kalman filtering systems, and network synthesis. It has enormous applications in the fields of super symmetric quantum mechanics and quantum chemistry and plays a key role in the theory of optimal control, stochastic control theory, financial mathematics, diffusion problems, econometric models, and dynamic games.

Modeling by delay is necessary in many applied physical problems, and to accomplish the purpose, delay differential equations have been used significantly. Delay differential equations arise inevitably in decision making, mathematical modelling of chemicals, biological and physiological processes, economic growth, neural networks, and delayed dynamics. For further applications of RDEs, one can see [23, 34, 59, 76] and the references mentioned in the following chapters.

In recent years, the problem of finding the approximate solution of these differential equations has grabbed attention and has been examined by many mathematicians. The methods already used for the numerical solution of Riccati differential equations are the variational iteration method (VIM)[38], the modified variational iteration method (MVIM)[1], homotopy perturbation method (HPM)[16], differential transform method (DTM)[75], and the Bezier curves method[40]. The Reproducing kernel Hilbert space method (RKHSM)[49] and Bezier control point method [39] are used to find the approximate solution of delay RDEs. In [23], semi-analytical solutions of some nonlinear proportional delay differential equations are discussed. In [5], author studied the numerical treatment of the stochastic delay differential equation to formulate a one-step scheme to approximate the solution of the problem. [80] studied the numerical inclusion of exact periodic solutions for the delay Duffing equation and proposed the existence of periodic solutions for the forced delay

Duffing equations based on the verified numerical computations.

The aim of this chapter is to present a numerical method which has a low computational cost and will allow us to solve RDEs and proportional delay RDEs. The method is based on the Haar wavelet basis and is named as Haar wavelet method (HWM). The idea is to convert a differential equation into a system of algebraic equations from which an approximate solution can be obtained. The method is tested on linear as well as nonlinear problems, and very promising results are obtained.

2.2 Haar Wavelet Basis and its Integration

To construct the Haar wavelet system $\{\mathfrak{h}_i(t)\}_{i=1}^{\infty}$ on $[\Gamma_1, \Gamma_2]$ two basic functions are required, namely

(a).The Haar scaling function (father wavelet):

$$\mathfrak{h}_1(t) = \mathbb{I}_{[\Gamma_1,\Gamma_2)}(t). \tag{2.2.1}$$

(b).The mother wavelet:

$$\mathfrak{h}_2(t) = \mathbb{I}_{[\Gamma_1,(\Gamma_1+\Gamma_2)/2)}(t) - \mathbb{I}_{[(\Gamma_1+\Gamma_2)/2,\Gamma_2)}(t), \tag{2.2.2}$$

where $\mathbb{I}_{[a,b]}(t)$ is characteristic/indicator function. Now for generating the Haar wavelet series, let j be dilation and k be translation parameter.

Then i-th Haar Wavelet is defined as:

$$\mathfrak{h}_i(t) = \begin{cases} 1 & \text{for } t \in [\vartheta_1(i), \vartheta_2(i)), \\ -1 & \text{for } t \in [\vartheta_2(i), \vartheta_3(i)), \\ 0 & otherwise, \end{cases} \tag{2.2.3}$$

where $\vartheta_1(i) = \Gamma_1 + (\Gamma_2 - \Gamma_1)k/2^j, \vartheta_2(i) = \Gamma_1 + (\Gamma_2 - \Gamma_1)(k + 0.5)/2^j, \vartheta_3(i) = \Gamma_1 + (\Gamma_2 - \Gamma_1)(k + 1)/2^j$. The index $i = 2^j + k + 1,\ j = 0, 1, \ldots, J$ where J is maximum level of wavelet and $k = 0, 1, \ldots, 2^j - 1$.

(c).Define scaling function space and wavelet space as follows

$$
\begin{aligned}
V_j &= span\{2^{j/2}\mathfrak{h}_1(2^j t - k), t \in [\Gamma_1, \Gamma_2]\}_{k=0}^{2^j-1}, \\
W_j &= span\{2^{j/2}\mathfrak{h}_2(2^j t - k), t \in [\Gamma_1, \Gamma_2]\}_{k=0}^{2^j-1}.
\end{aligned} \tag{2.2.4}
$$

Suppose $0 \leq J_0 < J$, then following relation holds:

$$
V_J = V_{J_0} \otimes W_{J_0} \otimes W_{J_0+1} \cdots \otimes W_{J-1}. \tag{2.2.5}
$$

The spaces V_j are such that $V_0 \subset V_1 \subset V_2 \cdots \subset L^2([\Gamma_1, \Gamma_2])$ and $\overline{\cup_{j=0}^{\infty} V_j} = L^2([\Gamma_1, \Gamma_2])$. Hence $L^2([\Gamma_1, \Gamma_2]) = V_0 \bigotimes(\bigotimes_{j_0}^{\infty} W_j)$ holds. It allows us to approximate any $f \in L^2([\Gamma_1, \Gamma_2])$ with following truncated Haar series:

$$
f_{approx}(t) \approx \sum_{i=1}^{2^{J+1}} a_i \mathfrak{h}_i(t). \tag{2.2.6}
$$

In the interval $[0, 1], \vartheta_1(i), \vartheta_2(i), \vartheta_3(i)$ becomes:

$$
\vartheta_1(i) = \frac{k}{2^j}, \ \vartheta_2(i) = \frac{(k + 0.5)}{2^j}, \ \vartheta_3(i) = \frac{(k + 1)}{2^j}.
$$

To apply the Haar wavelet following integrals are required:

$$
I_1\mathfrak{h}_i(t) = \int_0^t \mathfrak{h}_i(u)du, \ I_2\mathfrak{h}_i(t) = \int_0^t I_1\mathfrak{h}_i(u)du, \ \ldots \ I_n\mathfrak{h}_i(t) = \int_0^t I_{(n-1)}\mathfrak{h}_i(u)du.
$$

These integral can be calculated by analytic integration of (2.2.3),

$$
I_1\mathfrak{h}_i(t) = \begin{cases} t - \vartheta_1(i) & \text{for } t \in [\vartheta_1(i), \vartheta_2(i)), \\ \vartheta_3(i) - t & \text{for } t \in [\vartheta_2(i), \vartheta_3(i)), \\ 0 & otherwise, \end{cases} \tag{2.2.7}
$$

and

$$I_2\mathfrak{h}_i(t) = \begin{cases} \frac{1}{2}(t-\vartheta_1(i))^2 & \text{for } t \in [\vartheta_1(i), \vartheta_2(i)), \\ \frac{1}{2^{2j+2}} - \frac{1}{2}(\vartheta_3(i)-t)^2 & \text{for } t \in [\vartheta_2(i), \vartheta_3(i)), \\ \frac{1}{2^{2j+2}} & \text{for } t \in [\vartheta_3(i), 1), \\ 0 & \textit{otherwise}. \end{cases} \tag{2.2.8}$$

In general, the value of nth integral of (2.2.3) on interval $[0, 1]$ is

$$I_n\mathfrak{h}_i(t) = \frac{1}{n!}\begin{cases} 0 & \text{for } t \in [0, \vartheta_1(i)), \\ (t-\vartheta_1(i))^n & \text{for } t \in [\vartheta_1(i), \vartheta_2(i)), \\ (t-\vartheta_1(i))^n - 2(t-\vartheta_2(i))^n & \text{for } t \in [\vartheta_2(i), \vartheta_3(i)), \\ (t-\vartheta_1(i))^n - 2(t-\vartheta_2(i))^n + (t-\vartheta_3(i))^n & \text{for } t \in [\vartheta_3(i), 1). \end{cases} \tag{2.2.9}$$

In case $i = 1$, we have the n^{th} integral of scaling function evaluated from (2.2.1)

$$I_n\mathfrak{h}_i(t) = \frac{t^n}{n!}. \tag{2.2.10}$$

2.3 Description of Method

In order to solve equation (2.1.1) and equation (2.1.2), by Haar wavelet expansion, let

$$y'(t) = \sum_{i=1}^{2M} a_i\mathfrak{h}_i(t). \tag{2.3.1}$$

On integrating equation (2.3.1) from 0 to t with respect to t we compute

$$y(t) = \sum_{i=1}^{2M} a_i I_1\mathfrak{h}_i(t) + y(0), \tag{2.3.2}$$

also

$$y'(\alpha t) = \sum_{i=1}^{2M} a_i \mathfrak{h}_i(\alpha t), \tag{2.3.3}$$

and

$$y(\alpha t) = \sum_{i=1}^{2M} a_i I_1 \mathfrak{h}_i(\alpha t) + y(0). \tag{2.3.4}$$

Using equations (2.3.1), (2.3.2) in equation (2.1.1) and equations (2.3.3), (2.3.4) in equation (2.1.2) with collocation points $t_l = \frac{(l-0.5)}{2M}$, $l = 1, 2, \ldots, 2M$, we have the following system of equations

$$\begin{aligned}\sum_{i=1}^{2M} a_i \mathfrak{h}_i(t_l) =& q_1(t_l) + \left[\sum_{i=1}^{2M} a_i I_1 \mathfrak{h}_i(t_l) + y(0)\right] q_2(t_l) \\ &+ q_3(t_l)\left[\sum_{i=1}^{2M} a_i I_1 \mathfrak{h}_i(t_l) + y(0)\right]\left[\sum_{i=1}^{2M} a_i I_1 \mathfrak{h}_i(t_l) + y(0)\right],\end{aligned} \tag{2.3.5}$$

and

$$\begin{aligned}\sum_{i=1}^{2M} a_i \mathfrak{h}_i(t_l) =& \psi(t_l) + b\left[\sum_{i=1}^{2M} a_i I_1 \mathfrak{h}_i(t_l) + y(0)\right] \\ &+ c\left[\sum_{i=1}^{2M} a_i I_1 \mathfrak{h}_i(\alpha t_l) + y(0)\right]\left[d - (\sum_{i=1}^{2M} a_i I_1 \mathfrak{h}_i(\alpha t_l) + y(0))\right].\end{aligned} \tag{2.3.6}$$

Above systems of nonlinear equations can be solved using classical "Newton's method", by using these values of Haar coefficient a_i's obtained from equation (2.3.5) in equation (2.3.2), we get the approximate solution of equation (2.1.1), similarly using coeffiecients obtained form equation (2.3.6) in equation (2.3.2), we get the approximate solution of equation (2.1.2).

2.3.1 Convergence analysis of the Haar wavelet

Lemma 2.1. *Assume that $\omega(t) \in L^2(\mathbb{R})$ be a Lipschitz continuous (with $K = sup|\omega'(t)|$) on $[0,1)$, then the error norm at Jth level satisfies the following inequality*

$$\|e_j(t)\| \leq \sqrt{\frac{K}{7}} \frac{C}{2^{(3)2^{J-1}}}, \tag{2.3.7}$$

where K, C are some real constants.

Proof. For proof see [9]. □

2.4 Numerical Problems

Here we will present numerical problems and the discussion on the Haar wavelet method for solving different types of Riccati and proportional delay Riccati differential equations. We have shown that the performance of our technique is sharp and the absolute error is reduced significantly in some problems. We also calculated the experimental rate of convergence $R_c(J)$, as described in [68]. In the first part of this section, we consider quadratic Riccati differential equations. Then, we solve some delay-Riccati differential equations.

$$R_c(J) = \frac{log(E_c(J-1)/E_c(J))}{log(2)}, \tag{2.4.1}$$

where $E_c(J)$ is error at level J.

Problem 1. Consider the following, taken from [40]

$$y'(t) = 16t^2 - 5 + 8ty(t) + y^2(t), \quad 0 \leq t \leq 1, \quad y(0) = 1. \tag{2.4.2}$$

The exact solution of equation (2.4.2) is $y(t) = 1 - 4t$. Here we have solved this problem using Haar wavelet expansions and integral of the Haar wavelet. The values

Table 2.1: MAEs at different level of J (Problem 1).

Value of J	**MAEs**
2	$1.4654E-14$
3	$1.1546E-14$
4	$3.1086E-15$
5	$2.6645E-15$
6	$3.5527E-15$
7	$8.8818E-16$

Table 2.2: MAEs for Problem 1 with J=3.

HWM	**Bezier Curves Method**[40]
$5.3735E-14$	$5.3714E-04$

of Haar coefficients at level $J = 2$ are $a_1 = -4.000000, a_2 = 0.000000, a_3 = 0.000000, a_4 = 0.000000, a_5 = 0.000000, a_6 = 0.000000, a_7 = 0.000000, a_8 = 0.000000$. The coefficient a_1 is significantly close to -4 and rest of the coefficients are zero correct up to six decimal places. Therefore, from equation (2.3.2) solution is $a_1 I_1 h_1(t) + y(0)$ i.e.$-4t + 1$ which is same as exact solution. The error estimates at different levels of resolution are given in Table 2.1. We observed that good approximation can be achieve with the increase in level of resolution. A comparison between the Haar wavelet method and the Bezier Curves method [40] is reported in Table 2.2, which clearly shows that the absolute error is reduced significantly in our case as compared to the Bezier Curves method. Point wise error at $J = 3$ is shown in Table 2.3. Comparison between exact solution and numerical solution at $J = 3$ is shown in Fig.2.1 and we observed that both the curves visually coincide.

Problem 2. Solve the equation

$$y'(t) = e^t - e^{3t} + 2e^{2t}y(t) - e^t y^2(t), \quad 0 \leq t \leq 1, \quad y(0) = 1. \tag{2.4.3}$$

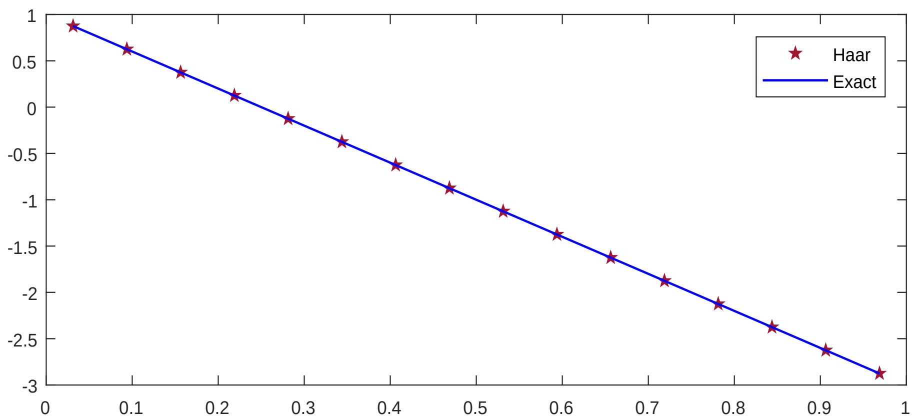

FIGURE 2.1: Comparison of exact and numerical solution at J =3.

TABLE 2.3: Comparison between exact solution and Haar solution (Problem 1).

$t_l = (l-0.5)/2^{J+1}$ $t(=1/32)$	**Haar solution**	**Exact**	**Error**
1	0.8750	0.8750	$0.0222E-014$
3	0.6250	0.6250	$0.0666E-014$
5	0.3750	0.3750	$0.0666E-014$
7	0.1250	0.1250	$0.0333E-014$
9	-0.1250	-0.1250	$0.0222E-014$
11	-0.3750	-0.3750	$0.0888E-014$
13	-0.6250	-0.6250	$0.1554E-014$
15	-0.8750	-0.8750	$0.1554E-014$
17	-1.1250	-1.1250	$0.1332E-014$
19	-1.3750	-1.3750	$0.1332E-014$
21	-1.6250	-1.6250	$0.1332E-014$
23	-1.8750	-1.8750	$0.0444E-014$
25	-2.1250	-2.1250	$0.0888E-014$
27	-2.3750	-2.3750	$0.2665E-014$
29	-2.6250	-2.6250	$0.4885E-014$
31	-2.8750	-2.8750	$0.8882E-014$

The exact solution of equation (2.4.3) is $y(t) = e^t$[40]. The maximum absolute error at different levels of resolution is shown in Table 2.4. From Table 2.4, we have observed that error is decreasing with the increase in resolution. The result is compared with the Bezier Curves method [40] in Table 2.6. A comparison between the exact solution and the numerical solution for $J = 4$ is depicted in Fig.2.2.

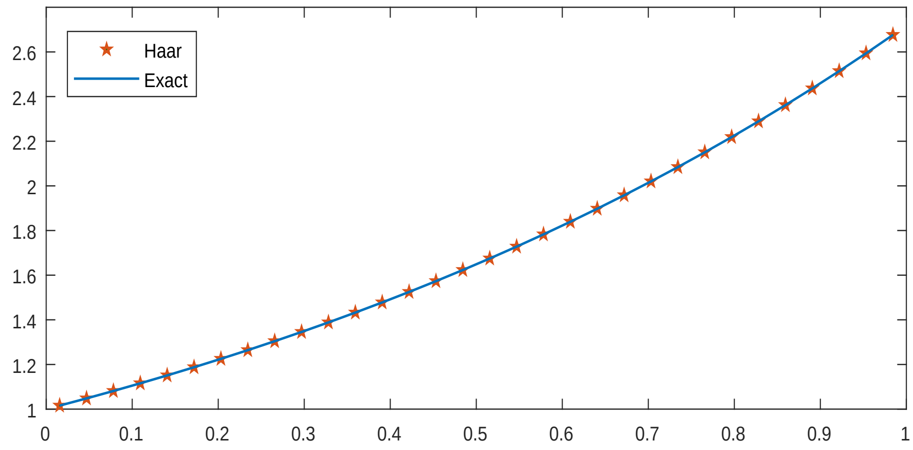

FIGURE 2.2: Comparison between exact and numerical solution (Problem 2).

TABLE 2.4: MAEs at different levels of J (Problem 2).

Value of J	MAEs
4	$2.5841E-04$
5	$6.5049E-05$
6	$1.6315E-05$
7	$4.0855E-06$
8	$1.0238E-06$
9	$2.5889E-07$

TABLE 2.5: MAEs at different levels of J (Problem 4).

Value of J	MAEs
5	$3.1062E-03$
6	$7.8308E-04$
7	$1.9648E-04$
8	$4.9204E-05$
9	$1.2307E-05$
10	$3.0790E-06$

TABLE 2.6: Comparison for Problem 2.

HWM	**Bezier Curves Method**[40]
$6.5049E-05$	$8.0175E-04$

Computer simulations indicate that by increasing resolution, a good approximate solution can be achieved.

Problem 3. In this example, we choose to solve the following Riccati differential equation

$$y'(t) = y(t) - 50ty^2 + f(t), \quad 0 \leq t \leq 1, \quad y(0) = 1. \tag{2.4.4}$$

The function $f(t)$ is chosen such that equation (2.4.4) has exact solution $y(t) =$

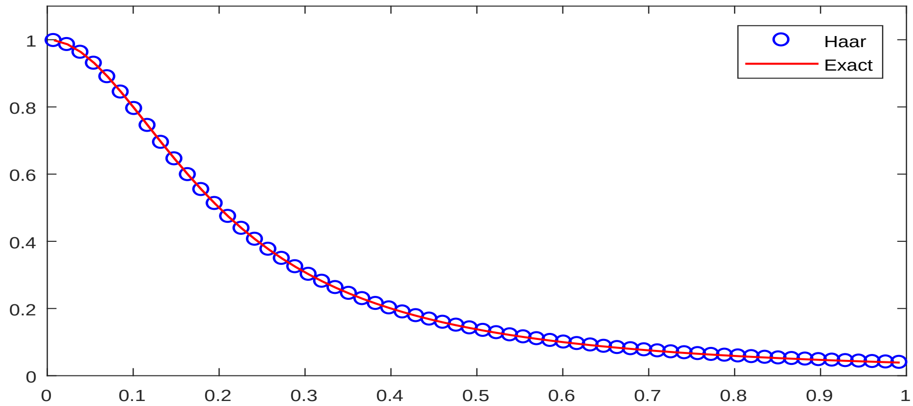

FIGURE 2.3: Comparison between exact and numerical solution (Problem 3).

$\frac{1}{1+25t^2}$. We have calculated the maximum absolute error and experimental rate of convergence at $J = 4, 5, 6, 7, 8, 9$. The maximum absolute error is decreasing from order 10^{-3} for $J = 4$ to order 10^{-6} for $J = 9$. Further, we observed that the maximum absolute error decreases by increasing the levels of resolution and the numerical rate of convergence approaches 2, thus confirming the theoretical results (studied by the authors in [68]). Finally, the comparison between approximate and exact solution is depicted in Fig.2.3

Problem 4. In this illustration we consider the following PDRDE

$$y'(t) = 1 - 2y^2(\frac{t}{2}), \quad 0 \leq t \leq 2\pi, \quad y(0) = 0. \tag{2.4.5}$$

The exact solution of equation (2.4.5) is $y(t) = sin(t)$[23]. In this problem $\alpha = 1/2$, which is the case of a retarded equation. We have solved this problem using Haar wavelet expansion and integral of the Haar wavelet. The maximum absolute error for different resolutions is shown in Table 2.5. A comparison between analytic and approximate solutions at $J = 5$ is shown in Fig.2.4. The maximum absolute error is $3.0790E - 06$ at $J = 10$. We observed that by increasing the value of J a good

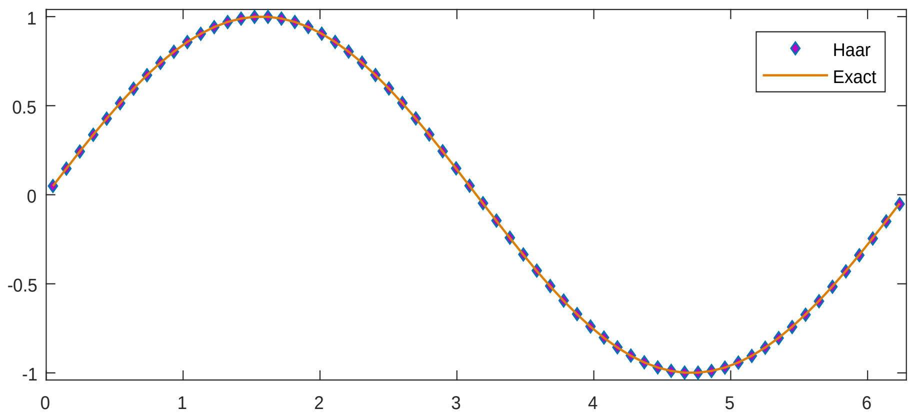

FIGURE 2.4: Comparison between exact and numerical solution (Problem 4).

approximation can be achieved.

Problem 5. Solve the delay equation

$$y'(t) = \frac{1}{4}y(t) + y(\frac{t}{2})(1 - y(\frac{t}{2})), \quad 0 \leq t \leq 1, \quad y(0) = 1. \tag{2.4.6}$$

The equation equation (2.4.6) is an example of proportional-delay variant of Riccati differential equation and it possesses the periodic solution

$$y(t) = \frac{1}{2} + \frac{1}{2}cos(\frac{\sqrt{2}t}{4}) + \frac{\sqrt{2}}{2}sin(\frac{\sqrt{2}t}{4}).$$

First, we will transform equation (2.4.6) into the following system of algebraic equations,

$$\sum_{i=1}^{2M} a_i \mathfrak{h}_i(t_l) - \frac{1}{4}\left[\sum_{i=1}^{2M} a_i I_1 \mathfrak{h}_i(t_l) + 1\right] - \left[\sum_{i=1}^{2M} a_i I_1 \mathfrak{h}_i(\frac{t_l}{2}) + 1\right]\left[1 - (\sum_{i=1}^{2M} a_i I_1 \mathfrak{h}_i(\frac{t_l}{2}) + 1)\right] = 0. \tag{2.4.7}$$

By solving the system of algebraic equation (2.4.7), we obtained the values of the Haar coefficients a_i. Using the values of a_i along with given initial condition $y(0) = 1$ in equation (2.3.2) approximate numerical solution for equation (2.4.6) is obtained. Maximum absolute error for different values of J is presented in Table

Table 2.7: MAEs (Problem 5).

Value of J	**MAEs**
3	$3.0352E-05$
4	$7.6091E-06$
5	$1.9048E-06$
6	$4.7652E-07$
7	$1.1917E-07$
8	$7.4500E-09$

Table 2.8: MAEs (Problem 6).

Value of J	**MAEs**
4	$5.8484E-04$
5	$1.5242E-04$
6	$3.8914E-05$
7	$9.8315E-06$
8	$2.4709E-06$
9	$6.1935E-07$

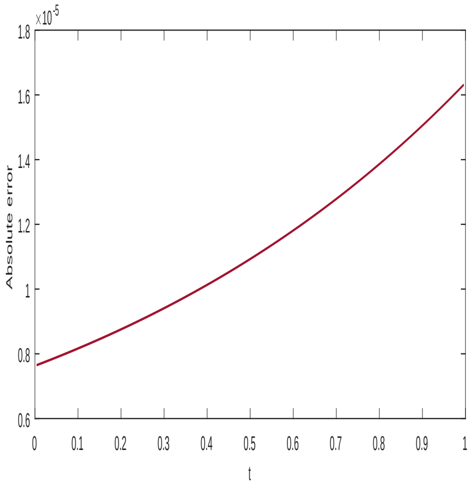

Figure 2.5: Absolute error (Problem 2) at J=6.

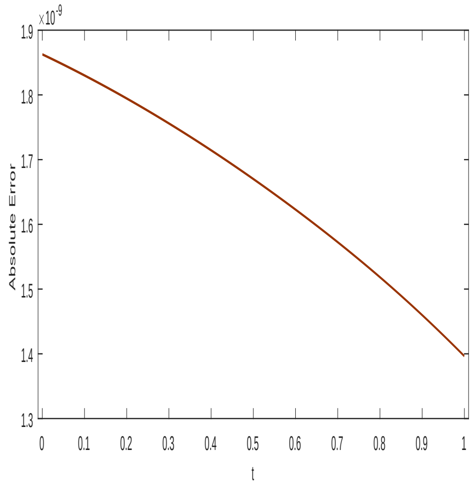

Figure 2.6: Absolute error(Problem 5) at J=10.

2.7 and the maximum absolute error is $7.4500E-09$ for $J = 8$. In Table 2.9 point wise error between exact solution and Haar solution at $J = 3$ is reported. Finally, comparison between exact solution and numerical solution at $J = 3$ is depicted graphically in Fig.2.7. We observed that a better approximation can be achieved with an increase in the value of J.

Problem 6. Solve the delay equation

$$y'(t) = -\frac{1}{8}y(t) + y(\frac{t}{2})(1 - y(\frac{t}{2})), \quad 0 \leq t \leq 4\pi, \quad y(0) = \frac{1}{4}. \tag{2.4.8}$$

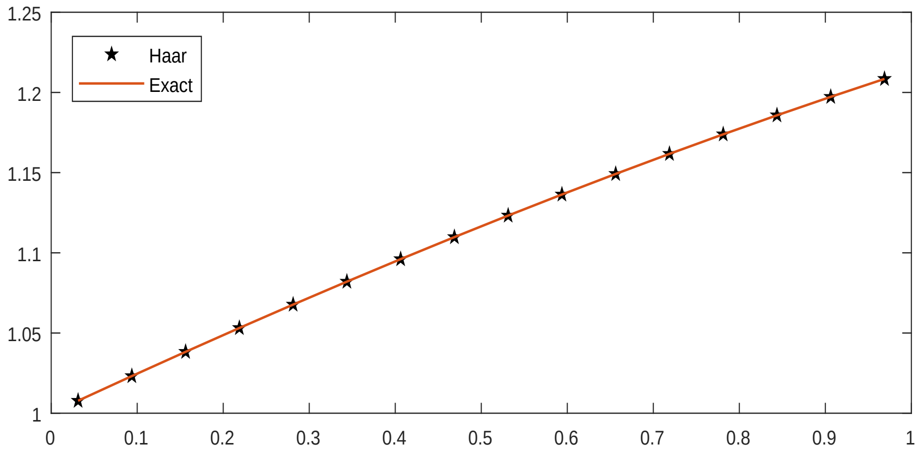

FIGURE 2.7: Comparison between exact and numerical solution (Problem 5).

TABLE 2.9: Comparison between exact solution and Haar solution (Problem 5).

$t_l = (l-0.5)/2^{J+1}$ $t(=1/32)$	**Haar solution**	**Exact solution**	**Error**
1	1.007751	1.007781	$0.303515E-004$
3	1.023128	1.023158	$0.300143E-004$
5	1.038250	1.038279	$0.296578E-004$
7	1.053109	1.053138	$0.292823E-004$
9	1.067697	1.067726	$0.288881E-004$
11	1.082009	1.082038	$0.284758E-004$
13	1.096036	1.096065	$0.280460E-004$
15	1.109773	1.109801	$0.275987E-004$
17	1.123212	1.123239	$0.271345E-004$
19	1.136346	1.136373	$0.266540E-004$
21	1.149170	1.149196	$0.261577E-004$
23	1.161677	1.161702	$0.256458E-004$
25	1.173860	1.173885	$0.251189E-004$
27	1.185715	1.185740	$0.245777E-004$
29	1.197235	1.197259	$0.240227E-004$
31	1.208414	1.208438	$0.234542E-004$

Note that equation (2.4.8) is first order Riccati differential equation with proportional delay. The exact solution for this problem is

$$y(t) = \frac{1}{2} - \frac{1}{4}cos(\frac{\sqrt{5}t}{8}) + \frac{\sqrt{5}}{4}sin(\frac{\sqrt{5}t}{8}).$$

On applying the numerical technique mentioned in section 3, the maximum absolute

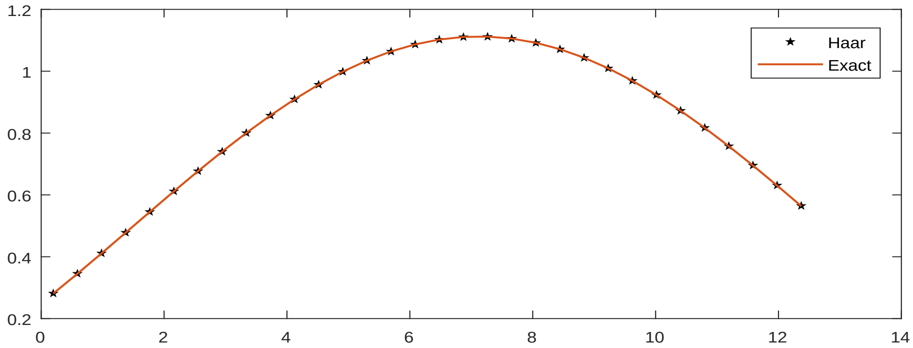

FIGURE 2.8: Comparison between exact and numerical solution (Problem 6).

error between the exact solution and the numerical solution at different values of J is recorded in Table 2.8. From Table 2.8 we have observed that the maximum absolute error decreases with the increase in resolution. The maximum absolute error is decreased from the order of 10^{-4} at $J = 4$ to 10^{-7} at $J = 9$ and the rate of convergence approaches 2, which follows the theoretical results mentioned in [68]. A comparison between the exact solution and the numerical solution at $J = 4$ is shown in Fig.2.8.

2.5 Summary

In this chapter[1], the Haar wavelet method has been successfully applied to find the numerical solution of Riccati differential equations and proportional-delay variants of Riccati differential equations, and several problems from the literature have been solved. Numerical results are compared with the Bezier Curves method and exact solutions. The numerical simulations show that our computation is much better in terms of accuracy and convergence.

[1]The content of this chapter is published in **Poincare Journal of Analysis and Applications .**(Scopus Indexed).

Chapter 3

Haar based numerical technique for solving proportional delay Dirichlet boundary value problems

3.1 Introduction

Boundary value problems(BVPs) are now prevalent in all applied sciences. The growing popularity of this branch of differential equations has prompted numerous researchers to investigate various physical models utilizing mathematical tools and computer simulation software. Many problems in science and technology such as study of the mechanical behavior of the nano material in nanomechanics[42], turbulence modeling[58], modeling of chemical reactors[47], study of molecular structure in chemical engineering[12], heat transfer model and study of deflection in cables can be formulated mathematically in BVPs for second order differential equations.

Another application of BVPs appears in mathematical modelling design to reflect the real mechanical properties of smart material[69]. The smart material, also called as intellectual material of the 21st century, is a material with shape memory effects. Such materials are widely used in medicine, engineering, aircraft building, construction, etc.

The main focus of this study is to develop a Haar wavelet-based numerical technique for solving the following proportional delay variant of the two-point boundary value problem

$$y''(t) = \Omega(t, y(t), y(qt), y'(t), y'(qt)),\ t \in [0,1], \qquad \text{with } y(0) = \zeta_1,\ y(1) = \zeta_2, \tag{3.1.1}$$

where Ω is analytic function, $q \in (0,1)$ and, ζ_1, ζ_2 are arbitrary constants.

The proportional delay variant of the delay differential equation is generally referred to as the Pantograph equation. The name Pantograph comes from Ockendon and Tayler's first work for collecting current by the Pantograph head of an electric locomotive. These equations are used in many different fields, such as number theory, probability theory on algebraic structure, economics, cell growth modelling, astrophysics, nonlinear dynamical systems, adaptive control, quantum mechanics, electrodynamics, engineering, and numerous others. [13, 35, 36, 111].

In many instances, it is difficult to obtain the exact solution of the delay differential models. As a result, the solutions to such equations have developed a lot of interest among researchers, and they have used a variety of numerical approaches to approximate the solutions to these equations. Agarwal and Chow extended the finite-difference method to offer the approximate solution to two-point boundary-value problems with deviating argument [3]. Li and Liu presented a novel numerical approach for solving multi-pantograph delay equations based on the Runge-Kutta scheme [61]. Shakeri et al. used the homotopy perturbation method (HPM) to solve certain delay differential equations [100]. To solve generalised pantograph equations, Saadatmandi et al. used a Lagrange multiplier-based variational iteration scheme (VIM) [93]. Both VIM and HPM yield correct results, but the computational cost is significant due to the use of symbolic integrations. Shakeri and Dehghan have investigated the numerical solution of delay differential equations using the adomain decomposition method [99]. Sedaghat et al. [96] adopted a Chebyshev polynomial based numerical method and approximate the solution of DDEs. The aim of the method [96] is to utilise the operational matrix and its derivative to simplify the problem into a series of algebraic equations from which the solution can be derived. Authors in [15, 33, 112, 115] have developed some numerical techniques based on collocation method in the recent past. These techniques are quite effective for investigating proportional delay differential equations.

The author is inspired by the aforementioned findings and adopted the Haar wavelet series approach for examining the approximate numerical solutions of Dirichlet boundary value problems of proportional delay nature. The method is suitable for solving BVPs since it takes the boundary condition into consideration automatically. Moreover, for a limited number of collocation points, high precision is achievable.

3.2 Construction of Method

We consider the boundary value problem of pantograph type as follows:

$$y''(t) = \Omega(t, y(t), y(qt), y'(t), y'(qt)),\ t \in [0,1], \qquad (3.2.1)$$

$$\text{with Dirichlet condition } y(0) = \zeta_1,\ y(1) = \zeta_2,$$

where Ω is analytic function, $q \in (0,1)$ and, ζ_1, ζ_2 are arbitrary constant.

In order to apply the Haar wavelet series techniques, firstly we expand the $y''(t)$ in terms of truncated Haar wavelet series as:

$$y''(t) = \sum_{i=0}^{2^{J+1}} a_i \mathfrak{h}_i(t). \tag{3.2.2}$$

Integrate equation (3.2.2) 0 *to* t, we get,

$$y'(t) = \sum_{i=0}^{2^{J+1}} a_i I_1 \mathfrak{h}_i(t) + y'(0). \tag{3.2.3}$$

Further integration yields,

$$y(t) = \sum_{i=0}^{2^{J+1}} a_i I_2 \mathfrak{h}_i(t) + y'(0)t + y(0). \tag{3.2.4}$$

Quantity $y'(0)$ in equation (3.2.3) and (3.2.4) are yet to determined for that integrate equation (3.2.3) from t *to* 1, we have

$$-y(t) = \sum_{i=0}^{2^{J+1}} a_i I_2 \mathfrak{h}_i(1) - \sum_{i=0}^{2^{J+1}} a_i I_2 \mathfrak{h}_i(t) + y'(0)(1-t) - y(1). \tag{3.2.5}$$

Now, from equation(3.2.4) and (3.2.5) we get,

$$y'(0) = -\sum_{i=0}^{2^{J+1}} a_i I_2 \mathfrak{h}_i(1) - y(0) + y(1).$$

Utilizing $y'(0),\ y(0) = \zeta_1,\ y(1) = \zeta_2$ in equation (3.2.4), we obtain the following

$$y(t) = \sum_{i=0}^{2^{J+1}} a_i I_2 \mathfrak{h}_i(t) + \Big(-\sum_{i=0}^{2^{J+1}} a_i I_2 \mathfrak{h}_i(1) - \zeta_1 + \zeta_2\Big)t + \zeta_1. \tag{3.2.6}$$

Also,

$$y(qt) = \sum_{i=0}^{2^{J+1}} a_i I_2 \mathfrak{h}_i(qt) + \Big(-\sum_{i=0}^{2^{J+1}} a_i I_2 \mathfrak{h}_i(1) - \zeta_1 + \zeta_2\Big)(qt) + \zeta_1. \tag{3.2.7}$$

Similarly, putting $y'(0) = -\sum_{i=0}^{2^{J+1}} a_i I_2 \mathfrak{h}_i(1) - y(0) + y(1),\ y(0) = \zeta_1,\ y(1) = \zeta_2$ in equation (3.2.3) we get,

$$y'(t) = \sum_{i=0}^{2^{J+1}} a_i I_1 \mathfrak{h}_i(t) - \sum_{i=0}^{2^{J+1}} a_i I_2 \mathfrak{h}_i(1) - \zeta_1 + \zeta_2, \tag{3.2.8}$$

and

$$y'(qt) = \sum_{i=0}^{2^{J+1}} a_i I_1 \mathfrak{h}_i(qt) - \sum_{i=0}^{2^{J+1}} a_i I_2 \mathfrak{h}_i(1) - \zeta_1 + \zeta_2. \tag{3.2.9}$$

Substituting equation (3.2.2) and equations (3.2.6) - (3.2.9), in equation (3.2.1), we have

$$\begin{aligned}\sum_{i=0}^{2^{J+1}} a_i \mathfrak{h}_i(t) =& \Omega\Bigg(t, \Big[\sum_{i=0}^{2^{J+1}} a_i I_2 \mathfrak{h}_i(t) + \Big(-\sum_{i=0}^{2^{J+1}} a_i I_2 \mathfrak{h}_i(1) - \zeta_1 + \zeta_2\Big)t + \zeta_1\Big],\\ & \Big[\sum_{i=0}^{2^{J+1}} a_i I_2 \mathfrak{h}_i(qt) + \Big(-\sum_{i=0}^{2^{J+1}} a_i I_2 \mathfrak{h}_i(1) - \zeta_1 + \zeta_2\Big)(qt) + \zeta_1\Big],\\ & \Big[\sum_{i=0}^{2^{J+1}} a_i I_1 \mathfrak{h}_i(t) - \sum_{i=0}^{2^{J+1}} a_i I_2 \mathfrak{h}_i(1) - \zeta_1 + \zeta_2\Big],\\ & \Big[\sum_{i=0}^{2^{J+1}} a_i I_1 \mathfrak{h}_i(qt) - \sum_{i=0}^{2^{J+1}} a_i I_2 \mathfrak{h}_i(1) - \zeta_1 + \zeta_2\Big]\Bigg).\end{aligned} \tag{3.2.10}$$

Discretisation of the above equation using collocation procedure leads to the algebraic system for $a_i^{,}s$. After determining $a_i^{,}s$ using Newton's iterative method or any other suitable method we get the approximate solution from equation (3.2.6).

3.3 Flow Chart

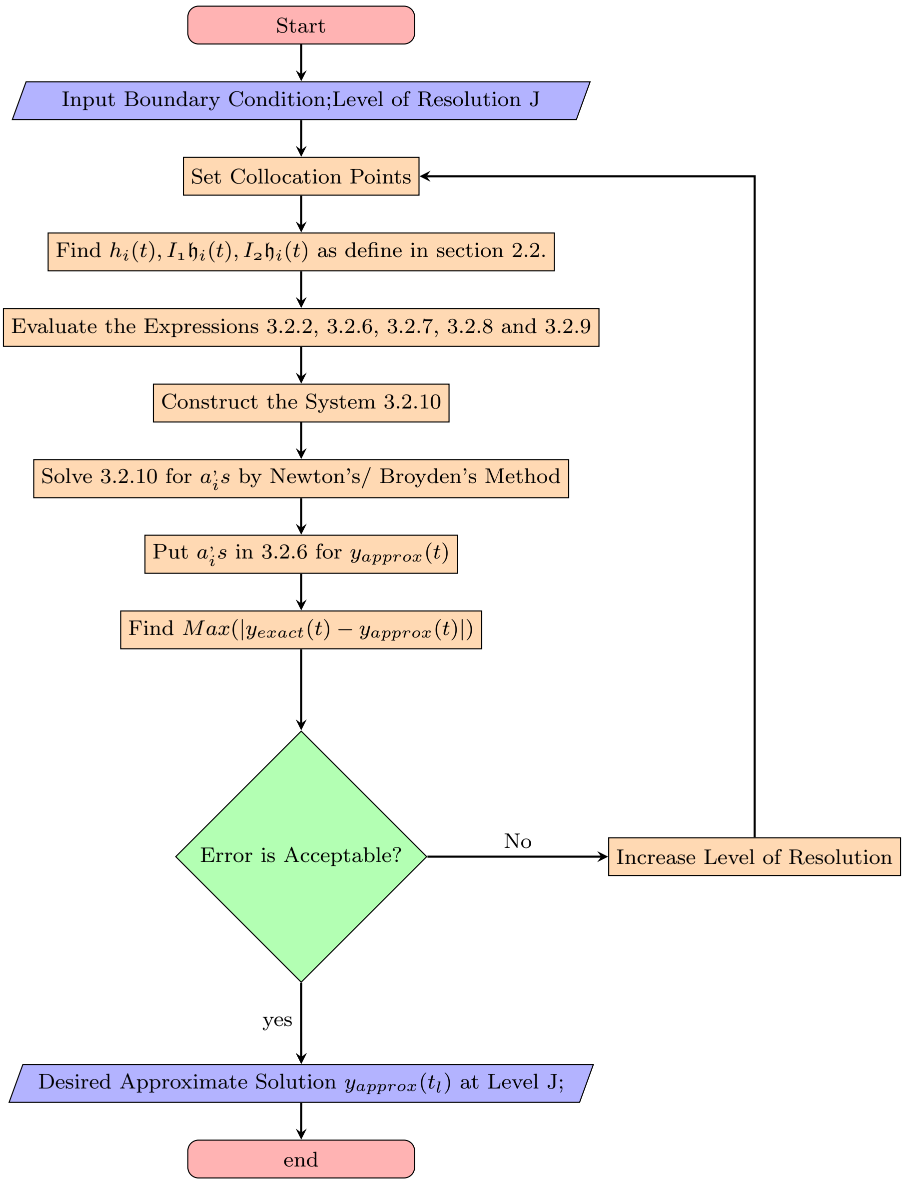

3.4 Illustrative Examples

Problem 1. Consider the boundary value problem

$$y''(t) - 1 - 2(1 + t^2/8)cos(t/2) + 2cos(t/2)y(t/2) = 0, \ t \in [0, 1], \qquad (3.4.1)$$

$$\text{with Dirichlet boundary condition } y(0) = 1, \ y(1) = \frac{3}{2} + sin(1).$$

Whereas, the exact solution of the problem is given by $y(t) = \frac{t^2}{2} + sin(t) + 1$.

Problem 2. Consider the boundary value problem

$$\begin{gathered} y''(t) + 2e^{-t} - y(t)/2 - e^{-t/2}y(t/2) = 0,\ t \in [0,1], \\ \text{with Dirichlet boundary condition } y(0) = 0,\ y(1) = e^{-1}, \end{gathered} \tag{3.4.2}$$

whose exact solution is $y(t) = te^{-t}$.

Problem 3. Let us assume the boundary value problem

$$\begin{gathered} y''(t) - 4e^{-t/2}sin(t/2)y(t/2) = 0,\ t \in [0,1], \\ \text{along with Dirichlet boundary condition } y(0) = 1,\ y(1) = e^{-1}cos(1), \end{gathered} \tag{3.4.3}$$

corresponding to the exact solution $y(t) = e^{-t}cos(t)$.

Problem 4. Assume the nonlinear two-point boundary value problem as

$$\begin{gathered} y''(t) - ((y(t))^2 + (y(t))^3)y(t/2) = 0,\ t \in [0,1], \\ \text{with Dirichlet boundary condition } y(0) = 1,\ y(1) = 1/2. \end{gathered} \tag{3.4.4}$$

The exact solution of the above nonlinear boundary value problem is $y(t) = \frac{1}{t+1}$.

Problem 5. Assume the following two-point boundary value problem

$$\begin{gathered} y''(t) - y'(t)y(t/2) + 8t^2y(t/2) + \ominus(t) = 0,\ t \in [0,1], \\ \text{subject to Dirichlet boundary condition } to\ y(0) = 1,\ y(1) = 3, \end{gathered} \tag{3.4.5}$$

and the $\ominus(t)$ is chosen such that the exact solution of problem (3.4.5) is $y(t) = 1 + t + t^3$.

3.5 Results and Discussions

The above problems are solved using the Haar wavelet series method. For each problem at different resolutions J, the maximum absolute error and experimental convergence rate are computed. These results are presented in Tables 3.1-3.8. Table

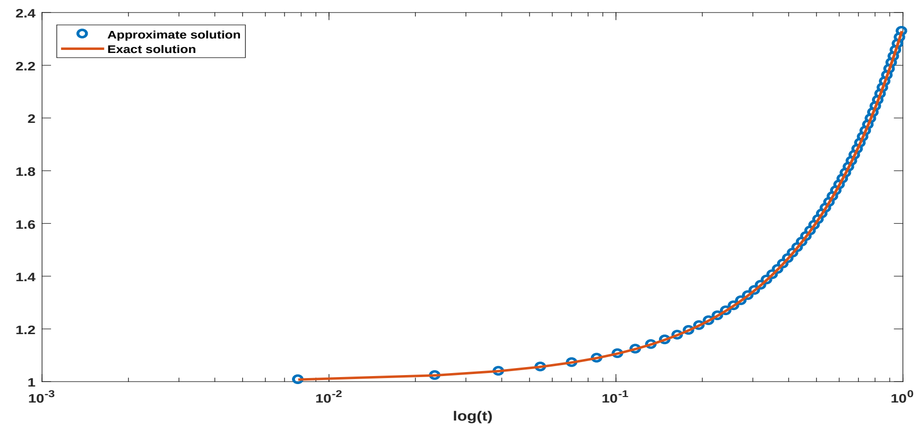

FIGURE 3.1: Plot for Problem 1 at J=5

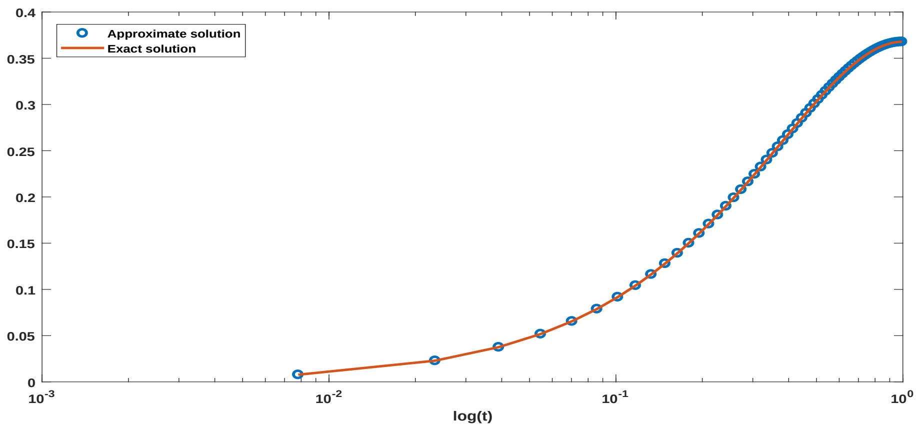

FIGURE 3.2: Plot for Problem 2 at J=5

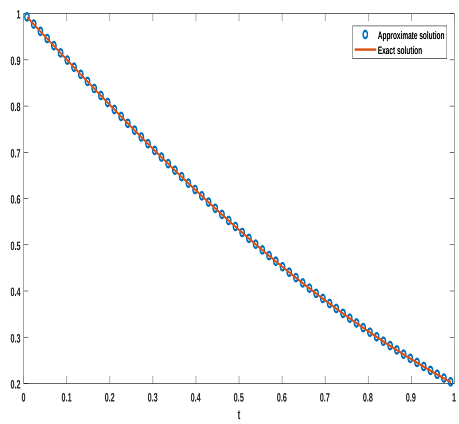

FIGURE 3.3: Solution curves for Problem 3 at J=5

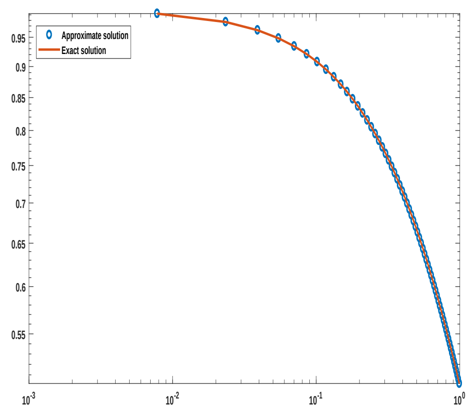

FIGURE 3.4: loglog Plot for Problem 4 at J=5

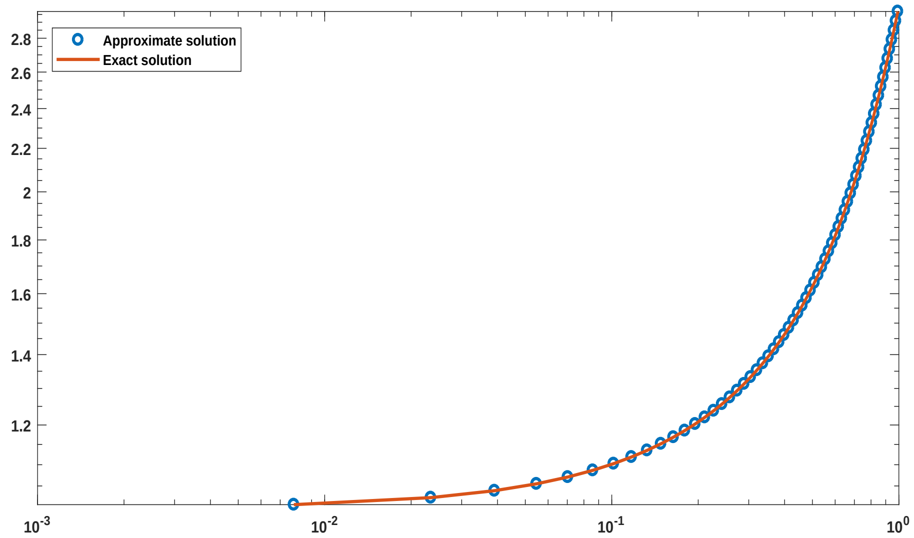

FIGURE 3.5: loglog Plot for Problem 5 at J=5

TABLE 3.1: MAEs for Problems 1 to 5.

J	**Problem 1**	**Problem 2**	**Problem 3**	**Problem 4**	**Problem 5**
1	$1.5997E-04$	$5.5835E-04$	$5.8345E-04$	$9.4871E-04$	$2.6907E-03$
2	$4.4574E-05$	$1.5644E-04$	$1.6306E-04$	$2.7026E-04$	$6.6283E-04$
3	$1.1324E-05$	$3.9757E-05$	$4.1522E-05$	$7.0508E-05$	$1.6553E-04$
4	$2.8500E-06$	$1.0014E-05$	$1.0454E-05$	$1.7787E-05$	$4.1311E-05$
5	$7.1382E-07$	$2.5082E-06$	$2.6172E-06$	$4.4582E-06$	$1.0331E-05$
6	$1.7831E-07$	$6.2735E-07$	$6.5449E-07$	$1.1152E-06$	$2.5828E-06$
7	$4.4275E-08$	$1.5692E-07$	$1.6362E-07$	$2.7884E-07$	$6.4569E-07$
8	$1.1342E-08$	$3.9226E-08$	$4.0890E-08$	$6.9712E-08$	$1.6142E-07$
9	$2.6235E-09$	$9.8905E-09$	$1.0218E-08$	$1.7427E-08$	$4.0355E-08$
10	$6.9708E-10$	$2.4508E-09$	$2.5589E-09$	$4.3559E-09$	$1.0088E-08$

TABLE 3.2: Rate of convergence $R_c = \frac{log\left(\frac{error(J-1)}{error(J)}\right)}{log(2)}$ for Problems 1 to 5.

J	**Problem 1**	**Problem 2**	**Problem 3**	**Problem 4**	**Problem 5**
1	−−−−−−−	−−−−−−−	−−−−−−−	−−−−	−−−−−
2	1.8435	1.8356	1.8392	1.8116	2.0213
3	1.9768	1.9763	1.9735	1.9385	2.0015
4	1.9903	1.9892	1.9898	1.9870	2.0025
5	1.9973	1.9973	1.9980	1.9963	1.9995
6	2.0012	1.9993	1.9996	1.9992	2.0000
7	2.0098	1.9992	2.0000	1.9998	2.0000
8	1.9648	2.0001	2.0005	2.0000	2.0000
9	2.1121	1.9877	2.0006	2.0001	2.0000
10	1.9121	2.0128	1.9975	2.0003	2.0001

Table 3.3: Comparison of errors.

Problem	**HWS**	**Bica[17]**
1	$1.7831E-07$ at $J=6$	$6.9097E-07$ at $h=\frac{\pi}{400}$
1	$6.9708E-10$ at $J=10$	$6.9100E-09$ at $h=\frac{\pi}{4000}$
2	$9.8905E-09$ at $J=9$	$1.2770E-08$ at $h=\frac{1}{1000}$

Table 3.4: Comparison between approximate and analytic solution at J=6.

	Problem 1		
t	y_{exact}	y_{approx}	$\lvert y_{exact}-y_{approx}\rvert$
0.1	1.1108	1.1108	$4.9295E-08$
0.2	1.2270	1.2270	$9.3465E-08$
0.3	1.3415	1.3415	$1.2867E-07$
0.4	1.4725	1.4725	$1.5786E-07$
0.5	1.6098	1.6098	$1.7498E-07$
0.6	1.7524	1.7524	$1.7727E-07$
0.7	1.8995	1.8995	$1.6214E-07$
0.8	2.0385	2.0385	$1.3054E-07$
0.9	2.1919	2.1919	$7.5335E-08$

Table 3.5: Comparison between approximate and analytic solution at J=6.

	Problem 2		
t	y_{exact}	y_{approx}	$\lvert y_{exact}-y_{approx}\rvert$
0.1	$9.4912E-02$	$9.4912E-02$	$2.8670E-07$
0.2	$1.6832E-01$	$1.6832E-01$	$4.7186E-07$
0.3	$2.2265E-01$	$2.2265E-01$	$5.7505E-07$
0.4	$2.6907E-01$	$2.6907E-01$	$6.2395E-07$
0.5	$3.0444E-01$	$3.0444E-01$	$6.1674E-07$
0.6	$3.3048E-01$	$3.3048E-01$	$5.6142E-07$
0.7	$3.4864E-01$	$3.4864E-01$	$4.6471E-07$
0.8	$3.5953E-01$	$3.5953E-01$	$3.4350E-07$
0.9	$3.6601E-01$	$3.6601E-01$	$1.8183E-07$

Table 3.6: Comparison between approximate and analytic solution at J=6.

	Problem 3		
t	y_{exact}	y_{approx}	$\lvert y_{exact} - y_{approx}\rvert$
0.1	$8.9490E-01$	$8.9490E-01$	$3.0232E-07$
0.2	$7.9563E-01$	$7.9563E-01$	$4.9807E-07$
0.3	$7.0701E-01$	$7.0701E-01$	$6.0542E-07$
0.4	$6.1535E-01$	$6.1535E-01$	$6.5268E-07$
0.5	$5.2907E-01$	$5.2907E-01$	$6.3862E-07$
0.6	$4.4879E-01$	$4.4879E-01$	$5.7344E-07$
0.7	$3.7491E-01$	$3.7491E-01$	$4.6661E-07$
0.8	$3.1255E-01$	$3.1255E-01$	$3.3853E-07$
0.9	$2.5139E-01$	$2.5139E-01$	$1.7510E-07$

Table 3.7: Comparison between approximate and analytic solution at J=6.

	Problem 4		
t	y_{exact}	y_{approx}	$\lvert y_{exact} - y_{approx}\rvert$
0.1	$9.0459E-01$	$9.0459E-01$	$7.0007E-07$
0.2	$8.2848E-01$	$8.2848E-01$	$1.0092E-06$
0.3	$7.6877E-01$	$7.6877E-01$	$1.1088E-06$
0.4	$7.1309E-01$	$7.1309E-01$	$1.0937E-06$
0.5	$6.6494E-01$	$6.6493E-01$	$9.9756E-07$
0.6	$6.2287E-01$	$6.2287E-01$	$8.4864E-07$
0.7	$5.8581E-01$	$5.8581E-01$	$6.6355E-07$
0.8	$5.5531E-01$	$5.5531E-01$	$4.6913E-07$
0.9	$5.2567E-01$	$5.2567E-01$	$2.3844E-07$

Table 3.8: Comparison between approximate and analytic solution at J=6.

	Problem 5		
t	y_{exact}	y_{approx}	$\lvert y_{exact} - y_{approx}\rvert$
0.1	1.1066	1.1066	$7.4140E-07$
0.2	1.2159	1.2159	$1.3630E-06$
0.3	1.3280	1.3280	$1.8446E-06$
0.4	1.4675	1.4675	$2.2490E-06$
0.5	1.6319	1.6319	$2.5062E-06$
0.6	1.8274	1.8274	$2.5806E-06$
0.7	2.0605	2.0605	$2.4239E-06$
0.8	2.3143	2.3143	$2.0191E-06$
0.9	2.6371	2.6371	$1.2202E-06$

3.1 demonstrate that error decreases with increase in resolution(J). In Table 3.2, we have calculated the rate of convergence by using the formula

$$R_c = \frac{\log(\frac{E_{J-1}}{E_J})}{\log(2)},$$

where E_J is the maximum absolute errors at resolution J. Also, from Table 3.2 one can observe that the experimental convergence rates in each problem tend to be 2, as described in [67]. The approximate and analytical solution curves of each problem are plotted in figures 3.1-3.5. We observed that both curves coincide, and a comparison drawn in Table 3.3 shows the method is more accurate and efficient.

3.6 Summary

This chapter[1] introduced the Haar wavelet-based numerical method to solve Dirichlet boundary value problems of proportional delay nature. The method is tested on benchmark problems and the results are compared with the existing method [17]. The accuracy and convergence rate of the technique have been validated by solving both linear and nonlinear problems. The MATLAB package is utilized to perform computer simulations, and the solutions obtained were compared with the analytical solutions.

[1]The content of this chapter is published in **International Journal of Nonlinear Analysis and Applications.**(ESCI, Scopus Indexed).

Chapter 4

Haar wavelet series method for solving simultaneous proportional delay differential equations

4.1 Introduction

In this study, we apply the Haar wavelet series method (HWSM) to solve the following simultaneous proportional delay differential equations:

$$
\begin{aligned}
&y_1'(t) = \Omega_1(t, y_1(t), y_2(t), \ldots, y_n(t), y_1(q_1 t), y_2(q_2 t), \ldots, y_n(q_\lambda t))\\
&y_2'(t) = \Omega_2(t, y_1(t), y_2(t), \ldots, y_n(t), y_1(q_1 t), y_2(q_2 t), \ldots, y_n(q_\lambda t))\\
&\vdots\\
&y_n'(t) = \Omega_n(t, y_1(t), y_2(t), \ldots, y_n(t), y_1(q_1 t), y_2(q_2 t), \ldots, y_n(q_\lambda t))\\
&y_\sigma(0) = y_{\sigma 0}, \quad \sigma = 1, 2, \ldots, n,
\end{aligned}
\tag{4.1.1}
$$

where Ω_σ's are analytical functions, and q_σ'$s \in (0,1), \sigma = 1, 2, \ldots, n$. These equations have been widely noticed in several models, such as biological models, aerospace systems, control theory, disease spread models, tumour growth models, etc. Therefore, this study is an important contribution in the field of applied mathematical modelling and numerical analysis. This method utilizes delayed Haar wavelet series and collocation points to transform the simultaneous proportional delay differential equations into a system of algebraic matrix equations with unknown coefficient matrices. The values of these unknown row matrices can be obtained by using a suitable solver. With these coefficients, the solution in terms of the collocated Haar wavelet series is obtained.

4.2 Description of Method

In this section, we apply the Haar wavelet series method for solving simultaneous proportional delay differential equation (4.1.1).

Let

$$\begin{aligned} y_1'(t) &= \sum_{i=1}^{2^{J+1}} a_i \mathfrak{h}_i(t), \\ y_2'(t) &= \sum_{i=1}^{2^{J+1}} b_i \mathfrak{h}_i(t), \\ &\vdots \\ y_n'(t) &= \sum_{i=1}^{2^{J+1}} c_i \mathfrak{h}_i(t), \end{aligned} \tag{4.2.1}$$

where a_i's, b_i'$s \ldots c_i$'s are Haar wavelet coefficients.

Now, by integrating equation (4.2.1), we have

$$\begin{aligned} y_1(t) &= \sum_{i=1}^{2^{J+1}} a_i I_1 \mathfrak{h}_i(t) + y_1(0), \\ y_2(t) &= \sum_{i=1}^{2^{J+1}} b_i I_1 \mathfrak{h}_i(t) + y_2(0), \\ &\vdots \\ y_n(t) &= \sum_{i=1}^{2^{J+1}} c_i I_1 \mathfrak{h}_i(t) + y_n(0). \end{aligned} \tag{4.2.2}$$

Also,

$$
\begin{aligned}
y_1(q_1t) &= \sum_{i=1}^{2^{J+1}} a_i I_1\mathfrak{h}_i(q_1t) + y_1(0), \\
y_2(q_2t) &= \sum_{i=1}^{2^{J+1}} b_i I_1\mathfrak{h}_i(q_2t) + y_2(0), \\
&\vdots \\
y_n(q_nt) &= \sum_{i=1}^{2^{J+1}} c_i I_1\mathfrak{h}_i(q_nt) + y_n(0),
\end{aligned}
\tag{4.2.3}
$$

where $y_\sigma(0)$'s are given initial conditions and q_σ's $\in (0,1), \sigma = 1, 2, \ldots, n$.

Now, upon plugging equations (4.2.1), (4.2.2) and (4.2.3) in the governing equation (4.1.1) along with the collocation points we get a system of an algebraic equations. After solving the system we obtain the unknowns Haar wavelet coefficients and finally using these coefficients in equation (4.2.2) approximate solution at collocation points can be obtained.

4.3 Algorithm

Input: Level of resolution J.

Step-1: Set collocation points $t_l = \frac{(l-0.5)}{2^{J+1}}, \quad l = 1, 2, 3 \ldots 2^{J+1}$.

Step-2: Compute Haar wavelets $\mathfrak{h}_i$ and integral of Haar wavelets $I_1\mathfrak{h}_i$ from equations (2.2.3) and (2.2.9), respectively.

Step-3: Assume $y'_\sigma(t) = \sum_{i=1}^{2^{J+1}} (a_i)_\sigma \mathfrak{h}_i(t)$ where $\sigma = 1, 2, \ldots n$ and i is wavelet index.

Step-4: Integration of Step-3 within the limits 0 to t yields,

$$y_\sigma(t) = \sum_{i=1}^{2^{J+1}} (a_i)_\sigma I_1\mathfrak{h}_i(t) + y_\sigma(0), \quad \sigma = 1, 2, \ldots, n.$$

Step-5: Upon using the expressions for $y'_\sigma(t)$'s, $y_\sigma(t)$'s , ..., $y_\sigma(q_\sigma t)$'s along with collocation points in equation (4.1.1), we get an algebraic system in unknown vectors $(a_i)_1, (a_i)_2, \ldots, (a_i)_n$.

Step-6: Solve the algebraic system for the unknown vectors $(a_i)_1, (a_i)_2, \ldots, (a_i)_n$.

Step-7: Utilize the values of the vectors $(a_i)_1, (a_i)_2, \ldots, (a_i)_n$ in Step-4 to obtained the unknown functions $y_1(t), y_2(t), \ldots, y_n(t)$.

Output: Approximate solution $y_1(t_l), y_2(t_l), \ldots, y_n(t_l)$ is obtained.

4.4 Implementation of Method on Test Problems

The efficiency and numerical validation of the method is demonstrated with the help of following test problems.

Problem 1: Consider the system

$$\begin{cases} y'_1(t) = y_1(t/2) + y_1(t) - y_2(t) + exp(-t) - exp(t/2) \\ y'_2(t) = -y_1(t/2) - y_1(t) - y_2(t) + exp(t) + exp(t/2) \\ with \;\; y_1(0) = y_2(0) = 1, \quad 0 \le t \le 1. \end{cases} \tag{4.4.1}$$

The system has exact solution $y_1(t) = \exp(t), y_2(t) = \exp(-t)$.

We have solved the above system of differential equation using the Haar wavelet series method. The maximum absolute error (MAE) at different levels of resolution is given in the Table 4.1. The Table 4.1 shows that the error decreases from $O(10-2)$ to $O(10-7)$, ensuring the method's convergence. Also, Fig 4.1 shows that approximate and exact curves match closely.

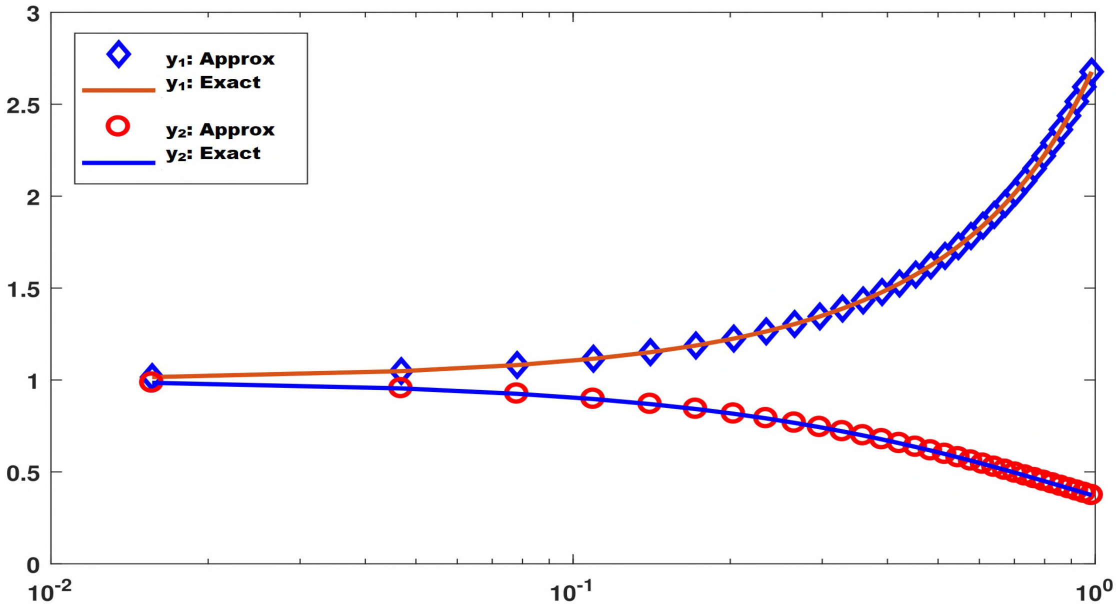

FIGURE 4.1: Exact and approximate solution of Problem 1.

TABLE 4.1: MAEs at different levels of J.

	Problem 1		**Problem 2**	
J	**MAE:**$y_1(t)$	**MAE:**$y_2(t)$	**MAE:**$y_1(t)$	**MAE:**$y_2(t)$
2.0	$1.3000E-02$	$5.4000E-03$	$7.3000E-03$	$7.3000E-03$
3.0	$3.4187E-03$	$1.4267E-03$	$1.9007E-03$	$1.9007E-03$
4.0	$8.7870E-04$	$3.6790E-04$	$4.8190E-04$	$4.8190E-04$
5.0	$2.2290E-04$	$9.3500E-05$	$1.2170E-04$	$1.2170E-04$
6.0	$5.6150E-05$	$2.3570E-05$	$3.0580E-05$	$3.0570E-05$
7.0	$1.4090E-05$	$5.9200E-06$	$7.6620E-06$	$7.6620E-06$
8.0	$3.5290E-06$	$1.4820E-06$	$1.9180E-06$	$1.9180E-06$
9.0	$8.8310E-07$	$3.7090E-07$	$4.7980E-07$	$4.7980E-07$

Problem 2: Consider the system

$$\begin{cases} y_1'(t) = \exp(t/2)y_2(t/2) + y_1(t) \\ y_2'(t) = \exp(t/2)y_1(t/2) + y_2(t) \\ with \quad y_1(0) = y_2(0) = 1, \quad 0 \leq t \leq 1. \end{cases} \tag{4.4.2}$$

The system has exact solution $y_1(t) = \exp(t), y_2(t) = \exp(t)$.

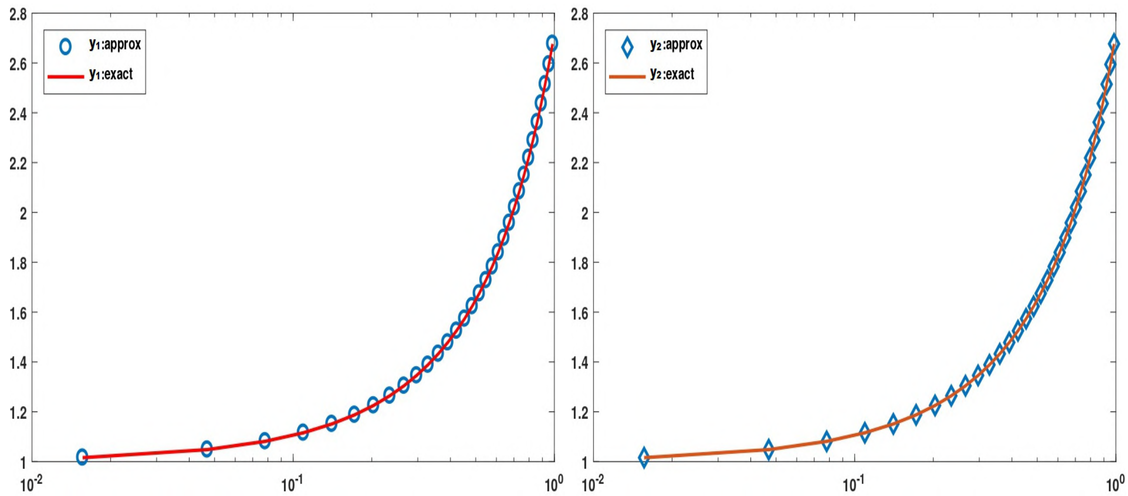

FIGURE 4.2: Exact and approximate solution of Problem 2.

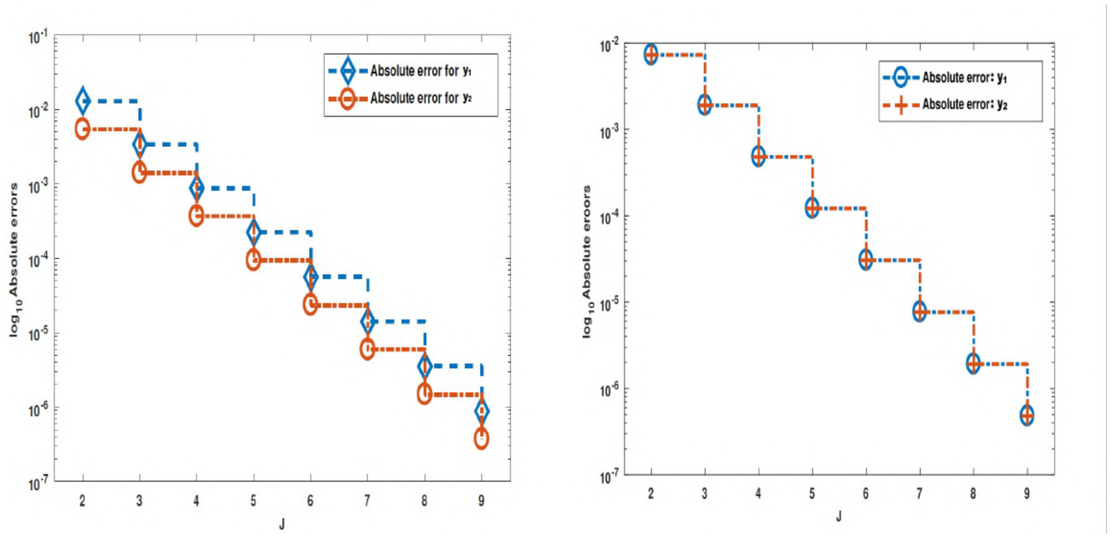

(Problem 1) (Problem 2)

FIGURE 4.3: Absolute error vs J.

The approximate solution of the aforementioned problem obtained using the Haar wavelet series approach is satisfactory. Computer simulation is carried out and the numerical results are presented in Table 4.1. The exact and approximate solution of Problem 2 is plotted in Fig 4.2 for J=4. Also, the convergence of the method can be observed in Fig 4.3.

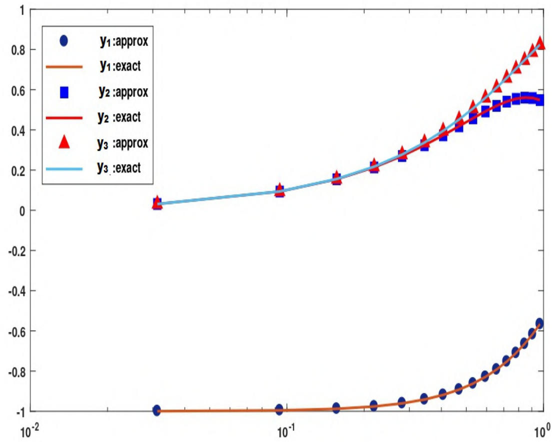

FIGURE 4.4: Exact and approximate solution of Problem 3.

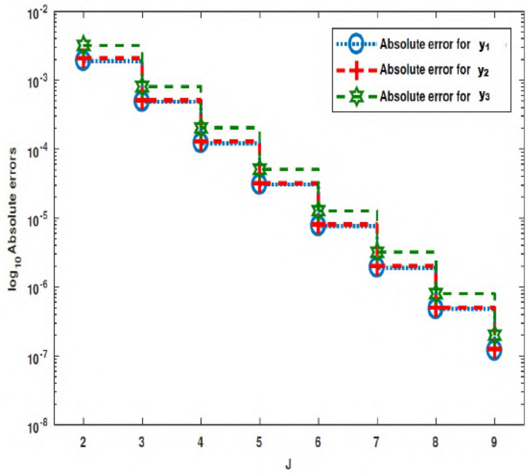

FIGURE 4.5: Absolute error vs J (Problem 3).

Problem 3: Consider the following non-linear proportional delay system:

$$\begin{cases} y_1'(t) = 2y_2(t/2) + y_3(t) + tcos(t/2) \\ y_2'(t) = -2y_3^2(t) + 1 - tsin(t) \\ y_3'(t) = y_2(t) - y_1(t) - tcos(t) \\ with \;\; y_1(0) = -1, y_2(0) = y_3(0) = 0, \quad 0 \leq t \leq 1. \end{cases} \tag{4.4.3}$$

Exact solution is $y_1(t) = -cos(t), y_2(t) = tcos(t), y_1, (t) = sin(t)$. In this case we have solved a non-linear system with three equations using the Haar wavelet series method. The exact and approximate solution for Problem 3 is plotted in Fig. 4.4. It is observed that both curves match closely. Absolute errors at different levels of resolution are depicted in Table 4.2 which shows that the computed numerical solution is satisfactory. Also, it is evident from Fig.4.5 that the accuracy of the solution is directly proportional to the value of J. Furthermore, in each case, the error was reduced from $O(10-2)$ to $O(10-7)$.

Table 4.2: MAEs at different levels of J (Problem 3).

J	**MAE:**$y_1(t)$	**MAE:**$y_2(t)$	**MAE:**$y_3(t)$
2.0	$1.9167E-03$	$2.0504E-03$	$3.1668E-03$
3.0	$4.8600E-04$	$5.1360E-04$	$8.0760E-04$
4.0	$1.2190E-04$	$1.2850E-04$	$2.0340E-04$
5.0	$3.0510E-05$	$3.2120E-05$	$5.1000E-05$
6.0	$7.6300E-06$	$8.0300E-06$	$1.2770E-05$
7.0	$1.9070E-06$	$2.0070E-06$	$3.1930E-06$
8.0	$4.7680E-07$	$5.0190E-07$	$7.9860E-07$
9.0	$1.1920E-07$	$1.2550E-07$	$1.9970E-07$

4.5 Summary

This chapter[1] discussed the Haar wavelet series method for linear and nonlinear simultaneous proportional delay differential equations with two and three dependent variables. Three illustrations at different counts of collocation points are solved to test the consistency, correctness, and efficacy of the method. The numerical results demonstrated in figures and tables illustrate the expected rate of convergence.

[1]The content of this chapter is accepted for publication In: **Advances in Mathematical Modelling, Applied Analysis and Computation**. Proceedings of ICMMAAC 2021. Lecture Notes in Networks and Systems, Springer, Singapore. (Scopus Indexed)

Chapter 5

A modified Haar wavelet series method to solve higher-order multi-pantograph equations arising in electrodynamics

5.1 Pantograph Equations

The functional-differential with proportional delay is known as the pantograph equation or generalized pantograph equations. The name pantograph first appeared in 1851 and was a device used in the construction of the electric locomotive. The mathematical model of the pantograph was first developed by Ockendon and Tyler [79]. The Pantograph equation is one of the most distinguished delay differential equations and has been an interest of many researchers [19, 35, 36]. The pantograph differential equations are encountered in studies of population dynamic models, quantum theory, control theory, cell growth models, disease spread models, and astrophysics [35]. These equations also have several industrial applications and play a central role in the mathematical modelling of the train's overhead current collection system [79]. The continuous electricity supply between the catenary and the train's motor is maintained by a device called a z-shape pantograph. The z-shape pantograph (also known as half pantograph) resembled the pantograph device for copying, writing, and drawing. It has a spring mechanism that pushes the contact shoe up against the wire to draw the electricity required to power the train.

Most of these equations can not be solvable exactly. Therefore, a numerical technique is required to obtain their approximate solutions. Variational iteration method [25], One leg-θ method [106], Two-stage R-K method [108], Reproducing kernel Hilbert space method (RKHSM) [64], Differential transform method [53], Adomain decomposition method [20], Perturbed iteration method [10] are some well known numerical techniques to solve such types of differential equations. Recently, in [8] time-invariant and time-varying first-order delay differential equations have been solved using the Haar wavelet collocation method. Some other collocation methods are also developed using Chebyshev Polynomials, Hermite Polynomials, and Bernoulli Polynomials. For details, readers may refer to [63, 103, 113] respectively.

Chen and Hsiao [24] gave an idea of utilizing Haar operational matrix of integration for solving differential equations. In the existing literature, the development and application of the Haar wavelet collocation method (HWCM) for solving differential equations are based on the method given by Chen and Hsiao. Later this idea has been extended to solve a wide range of problems [60]. Marzban and Razzaghi [71] adapted the rationalized Haar wavelet approach for solving nonlinear optimal control problems. The HWCM is also a efficient tool in structural mechanics, Hariharan [46] applied the Haar wavelet-based technique for solving the finite length beam equation. Lepik [60] discussed buckling of elastic beams using the Haar wavelet method. In [84] Patra and Saha obtained the solution of stiff point kinetics equations using wavelet operational method based on the Haar wavelet. In the recent past, the Chen-Hsiao technique has been extended to solve delay differential equations.

Aziz and Amin[8] investigated the approximate solution of delay differential as well as partial delay differential equations. Raza et al. [89] transformed the delay term using Taylor series expansion and then applied the Haar wavelet collocation method to solve singularly perturbed differential-difference equations and singularly perturbed convection delayed dominated diffusion equations. Abdullah and Rafiq [2] combined the backward Euler method and the HWCM to obtain the approximate solution of the Chen-Lee-Liu equation.

Here we have applied a modified Haar wavelet series method (MHWSM) instead of the conventional Haar wavelet collocation method. Instead of the highest (n^{th}) order derivative, we expanded the$(n+1)^{th}$ order derivative involved in the differential equations in terms of the Haar series. The MHWSM produced a smoother solution than the Haar wavelet collocation method, therefore a significant decrease in absolute error is expected.

5.2 Construction of Method

Let us assume a n^{th} order pantograph equation of the form

$$y^n(t) = \varphi\left(g(t), y(q_0 t), y^1(q_1 t), y^2(q_2 t)\dots y^n(q_n t)\right), \quad \forall\ t \in [t_0, t_f] \tag{5.2.1}$$

$$\text{with} \quad y^\eta(t_0) = y_0^\eta,$$

where $\varphi : [t_0, t_f] \times \underbrace{R \times R \cdots \times R}_{\text{(n+1)-times}} \mapsto R$ is a differentiable function, $g(t)$ is continuous on $[t_0, t_f]$ and $q_0, q_1 \dots q_n$ are real constants lies in $(0, 1]$. Also, $y^1, y^2 \dots y^n$ denotes the first, second and n^{th} order derivatives, respectively and y_0^η are initial value conditions $\eta = 0, 1, 2 \dots n-1$. Put $t = t_0$ in equation (5.2.1) for $y^n(t_0)$.

In order to solve equation (5.2.1) we have established the following algorithm using Haar wavelet series equation (2.2.3). Let us suppose $y^{n+1}(t)$ be square integrable function. Therefore, we can write

$$y^{n+1}(t) = \sum_{i=1}^{2M} a_i \mathfrak{h}_i(t). \tag{5.2.2}$$

Integrating equation (5.2.2) r times with respect to t, we have the following relation

$$y^{n+1-r}(t) = \sum_{i=1}^{2M} a_i I_r \mathfrak{h}_i(t) + \sum_{\eta=n+1-r}^{n} \frac{y^{\eta}(t_0)(t)^{\eta-(n+1-r)}}{(\eta-(n+1-r))!}. \tag{5.2.3}$$

Taking $r = n+1$ in relation equation (5.2.3), we have $y(t)$ as

$$y(t) = \sum_{i=1}^{2M} a_i I_{n+1} \mathfrak{h}_i(t) + \sum_{\eta=0}^{n} \frac{y^{\eta}(t_0)(t)^{\eta}}{(\eta)!}. \tag{5.2.4}$$

Also,

$$y(q_0 t) = \sum_{i=1}^{2M} a_i I_{n+1} \mathfrak{h}_i(q_0 t) + \sum_{\eta=0}^{n} \frac{y^{\eta}(t_0)(q_0 t)^{\eta}}{(\eta)!}. \tag{5.2.5}$$

Similarly,

$$y^{1}(q_1 t) = \sum_{i=1}^{2M} a_i I_{n} \mathfrak{h}_i(q_1 t) + \sum_{\eta=1}^{n} \frac{y^{\eta}(t_0)(q_1 t)^{\eta-1}}{(\eta-1)!}, \tag{5.2.6}$$

$$\vdots$$

$$y^{n}(q_n t) = \sum_{i=1}^{2M} a_i I_{1} \mathfrak{h}_i(q_n t) + y^{n}(t_0). \tag{5.2.7}$$

Now, substituting equations (5.2.3 - 5.2.7) in equation (5.2.1), we get

$$\sum_{i=1}^{2M} a_i I_1 \mathfrak{h}_i(t) + y^n(t_0) = \varphi\Bigg(g(t), \sum_{i=1}^{2M} a_i I_{n+1}\mathfrak{h}_i(q_0 t) + \sum_{\eta=0}^{n} \frac{y^\eta(t_0)(q_0 t)^\eta}{(\eta)!}, \sum_{i=1}^{2M} a_i I_n \mathfrak{h}_i(q_1 t) + \sum_{\eta=1}^{n} \frac{y^\eta(0)(q_1 t)^{\eta-1}}{(\eta-1)!}, \ldots, \sum_{i=1}^{2M} a_i I_1 \mathfrak{h}_i(q_n t) + y^n(0)\Bigg). \tag{5.2.8}$$

Moreover, utilizing collocation points $t_l = \frac{l-0.5}{2M}, l = 1, 2, \ldots 2M$ in equation (5.2.8), we obtain

$$\sum_{i=1}^{2M} a_i I_1 \mathfrak{h}_i(t_l) + y^n(t_0) = \varphi\Bigg[g(t_l), \sum_{i=1}^{2M} a_i I_{n+1}\mathfrak{h}_i(q_0 t_l) + \sum_{\eta=0}^{n} \frac{y^\eta(t_0)(q_0 t_l)^\eta}{(\eta)!}, \sum_{i=1}^{2M} a_i I_n \mathfrak{h}_i(q_1 t_l) + \sum_{\eta=1}^{n} \frac{y^\eta(t_0)(q_1 t_l)^{\eta-1}}{(\eta-1)!}, \ldots, \sum_{i=1}^{2M} a_i I_1 \mathfrak{h}_i(q_n) + y^n(t_0)\Bigg]. \tag{5.2.9}$$

Now, one can determine the coefficients $a_i^{'}s$ by using any iterative techniques like Newton's method or Broyden's method. Finally, the solution is obtained by substituting $a_i^{'}s$ in equation (5.2.4).

5.3 Algorithm

Input: level of resolution J.

Step-1: Set collocation points $t_l = \frac{(l-0.5)}{2M}, \quad l = 1, 2, 3 \ldots 2M, M = 2^J$.

Step-2: Compute Haar wavelets $\mathfrak{h}_i(t)$ and integral of Haar wavelets $I_n\mathfrak{h}_i(t)$ from equations (1.2.1) and (1.2.2), respectively.

Step-3: Construct the system (5.2.9) by using Eqs. (5.2.3-5.2.7) and collocation points t_l sets in step 1.

Step-4: Apply Newton's method to the system (5.2.9) for unknowns $a_i^{'}s$.

Step-5: Put $a_i^{'}s$ in Eq. (5.2.4).

Output: Approximate solution $y_h(t_l)$.

5.4 Numerical Experiment

To check the applicability and efficiency of our technique, we have solved second-order linear and non-linear differential equations, integro differential equations, a third-order, and a fourth-order differential equation of pantograph nature. All computer simulations are carried out in MATLAB and are reported in tables and figures.

Problem 1. Consider the pantograph equation

$$\begin{aligned} &y^{''}(t) = \tfrac{3}{4}y(t) + y\left(\tfrac{t}{2}\right) + y^{'}\left(\tfrac{t}{2}\right) + \tfrac{1}{2}y^{''}\left(\tfrac{t}{2}\right) - t^2 - t + 1,\ t \in [0,1], \\ &y(0) = 0,\ y^{'}(0) = 0. \end{aligned} \tag{5.4.1}$$

The exact solution of equation (5.4.1) from [64] is $y_e = t^2$.

The present technique is successfully applied on equation (5.4.1) and the result is compared with some existing methods [25, 64, 106, 107, 108]. Wavelet coefficients are calculated using the classical Newton's method by choosing an appropriate initial guess. We observed that the maximum absolute error is zero for $J = 2, 3, 4, \ldots, 9$. Also, it is evident from Table 5.1 and Table 5.2 that our method has easy applicability and produces better results. Figure 5.1 shows that both exact and approximate solutions coincide visually.

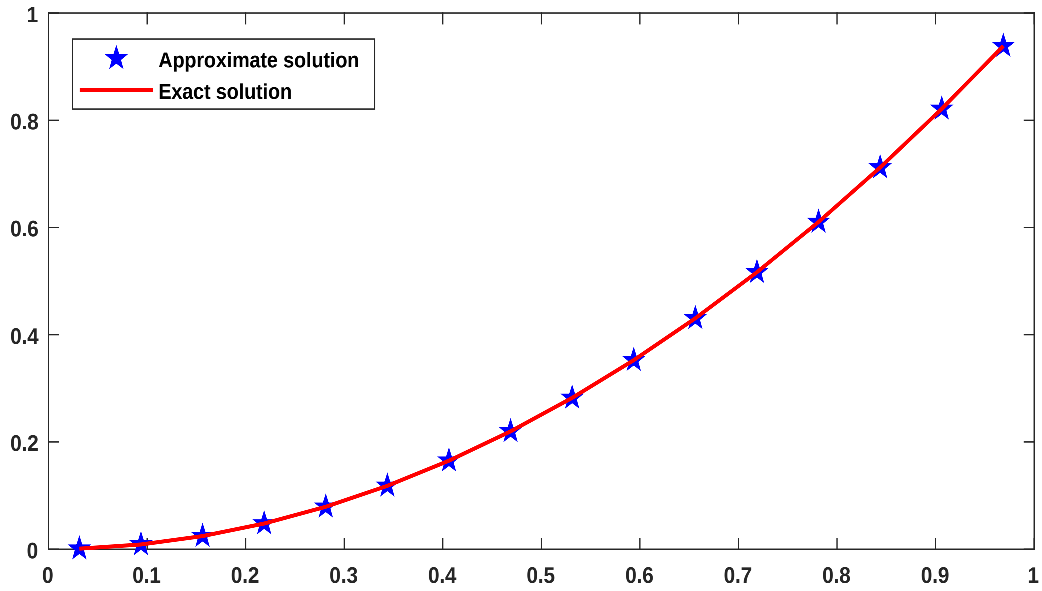

FIGURE 5.1: Comparison of exact and approximate solution (Problem 1).

TABLE 5.1: Error comparison with existing method (Problem 1).

Our method $J=2$	**Two-stage**[108] **order-one RKM**	**One-leg** θ**-method** $(\theta=0.8)$[106]	**VIM**[25] $n=5$	**VIM**[25] $n=5$	**RKHSM** $n=100$[64]
0	$5.34E-03$	$2.81E-01$	$1.11E-02$	$5.55E-03$	$4.92E-04$

Problem 2. In this Example we consider a second order nonlinear pantograph equation

$$y''(t) = -y(t) + 5\left(y\left(\tfrac{t}{2}\right)\right)^2,\ t \in [0,1], \qquad y(0)=1,\ y'(0)=-2. \tag{5.4.2}$$

Approximate solution of equation (5.4.2) is obtained with the present algorithm. Our solution is compared with exact solution $y_e = \exp(-2t)$ in Table 5.3 and Figure 5.2. We have observed that maximum absolute errors are decreased from order of 10^{-3} for $J=2$ to order of 10^{-7} for $J=9$.

Table 5.2: Comparison of exact and approximate solution (Problem 1).

$t(=1/32)$	**Present method**	**Exact solution**
1	0.00097656250	0.00097656250
3	0.00878906250	0.00878906250
5	0.02441406250	0.02441406250
7	0.04785156250	0.04785156250
9	0.07910156250	0.07910156250
11	0.11816406250	0.11816406250
13	0.16503906250	0.16503906250
15	0.21972656250	0.21972656250
17	0.28222656250	0.28222656250
19	0.35253906250	0.35253906250
21	0.43066406250	0.43066406250
23	0.51660156250	0.51660156250
25	0.61035156250	0.61035156250
27	0.71191406250	0.71191406250
29	0.82128906250	0.82128906250
31	0.93847656250	0.93847656250

Table 5.3: MAEs at different levels of J (Problem 2).

J	**max** $\lvert y_{exact} - y_{approx}\rvert$
3	$7.4217E-04$
4	$1.9187E-04$
5	$4.8675E-05$
6	$1.2252E-05$
7	$3.0729E-06$
8	$7.6943E-07$
9	$1.9248E-07$

Table 5.4: MAEs at different levels of J (Problem 4).

J	**max** $\lvert y_{exact} - y_{approx}\rvert$
3	$8.2836E-04$
4	$2.1882E-04$
5	$5.6115E-05$
6	$1.4201E-05$
7	$3.5715E-06$
8	$8.9555E-07$
9	$2.2414E-07$

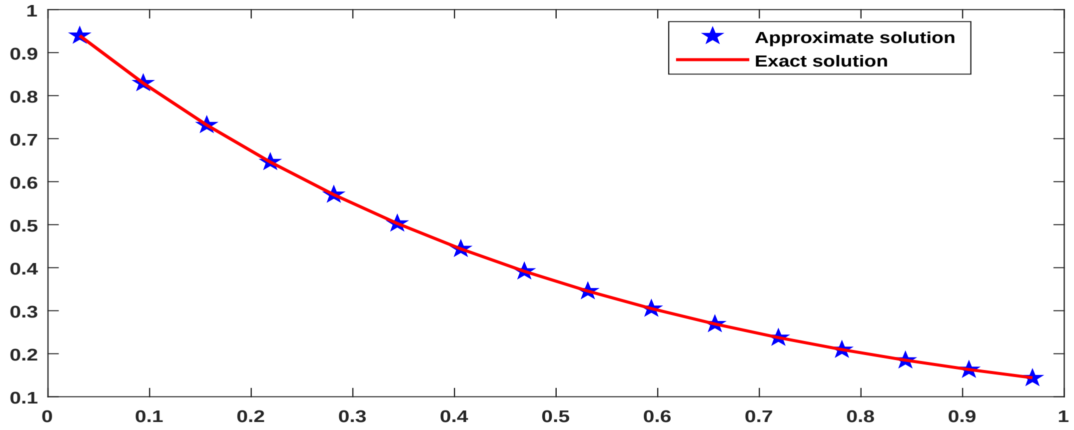

FIGURE 5.2: Comparison of exact and approximate solution (Problem 2).

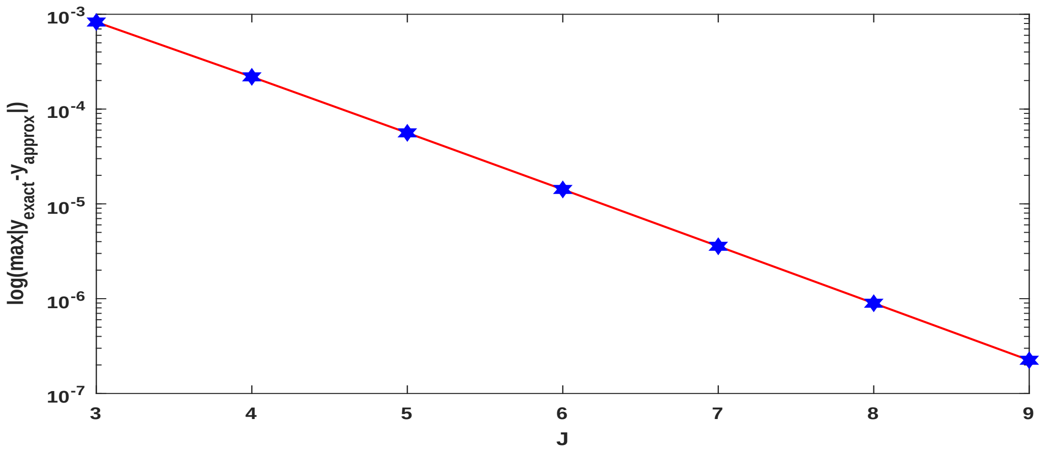

FIGURE 5.3: Maximum absolute errors vs J (Problem 2).

Problem 3. Let us consider the following second order pantograph type initial value problem mention in [64],

$$y^{''}(t) = y^{'}\left(\frac{t}{2}\right) - \frac{t}{2}y^{''}\left(\frac{t}{2}\right) + 2,\ t \in [0,1], \tag{5.4.3}$$

$$y(0) = 1,\ y^{'}(0) = 0.$$

We have solve this example using present method. The approximate function to be sought is $y_h = \sum_{i=1}^{2M} a_i * I_3\mathfrak{h}_i(t) + t^2 + 1$. A computer simulation is carried out and it is observed that the maximum absolute error is zero for $J = 2, 3, \ldots, 9$. A comparison

TABLE 5.5: Comparison of exact and approximate solution (Problem 3).

$t(= 1/16)$	**Present method**	**Exact solution**
1	1.003906250	1.003906250
3	1.035156250	1.035156250
5	1.097656250	1.097656250
7	1.191406250	1.191406250
9	1.316406250	1.316406250
11	1.472656250	1.472656250
13	1.660156250	1.660156250
15	1.878906250	1.878906250

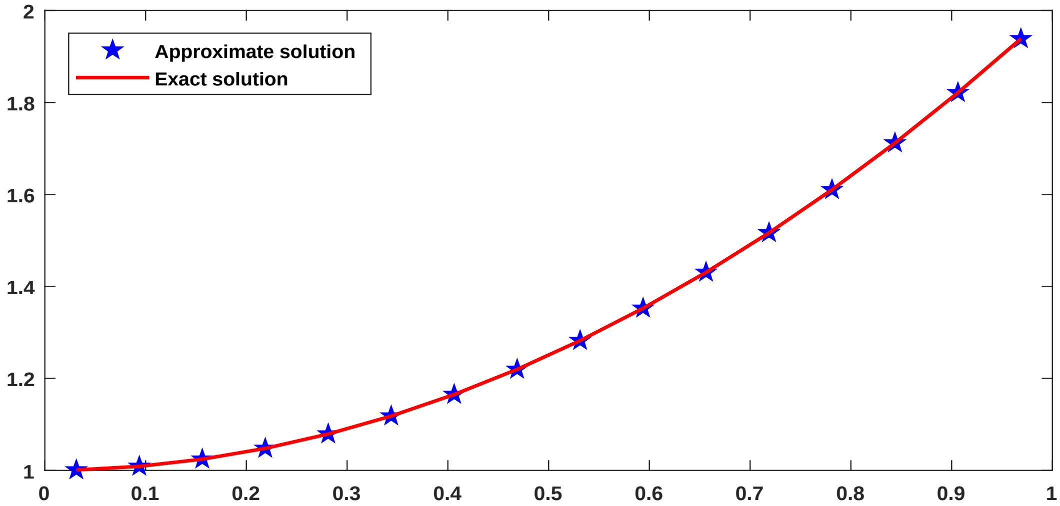

FIGURE 5.4: Comparison of approximate and exact solution (Problem 3).

between the approximate solution and the exact solution is demonstrated in Table 5.5 and Figure 5.4, which show that both solutions coincide.

Problem 4. We consider a nonlinear integro-differential equation with proportional delay in kernal

$$y'(t) + \left(\frac{t}{2} - 2\right) y(t) - 2 \int_0^t \left(y\left(\frac{s}{2}\right)\right)^2 ds = 1, \;\; t \in [0, 1], \qquad (5.4.4)$$

$$y(0) = 0.$$

Table 5.6: Comparison of exact and approximate solution (Problem 4).

$t(=1/32)$	**Present method**	**Exact solution**	$\lvert y_{exact} - y_{approx}\rvert$
1	0.0322421468	0.0322419814	$0.1653E-6$
3	0.1029618079	0.1029642319	$0.2423E-5$
5	0.1826661951	0.1826747572	$0.8562E-5$
7	0.2722202080	0.2722387735	$0.1856E-4$
9	0.3725622277	0.3725957133	$0.3348E-4$
11	0.4847113430	0.4847651995	$0.5385E-4$
13	0.6097726143	0.6098534812	$0.8086E-4$
15	0.7489450753	0.7490603671	$0.1152E-3$
17	0.9035281845	0.9036866916	$0.1585E-3$
19	1.0749307939	1.0751423553	$0.2115E-3$
21	1.2646789302	1.2649549829	$0.2760E-3$
23	1.4744259044	1.4747792434	$0.3533E-3$
25	1.7059615777	1.7064068834	$0.4453E-3$
27	1.9612238562	1.9617775258	$0.5536E-3$
29	2.2423096473	2.2429902915	$0.6806E-3$
31	2.5514879480	2.5523163047	$0.8283E-3$

Equation (5.4.4) can be reduced to following second order nonlinear pantograph equation

$$\begin{aligned} &y''(t) + \left(\tfrac{t}{2} - 2\right) y'(t) + \tfrac{1}{2} y(t) - 2\left(y\left(\tfrac{t}{2}\right)\right)^2 = 1,\ t \in [0,1], \\ &y(0) = 0,\ y'(0) = 1. \end{aligned} \tag{5.4.5}$$

Now we have applied the present algorithm to equation (5.4.5) and obtained its approximate solution. The exact solution $y_e = t\exp(t)$, is compared to the approximate solution and results are shown in Table 5.4 and Table 5.6. We have observed that maximum absolute errors are decreased from order of 10^{-4} for $J = 3$ to order of 10^{-7} for $J = 9$. We have verified in Figure 5.5 that both solutions visually coincide.

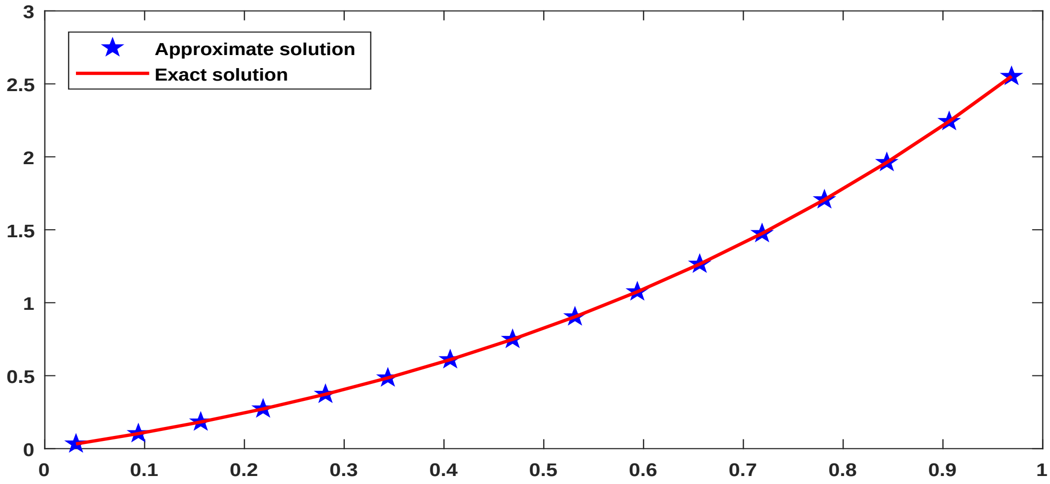

FIGURE 5.5: Comparison of exact and approximate solution (Problem 4).

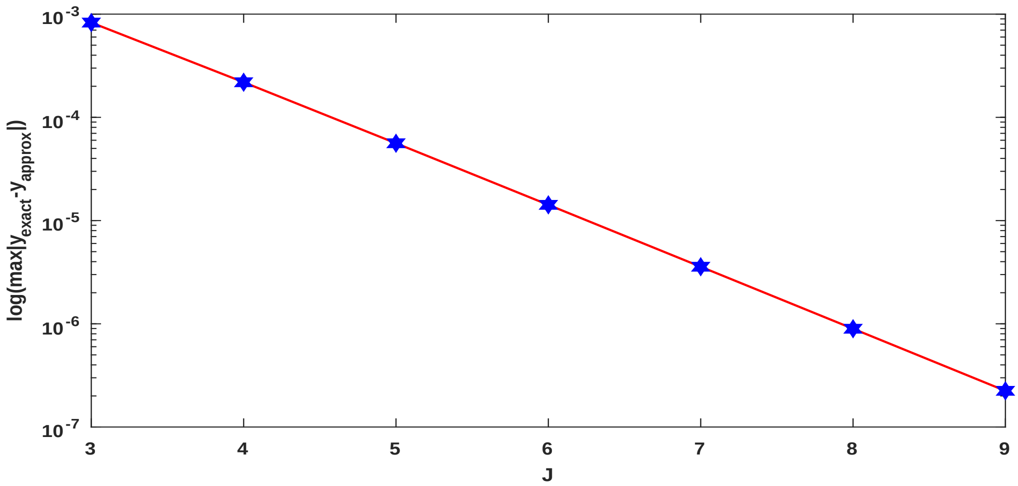

FIGURE 5.6: Absolute errors vs J (Problem 4).

TABLE 5.7: Error comparison with existing method (Problem 5).

Our method $J = 2$	**Two-stage[108] order-one RKM**	**VIM[25]** $n = 4$	**VIM[25]** $n = 5$	**VIM[25]** $n = 6$
$6.92214E - 10$	$7.34E - 02$	$3.21E - 04$	$4.01E - 05$	$1.26E - 06$

Problem 5. In this Example we consider a third-order pantograph equation

$$y'''(t) = y(t) + y'\left(\frac{t}{2}\right) + y''\left(\frac{t}{3}\right) + \frac{1}{2}y'''\left(\frac{t}{4}\right) - t^4 - \frac{t^3}{2} - \frac{4}{3}t^2 + 21t, \ t \in [0, 1],$$
$$y(0) = y'(0) = y''(0) = 0. \tag{5.4.6}$$

TABLE 5.8: Comparison of exact and approximate solution (Problem 5).

$t(=\frac{1}{16})$	**Present method**	**Exact solution**	$\lvert y_{exact} - y_{approx} \rvert$
1	0.000015258789160	0.000015258789063	$0.00098E-10$
3	0.001235961921205	0.001235961914063	$0.07143E-10$
5	0.009536743166434	0.009536743164063	$0.02372E-10$
7	0.036636352518005	0.036636352539063	$0.21057E-10$
9	0.100112915165484	0.100112915039063	$1.26421E-10$
11	0.223403930795185	0.223403930664063	$1.31123E-10$
13	0.435806274199234	0.435806274414063	$2.14829E-10$
15	0.772476195596849	0.772476196289063	$6.92214E-10$

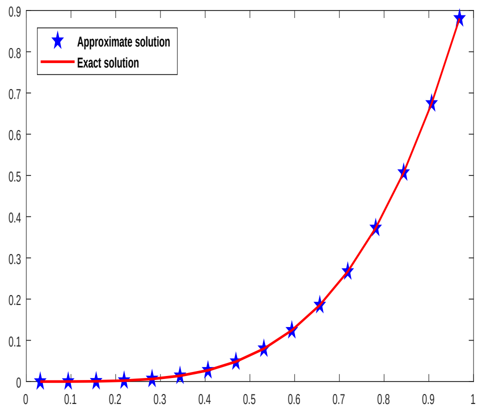

FIGURE 5.7: Comparison of exact and approximate solution (Problem 5).

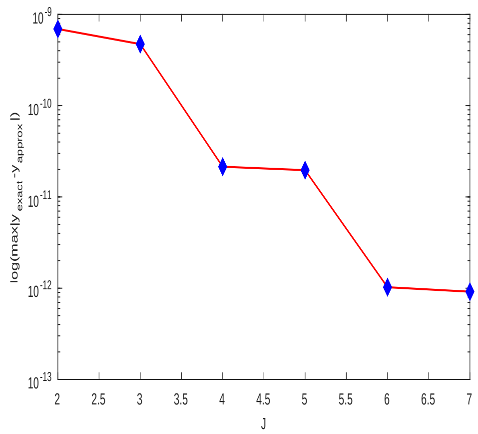

FIGURE 5.8: Maximum absolute errors vs J (Problem 5).

We have applied the present algorithm to equation (5.4.6). A comparison between approximate and exact solution $y_e = t^4$ demonstrated in Figure 5.7 and it shows that both solutions visually coincide. The wavelet coefficients are calculated using the classical Newton's method with an appropriate initial guess. In addition, we discovered that the maximum absolute error for $J = 2$ is $O(10)^{-10}$. From Tables 5.7, 5.8 and 5.9 we conclude that the present method is more efficient and produces much better results.

Problem 6. Now we consider a fourth order nonlinear multi-pantograph equation

TABLE 5.9: MAEs at different levels of J (Problem 5).

J	$\max\ \lvert y_{exact} - y_{approx}\rvert$
2	$6.9221E - 10$
3	$4.7252E - 10$
4	$2.1423E - 11$
5	$1.9649E - 11$
6	$1.0246E - 12$
7	$9.1538E - 13$

TABLE 5.10: MAEs at different levels of J (Problem 6).

J	$\max\lvert y_{exact} - y_{approx}\rvert$
4	$4.3588E - 05$
5	$1.9020E - 05$
6	$4.8286E - 06$
7	$2.2318E - 06$
8	$5.5998E - 07$
9	$2.6855E - 07$

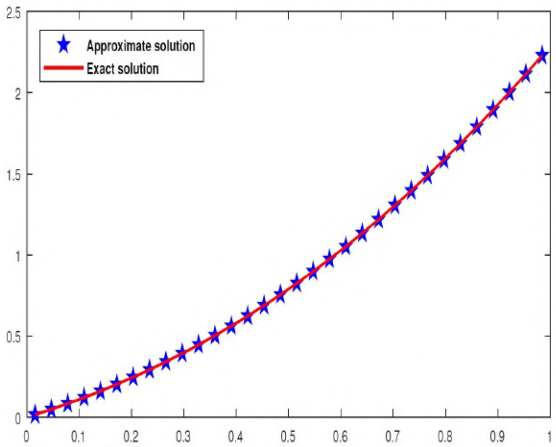

FIGURE 5.9: Comparison of exact and approximate solution (Problem 6).

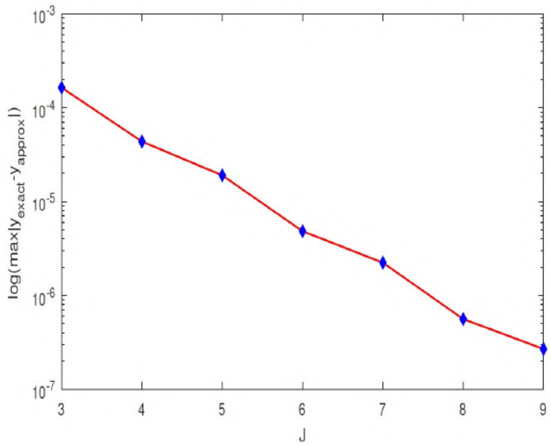

FIGURE 5.10: Maximum absolute errors vs J (Problem 6).

$$y^{iv}(t) = y''\left(\tfrac{t}{2}\right)\left(y^{iv}\left(\tfrac{t}{4}\right) - y(t)\right) + \lambda(t),\ t \in [0,1],$$
$$y(0) = 0,\ y'(0) = 1,\ y''(0) = 2,\ y'''(0) = 2, \tag{5.4.7}$$

where $\lambda(t)$ is supplied in such a way that the system has the exact solution $y_e = e^t sin(t)$. Carrying out the numerical technique mentioned in section 3, we have obtained the approximate solution of equation (5.4.7) for different values of J. Maximum absolute errors are computed at different resolutions (table 5.10). Moreover, the exact solution and approximate solution are plotted in figure 5.9 for $J = 4$. Based on the obtained results, it is realized that the method is efficient for tackling such problems.

5.5 Summary

This chapter[1] modified the traditional Haar wavelet series method and utilized the method to obtain the solutions of second and higher-order Pantograph equations. A short account of applications of pantograph equations in electrodynamics was also presented. The method was tested in numerical simulations and compared with other methods.

[1]Accepted for publication in **Jordon Journal of Mathematics and Statistics.**(ESCI, Scopus Indexed).

Chapter 6

A collocation method for solving proportional delay Riccati differential equations of fractional order

6.1 Introduction

Over the last few years, the subject of fractional calculus has provided more generalized methods to describe the behaviours of several physical systems. Fractional order models have attracted the attention of researchers since differential equations involving non integer derivative demonstrate the dynamics of many systems more realistically, for instance bio-engineering[65], viscoelasticity[66], diffusion[72], chaos theory, Fractional capacitor theory[86], electromagnetism[114], electrochemistry[81], and many others[30, 104]. Also, in recent years, several authors have contributed a large literature on the analysis and applications of fractional differential equations, namely [32, 55, 85]. Furthermore, several authors suggested different definitions of fractional derivatives. The Riemann-Liouville and Liouville-Caputo define a fractional derivative, which has significant importance in the field of fractional calculus but has certain limitations due to singular local power kernel[55, 85]. Caputo and Fabrizio propose a new definition of fractional derivatives using exponential decay kernel[22]. Recently, Atangana and Baleanu suggested another fractional derivative which is based on the concept of ML function [7]. Furthermore, some authors suggested more interesting definitions where time-dependent variable-order fractional derivative and integral $\alpha(t)$ is involved [95].

Delay differential equations (DDEs) form a special class of differential equations in which the rate of solution depends on the present as well as some previous value of the dependent variable and/or their derivative. DDEs are widely used to model processes in physical sciences, biosciences, engineering, electrodynamics, and economics. Depending upon the nature of delay/lag τ , DDEs have various formats such as DDEs with constant delay, DDEs with time dependent delay $\tau(t)$, DDEs with state dependent delay $\tau(t, y)$, Neutral DDEs, and proportional DDEs or Pantograph equations. Herein, the subject of our interest is the following fractional order proportional delay Riccati differential equation(PDRDE):

$$\begin{cases} \chi^{\alpha}(t) = \Omega(t) + c_1(t)\chi(t) + c_2(t)\chi(qt)(c_3(t) - \chi(qt)), \\ \\ with \;\; \chi(0) = \chi_0, \quad 0 \leq t \leq 1, \quad 0 < \alpha < 1, \end{cases} \tag{6.1.1}$$

where Ω, c_1, c_2, c_3 are analytical functions, and $q \in (0, 1)$. Note that when $q = 1$, equation (6.1.1) become ordinary Riccati fractional differential equation.

Due to the involvement of fractional derivatives and delay terms, the computational complexity of these equations increases, making it too complicated to solve these equations analytically. Also, in some cases, the analytical solution of these equations does not exist, so an efficient numerical technique is necessary to find the approximate solution.

In recent years, many authors have shown an interest in solving delay differential equations. Some of them are as follows. In [116] Yuzbasi & Sezer have introduced approximation method based on exponential polynomial and collocation point for solving pantograph equations, Bahsi & Cevik [11] solved proportional DDEs numerically using perturbation-iteration method, Davaeifar & Rashidinia[29] has proposed a collocation method using first Boubaker polynomials for solving multipantograph equations. Further, in [94] Sakar et al. employed iterative reproducing kernel method for solving Riccati differential equations, Muthukumar & Ganesh [77]used shifted jacobi polynomial to develop numerical technique for solving fractional delay differential equations, Li & Wang [62] represent solution of linear fractional DDEs of Riemann-Liouville type using the Mittage-Leffler function. Ali et al. [6] used the spectral collocation method to solve fractional order DDEs, Ghomanjani & Shateyi [41] developed approximation scheme using Genocchi polynomial for solving quadratic Riccati DEs, Multipantograph DDEs and optimal control systems with pantograph delays, Jafari et al. [51] provide transferred Legendre pseudospectral method to solve pantograph DDEs, Izadi & Srivastava[50] produced numerical solution of the Lane Emeden pantograph DDEs using Bessels polynomials and collocation points. Panghal & Kumar [83] used a neural network technique to solve multipantograph type DDEs.

The Haar wavelet is a compact support box function which takes only three values $\{0, \pm 1\}$. In the last two decades, it has been used to solve a wide variety of differential equations. The detailed applications of the Haar wavelet can be found in the monograph and references therein in [60, 87]. In [97] Shah et al. proposed a numerical technique using Haar wavelet for solving fractional differential equations. Recently, Oruc et al. [82] presented Haar wavelet and finite difference based scheme to solve the two-dimensional time fractional reaction–sub-diffusion equation. Akmal

& Arshad [88] solved neutral DDEs using Haar wavelet bases, Abdullah & Rafiq[2] combined the backward Euler method and Haar wavelet collocation method to obtain the approximate solution of the Chen-Lee-Liu equation. Motivated by the above literature, we aim to apply the Haar wavelet series method (HWSM) to solve the proportional delay Riccati differential equation of fractional order with Caputo derivative.

Some fundamental definitions related to fractional calculus,

Definition 6.1. "The **Riemann-Liouville integral** operator of order $\alpha > 0$ of a function $g(t),\ t \in (c, d)$ is represented as:

$$_{RL}\mathcal{J}^{\alpha}_{c,t}g(t) = \frac{1}{\Gamma(\alpha)} \int_{c}^{t} (t-u)^{\alpha-1} g(u)du, \tag{6.1.2}$$

where $\Gamma(\cdot)$ is Euler's gamma function."

Definition 6.2. "The **Riemann-Liouville derivative** of order $\alpha > 0$ of a function $g(t),\ t \in (c, d)$ is defined as:

$$_{RL}\mathcal{D}^{\alpha}_{c,t}g(t) = \frac{1}{\Gamma(\zeta-\alpha)} \frac{d^{\zeta}}{dt^{\zeta}} \int_{0}^{t} (t-u)^{\zeta-\alpha-1} g(u)du, \tag{6.1.3}$$

$\zeta - 1 < \alpha < \zeta,\ \zeta \in \mathbb{N}$. In particular, for $0 < \alpha < 1$, we have $n = 1$, and hence,

$$_{RL}\mathcal{D}^{\alpha}_{c,t}g(t) = \frac{1}{\Gamma(1-\alpha)} \frac{d}{dt} \int_{c}^{t} (t-u)^{-\alpha} g(u)du." \tag{6.1.4}$$

Definition 6.3. "The **Caputo fractional derivative** of order $\alpha > 0$ of a function $g(t),\ t \in (c, d)$ is defined as:

$$_{C}\mathcal{D}^{\alpha}_{c,t}g(t) = \frac{1}{\Gamma(\zeta-\alpha)} \int_{c}^{t} (t-u)^{\zeta-\alpha-1} g^{(\zeta)}(u)du, \tag{6.1.5}$$

$\zeta - 1 < \alpha < \zeta,\ \zeta \in \mathbb{N}$. In particular, for $0 < \alpha < 1$, we have $n = 1$, and hence,

$$ {}_C\mathcal{D}^{\alpha}_{c,t} g(t) = \frac{1}{\Gamma(1-\alpha)} \int_c^t (t-u)^{-\alpha} g'(u) du." \tag{6.1.6}$$

To apply the Haar wavelet following integral on Interval [0,1] is required :

$$\mathcal{P}_i^{\alpha}(t) = \frac{1}{\Gamma(\alpha+1)} \int_0^t (t-u)^{\alpha} \mathfrak{h}_i(u) du.$$

The R-L integration of (2.2.3) yields,

$$\mathcal{P}_i^{\alpha}(t) = \frac{1}{\Gamma(\alpha+1)} \begin{cases} \phi_1(t) & t \in [\vartheta_1(i), \vartheta_2(i)), \\ \phi_2(t) & t \in [\vartheta_2(i), \vartheta_3(i)), \\ \phi_3(t) & t \in [\vartheta_3(i), 1), \\ 0 & otherwise, \end{cases} \tag{6.1.7}$$

$\phi_1(t) = (t - \vartheta_1(i))^{\alpha}$,

$\phi_2(t) = [(t - \vartheta_1(i))^{\alpha} - 2(t - \vartheta_2(i))^{\alpha}]$,

$\phi_3(t) = [(t - \vartheta_1(i))^{\alpha} - 2(t - \vartheta_2(i))^{\alpha} + (t - \vartheta_3(i))^{\alpha}]$,

where $\vartheta_1(i) = k/2^j, \vartheta_2(i) = (k + 0.5)/2^j, \vartheta_3(i) = (k + 1)/2^j$.

The index $i = 2^j + k + 1,\ j = 0, 1, \ldots, J,$ where J is maximum level of wavelet and $k = 0, 1, \ldots, 2^j - 1$.

6.2 Description of Method

In this section we present Haar wavelet series method (HWSM) to find the approximate solution of the proportional delay Riccati differential equation of fractional order represented in equation (6.1.1). For that, we approximate $\chi^{\alpha}(t)$ present in equation (6.1.1) by truncated Haar wavelet series as follows:

$$\chi^{\alpha}(t) = \sum_{i=1}^{2^{J+1}} a_i \mathfrak{h}_i(t). \tag{6.2.1}$$

R-L Integration of (6.2.1) from 0 *to* t yields,

$$\chi(t) = \sum_{i=1}^{2^{J+1}} a_i \mathcal{P}_i^{\alpha}(t) + \chi(0). \tag{6.2.2}$$

Now replace t by qt in equation (6.2.2), we get,

$$\chi(qt) = \sum_{i=1}^{2^{J+1}} a_i \mathcal{P}_i^{\alpha}(qt) + \chi(0). \tag{6.2.3}$$

Using equations (6.2.1) to (6.2.3) in equation,(6.1.1) we get,

$$\begin{aligned} \sum_{i=1}^{2^{J+1}} a_i \mathfrak{h}_i(t) &= \Omega(t) + c_1(t)(\sum_{i=1}^{2^{J+1}} a_i \mathcal{P}_i^{\alpha}(t) + \chi(0)) \\ &+c_2(t)(\sum_{i=1}^{2^{J+1}} a_i \mathcal{P}_i^{\alpha}(qt) + \chi(0))(c_3(t) \\ &-(\sum_{i=1}^{2^{J+1}} a_i \mathcal{P}_i^{\alpha}(qt) + \chi(0))). \end{aligned} \tag{6.2.4}$$

Discretize the system (6.2.4) with the chosen collocation points $t_l = \frac{(l-0.5)}{2^{J+1}}$, we get,

$$\begin{aligned} \sum_{i=1}^{2^{J+1}} a_i \mathfrak{h}_i(t_l) &= \Omega(t_l) + c_1(t_l)(\sum_{i=1}^{2^{J+1}} a_i \mathcal{P}_i^{\alpha}(t_l) + \chi(0)) \\ &+c_2(t_l)(\sum_{i=1}^{2^{J+1}} a_i \mathcal{P}_i^{\alpha}(qt_l) + \chi(0))(c_3(t_l) \\ &-(\sum_{i=1}^{2^{J+1}} a_i \mathcal{P}_i^{\alpha}(qt_l) + \chi(0))). \end{aligned} \tag{6.2.5}$$

Solve the above system for Haar wavelet coefficients $a_i^{,}s$. Plugging these coefficients into the equation (6.2.2) produces the approximate solution $\chi(t_l)$.

6.3 Applications and Numerical Results

The combination of fractional calculus with the theory of delay differential equations has enhanced the mathematical description of a number of real-world phenomena during the past few years. On the other hand, several numerical treatment has been developed for solving fractional differential models. However, very few researchers have thoroughly investigated fractional differential equations with delay.

In this section, we shall be concerned with numerical treatment of some fractional order delay differential equations using Haar wavelet series method (HWSM). Before solving numerical examples, we shall state some real world applications of HWSM from existing literature. In Dec-2019 a threatful outbreak called the novel corona virus-2019 disease brought the world to its knees and took daily life to a grinding halt in much of the world. The researchers claim that the virus was initiated in the Chinese city of Wuhan. Planet-wide research to identify the symptoms, to control its spread, and to cure & eradicate the disease is still in full swing. In an attempt kamal shah et al. [98] study the transmission dynamics of the novel coronavirus-2019 and construct a fractional order differential mathematical model by considering three compartments including the susceptible population, infected population, and recovered population. Further, the solution of the model is computed using the Haar wavelet collocation method. Hence the method is proven as efficient tool in infectious disease spread modeling. Several recent studies which have promoted Haar wavelet as favorable mathematical tool are [57, 73, 102].

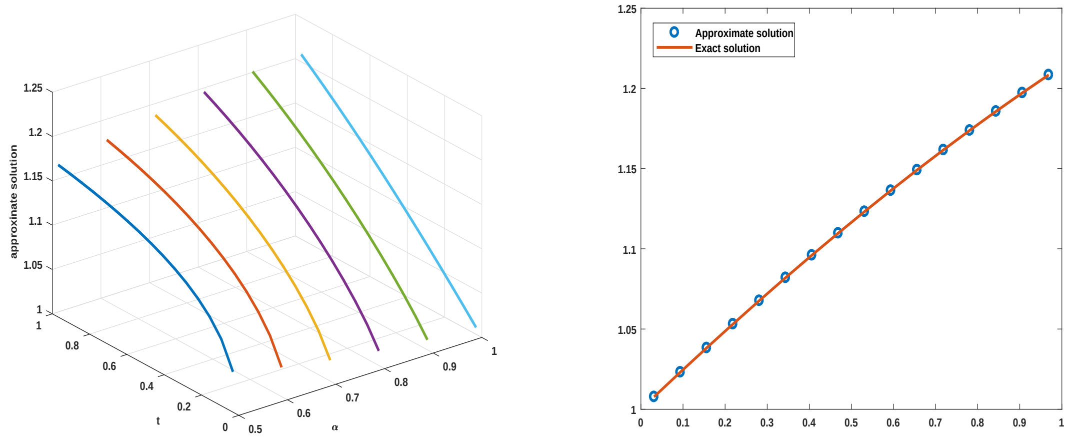

FIGURE 6.1: Problem 1.

Problem 1: Consider the following fractional order PDRDE

$$y^{\alpha}(t) = \frac{1}{4}y(t) + y(\frac{t}{2})(1 - y(\frac{t}{2})), 0 \leq \alpha \leq 1, t \in (0,1), \tag{6.3.1}$$

with initial condition $y(0) = 1$, and possesses the exact solution

$$y(t) = \frac{1}{2} + \frac{1}{2}cos(\frac{\sqrt{2}t}{4}) + \frac{\sqrt{2}}{2}sin(\frac{\sqrt{2}t}{4})$$

when $\alpha = 1$.

The approximate solution of (6.3.1) is computed using HWSM. The solution behaviour at $\alpha = 0.5, 0.6, 0.7, 0.8, 0.9, 1$ is presented graphically in Fig. 6.1. Also, we have presented solutions for $\alpha = 0.5, 0.7, 0.9, 1$ at selected collocation points in Table 6.1. Maximum absolute errors (MAEs) at different wavelet levels J are demonstrated in Table 6.4.

Problem 2: Solve the following fractional order PDRDE

$$y^{\alpha}(t) = \frac{1}{2}exp(\frac{t}{2})y(\frac{t}{2}) + \frac{1}{2}y(t), 0 \leq \alpha \leq 1, t \in (0,1) \tag{6.3.2}$$

TABLE 6.1: Approximate solution at $\alpha = 0.5, 0.7, 0.9, 1$ when J=3 (Problem 1).

t_l	$\alpha = 0.5$	$\alpha = 0.7$	$\alpha = 0.9$	$\alpha = 1$	y_{exact}
0.0313	1.0455	1.0235	1.0113	1.0078	1.0078
0.1563	1.0933	1.0692	1.0473	1.0383	1.0383
0.2813	1.1173	1.1000	1.0784	1.0677	1.0677
0.4063	1.1335	1.1243	1.1065	1.0960	1.0961
0.5313	1.1456	1.1442	1.1322	1.1232	1.1232
0.6563	1.1551	1.1609	1.1558	1.1492	1.1492
0.7813	1.1627	1.1751	1.1775	1.1739	1.1739
0.9063	1.1689	1.1872	1.1973	1.1972	1.1973

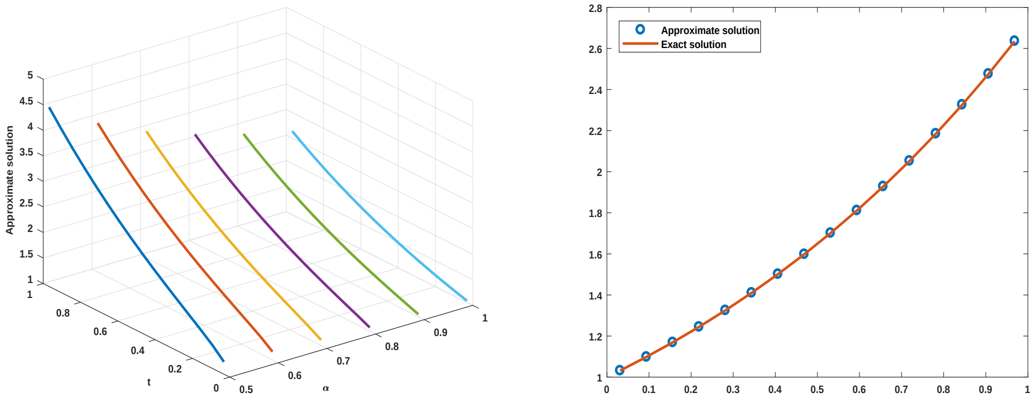

FIGURE 6.2: Problem 2.

with initial condition $y(0) = 1$, and has the exact solution $y(t) = exp(t)$ when $\alpha = 1$.

The approximate solution of (6.3.2) is computed using HWSM. The solutions behavior at $\alpha = 0.5, 0.6, 0.7, 0.8, 0.9, 1$ is presented graphically in Fig. 6.2. Also, we have presented solutions for $\alpha = 0.5, 0.7, 0.9, 1$ at selected collocation points in Table 6.2. Maximum absolute errors (MAEs) at different wavelet levels J are demonstrated in table 6.4.

Problem 3: Solve the following fractional order PDRDE

$$y^{\alpha}(t) = -\frac{1}{8}y(t) + y(\frac{t}{2})(1 - y(\frac{t}{2})), 0 \leq \alpha \leq 1, t \in (0, 1), \tag{6.3.3}$$

Table 6.2: Approximate solution at $\alpha = 0.5, 0.7, 0.9, 1$ when J=3 (Problem 2).

t_l	$\alpha = 0.5$	$\alpha = 0.7$	$\alpha = 0.9$	$\alpha = 1$	y_{exact}
0.0313	1.2426	1.1065	1.0480	1.0323	1.0317
0.1563	1.6442	1.3661	1.2183	1.1697	1.1691
0.2813	1.9987	1.6148	1.3998	1.3255	1.3248
0.4063	2.3653	1.8796	1.6007	1.5021	1.5012
0.5313	2.7606	2.1698	1.8255	1.7021	1.7011
0.6563	3.1951	2.4919	2.0782	1.9288	1.9276
0.7813	3.6775	2.8520	2.3632	2.1857	2.1842
0.9063	4.2165	3.2561	2.6849	2.4768	2.4750

Table 6.3: Approximate solution at $\alpha = 0.5, 0.7, 0.9, 1$ when J=3 (Problem 3).

t_l	$\alpha = 0.5$	$\alpha = 0.7$	$\alpha = 0.9$	$\alpha = 1$	y_{exact}
0.0313	0.2825	0.2655	0.2572	0.2549	0.2549
0.1563	0.3248	0.2985	0.2810	0.2747	0.2746
0.2813	0.3522	0.3243	0.3031	0.2947	0.2947
0.4063	0.3743	0.3472	0.3246	0.3150	0.3150
0.5313	0.3935	0.3684	0.3457	0.3355	0.3355
0.6563	0.4106	0.3883	0.3665	0.3562	0.3562
0.7813	0.4263	0.4073	0.3871	0.3770	0.3770
0.9063	0.4407	0.4255	0.4075	0.3981	0.3981

with initial condition $y(0) = \frac{1}{4}$, and the exact solution

$$y(t) = \frac{1}{2} - \frac{1}{4}cos(\frac{\sqrt{5}t}{8}) + \frac{\sqrt{5}}{4}sin(\frac{\sqrt{5}t}{8})$$

when $\alpha = 1$.

The approximate solution of (6.3.3) is computed using HWSM. The Solution behavior at $\alpha = 0.5, 0.6, 0.7, 0.8, 0.9, 1$ is presented graphically in Fig. 6.3. Also, we have presented solution for $\alpha = 0.5, 0.7, 0.9, 1$ at selected collocation points in table 6.3. Maximum absolute errors (MAEs) at different wavelet levels J are demonstrated in Table 6.4.

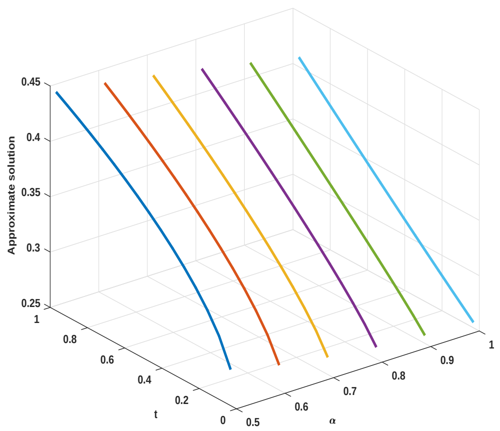

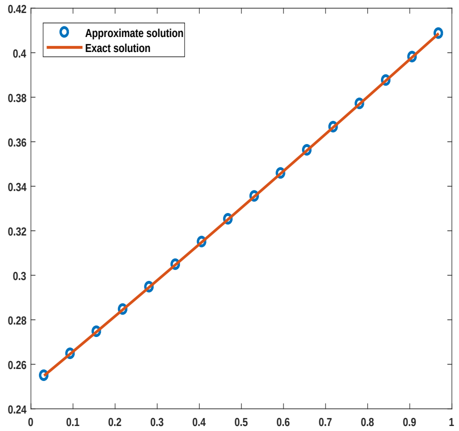

FIGURE 6.3: Problem 3.

TABLE 6.4: Maximum absolute error(MAE) $max|y_{approx} - y_{exact}|$.

J	**Problem** 1	**Problem** 2	**Problem** 3	**Problem** 4
3	$3.0351E-05$	$1.8900E-03$	$9.4852E-06$	$2.8315e-08$
4	$7.6090E-06$	$4.8189E-04$	$2.3778E-06$	$1.1102e-16$
5	$1.9048E-06$	$1.2167E-04$	$5.9526E-07$	$1.1102e-16$
6	$4.7652E-07$	$3.0572E-05$	$1.4891E-07$	$-$
7	$1.1917E-07$	$7.6623E-06$	$3.7240E-08$	$-$
8	$2.9797E-08$	$1.9178E-06$	$9.3117E-09$	$-$
9	$7.4499E-09$	$4.7979E-07$	$2.3281E-09$	$-$
10	$1.8620E-09$	$1.1996E-07$	$5.8205E-10$	$-$

Problem 4: Now for comparison we choose the following fractional Riccati differential equation from literature [94]

$$y^{\alpha}(t) = t^3y^2(t) - 2t^4y(t) + t^5, 0 \leq \alpha \leq 1, t \in (0, 1) \tag{6.3.4}$$

with initial condition $y(0) = 0$, and has the exact solution $y(t) = t$ when $\alpha = 1$. The aforementioned problem has been solved by means of HWSM and FDE solver. It is noted that the HWSM provides better accuracy and converges towards an exact solution, which has been asserted with the help of the graphical plot 6.4. To analyse the solution behaviour, a tabular (6.5) comparison is performed with $\alpha = 0.5, 0.6, 0.7, 0.8, 0.9, 1$. Also, maximum absolute errors and a comparison with IRKHSM are presented in table 6.4 and table 6.7.

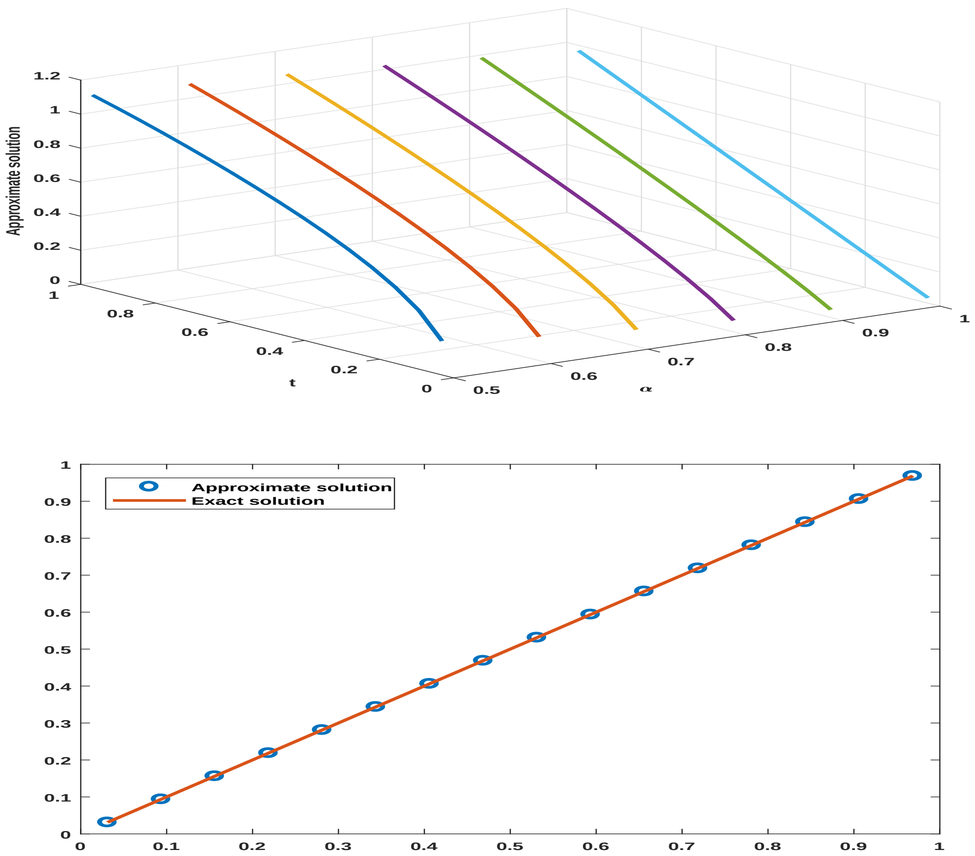

FIGURE 6.4: Problem 4.

TABLE 6.5: Approximate solution at $\alpha = 0.5, 0.7, 0.9, 1$ (Problem 4).

t_l	$\alpha = 0.5$	$\alpha = 0.7$	$\alpha = 0.9$	$\alpha = 1$	y_{exact}
0.0313	0.1995	0.0973	0.0460	0.0313	0.0313
0.1563	0.4461	0.3001	0.1956	0.1563	0.1563
0.2813	0.5990	0.4530	0.3320	0.2813	0.2813
0.4063	0.7215	0.5863	0.4622	0.4063	0.4063
0.5313	0.8277	0.7080	0.5885	0.5313	0.5313
0.6563	0.9236	0.8220	0.7119	0.6562	0.6563
0.7813	1.0115	0.9300	0.8329	0.7812	0.7813
0.9063	1.0920	1.0332	0.9521	0.9062	0.9063

TABLE 6.6: Comparison of MAE(Problem 4).

HWSM	**HWSM**	**IRKHSM**
$J = 3$	$J = 4$	$N = 4$[94]
$2.8315E - 08$	$1.1102E - 16$	$2E - 07$

TABLE 6.7: Comparison of HWSM vs FDE Solver .

t_l	$\alpha =$ 0.5 HWSM	$\alpha =$ 0.5 fde Solver	$\alpha =$ 0.7 HWSM	$\alpha =$ 0.7 fde Solver	$\alpha =$ 0.9 HWSM	$\alpha =$ 0.9 fde Solver	$\alpha = 1$ HWSM	$\alpha = 1$ fde Solver	$\alpha = 1$ MAE HWSM	$\alpha = 1$ MAE fde Solver[37]
0.03125	0.199471	0.031250	0.097275	0.031250	0.045951	0.031250	0.031250	0.031250	0	0
0.09375	0.345504	0.313356	0.209889	0.189275	0.123510	0.116997	0.093750	0.093749	0	$2.011643E-07$
0.15625	0.446102	0.430277	0.300120	0.287972	0.195600	0.191261	0.156250	0.156248	0	$1.132459E-06$
0.21875	0.528002	0.520157	0.379851	0.372261	0.264780	0.261731	0.218750	0.218748	0	$1.132459E-06$
0.28125	0.599044	0.596201	0.452972	0.448408	0.331986	0.329847	0.281250	0.281248	0	$1.132459E-06$
0.34375	0.662854	0.663572	0.521399	0.519067	0.397705	0.396267	0.343750	0.343748	0	$1.132459E-06$
0.40625	0.721469	0.724935	0.586262	0.585689	0.462240	0.461370	0.406250	0.406248	0	$1.132460E-06$
0.46875	0.776156	0.781869	0.648303	0.649179	0.525794	0.525402	0.468750	0.468748	0	$1.132464E-06$
0.53125	0.827741	0.835373	0.708035	0.710147	0.588514	0.588534	0.531250	0.531248	0	$1.132477E-06$
0.59375	0.876778	0.886100	0.765831	0.769025	0.650511	0.650894	0.593749	0.593748	$1.998401E-15$	$1.132511E-06$
0.65625	0.923624	0.934470	0.821966	0.826125	0.711872	0.712579	0.656249	0.656248	$4.596323E-14$	$1.132594E-06$
0.71875	0.968496	0.980737	0.876642	0.881675	0.772664	0.773664	0.718749	0.718748	$1.536992E-12$	$1.132784E-06$
0.78125	1.011508	1.025027	0.930006	0.935838	0.832943	0.834211	0.781249	0.781248	$2.236499E-11$	$1.133185E-06$
0.84375	1.052690	1.067373	0.982160	0.988726	0.892753	0.894268	0.843749	0.843748	$2.876829E-10$	$1.133985E-06$
0.90625	1.092022	1.107743	1.033172	1.040415	0.952131	0.953874	0.906249	0.906248	$3.129013E-09$	$1.135503E-06$
0.96875	1.129461	1.146071	1.083086	1.090949	1.011104	1.013060	0.968749	0.968748	$2.831572E-08$	$1.138263E-06$

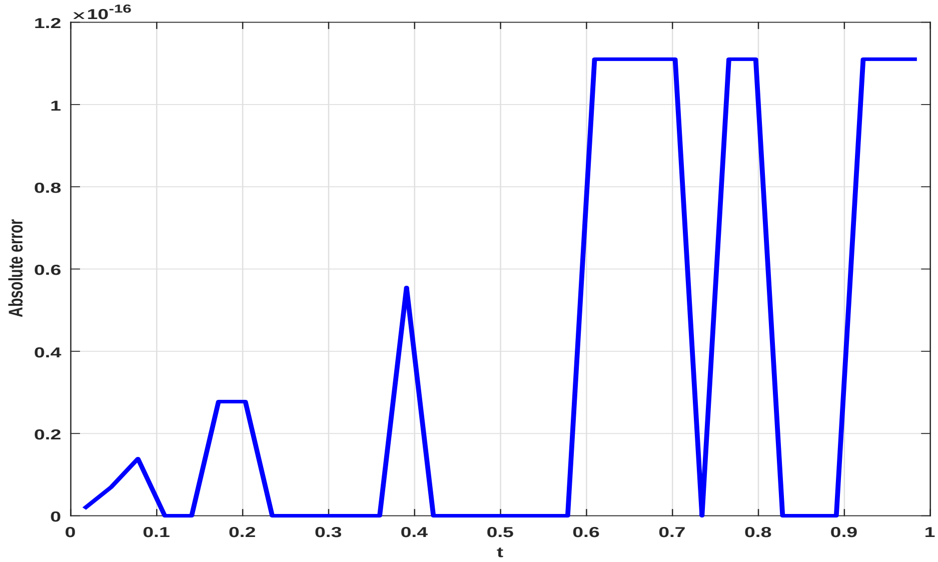

FIGURE 6.5: Absolute error at wavelet level $J = 4$ (Problem 4).

6.4 Summary

In this chapter[1], a collocation method based on the delayed Haar basis and their fractional integrals is discussed for the approximation of fractional proportional delay Riccati differential equations. A short account of fractional calculus and its applications was also presented. The applicability and utility of the method are tested by solving a few benchmark problems. The results we obtained are very promising.

[1]Accepted for publication in ICNAAO-2021, **Springer Proceeding in Mathematics and Statistics.** (Scopus Indexed)

Concluding Remarks

The work presented in this thesis has focused on establishing accurate, stable, and efficient numerical techniques for solving a particular class of delay differential equations known as proportional delay differential equations.

A numerical technique, presented in chapter 2, was designed to solve proportional delay Riccati differential equations. In this technique, Haar wavelets are preferred primarily due to their low computational cost and mathematical simplicity. Several examples have been solved to demonstrate the efficiency and accuracy of the technique. Numerical comparisons have been made between the implementations of the proposed method, the Bezier Curves Method, and the exact solution. The numerical experiment indicates that the Haar wavelet method has given an accuracy which varies between $O(10^{-05})-O(10^{-09})$ for the different resolutions of the wavelet. The method is extended and developed to solve Dirichlet BVPs of proportional delay nature and simultaneous proportional delay differential equations, as presented in chapters 3 and 4, respectively. The method has proven to be an efficient mathematical tool for solving BVPs because it can automatically incorporate boundary conditions. Several benchmark problems have been solved, maximum absolute errors and convergence rates are calculated. The accuracy for BVPs varies between $O(10^{-04}) - O(10^{-10})$ when J varies from 1 to 10 (Table 3.1). Also, the convergence rate for proportional delay IVPs and BVPs matches closely with the theoretical value, i.e., 2 (Table 3.2). Similarly, the method is extended to solve simultaneous proportional delay differential equations. Some linear and non-linear problems with two and three unknown functions are solved, and a comparison has been made between the solution obtained via the Haar wavelet series method and the exact solution. Figure 4.3 and 4.5 show that an increase in resolution contributes to the decrease in maximum absolute errors, and the method performs well even for the system of equations.

In chapter 5, a modified Haar wavelet approach is established to investigate the solution of higher-order multipanotgraph DEs arising in electrodynamics. In this modified approach, instead of the highest derivative (n^{th}) functions present in differential equations, the $(n+1)^{th}$ derivative of the unknown function is expanded into the Haar wavelets series with unknown coefficients, and the other derivatives are obtained through integration. This approach transforms the problem into a set of algebraic equations and thus simplifies the solution process. Numerical results show that the method is effective, robust, and comparable with existing methods (see, Table 5.1, 5.7), such as the Two-stage RKM, One-leg θ, VIM, and RKHS method.

Finally, in chapter 6, fractional integrals of Haar wavelets in the R-L sense are defined, and then an efficient Haar wavelets-based algorithm is established to obtain the numerical solution of fractional order proportional delay Riccati DEs. The outcomes of the numerical simulations in Table 6.6 and 6.7 indicate the superiority of HWSM over IRKHSM and FDESOLVER. The accuracy varies between $O(10^{-05}) - O(10^{-10})$ (Table 6.4) when J varies from 3 to 10, and in one case, it varies between $O(10^{-08}) - O(10^{-16})$ (Table 6.7).

A possible future research direction could be:

A Numerical method for solving delay fractional order partial DEs.

To design and investigate fractional delay differential models using wavelets.

Bibliography

[1] Tamer A Abassy, Magdy A El-Tawil, and Hanafi El Zoheiry. "Toward a modified variational iteration method". In: *Journal of Computational and Applied Mathematics* 207.1 (2007), pp. 137–147.

[2] Abdullah Abdullah and Mohd Rafiq. "A new numerical scheme based on Haar wavelets for the numerical solution of the Chen–Lee–Liu equation". In: *Optik* 226 (2021), p. 165847.

[3] RP Agarwal and YM Chow. "Finite-difference methods for boundary-value problems of differential equations with deviating arguments". In: *Computers & Mathematics with Applications* 12.11 (1986), pp. 1143–1153.

[4] Khalil Ahmad and Firdous Ahmad Shah. "Introduction to Wavelets with Applications". In: *Real World Education Publishers, New Delhi* (2013).

[5] B. Akhtari. "Numerical treatment of stochastic delay differential equations: A global error bound". In: *Journal of Computational and Applied Mathematics* 361 (2019), pp. 249–270.

[6] Khalid K Ali, Mohammad A Abd El Salam, and Emad M Mohamed. "Chebyshev operational matrix for solving fractional order delay-differential equations using spectral collocation method". In: *Arab Journal of Basic and Applied Sciences* 26.1 (2019), pp. 342–353.

[7] Abdon Atangana and Dumitru Baleanu. *New Fractional Derivatives with Nonlocal and Non-Singular Kernel: Theory and Application to Heat Transfer Model*. 2016. arXiv: `1602.03408 [math.GM]`.

[8] Imran Aziz and Rohul Amin. "Numerical solution of a class of delay differential and delay partial differential equations via Haar wavelet". In: *Applied mathematical modelling* 40.23-24 (2016), pp. 10286–10299.

[9] Imran Aziz, Božidar Šarler, et al. "The numerical solution of second-order boundary-value problems by collocation method with the Haar wavelets". In: *Mathematical and Computer Modelling* 52.9-10 (2010), pp. 1577–1590.

[10] M Mustafa Bahşi and Mehmet Çevik. "Numerical solution of pantograph-type delay differential equations using perturbation-iteration algorithms". In: *Journal of Applied Mathematics* 2015 (2015).

[11] M Mustafa Bahşi and Mehmet Çevik. "Numerical solution of pantograph-type delay differential equations using perturbation-iteration algorithms". In: *Journal of Applied Mathematics* 2015 (2015).

[12] Dumitru Baleanu et al. "A novel modeling of boundary value problems on the glucose graph". In: *Communications in Nonlinear Science and Numerical Simulation* 100 (2021), p. 105844.

[13] Alfredo Bellen and Marino Zennaro. *Numerical methods for delay differential equations*. Oxford university press, 2013.

[14] J. Bernoulli. "Modus generalis construendi omnes æquationes differentiales primi gradus, Acta Eruditorum". In: *Publicata Lipsiæ* (1694), pp. 435–437.

[15] Ali H Bhrawy et al. "A Legendre-Gauss collocation method for neutral functional-differential equations with proportional delays". In: *Advances in Difference Equations* 2013.1 (2013), p. 63.

[16] Jafar Biazar and Behzad Ghanbari. "The homotopy perturbation method for solving neutral functional-differential equations with proportional delays". In: *Journal of King Saud University-Science* 24.1 (2012), pp. 33–37.

[17] Alexandru Mihai Bica, Mircea Curila, and Sorin Curila. "About a numerical method of successive interpolations for two-point boundary value problems with deviating argument". In: *Applied mathematics and computation* 217.19 (2011), pp. 7772–7789.

[18] Steven L. Brunton and J. Nathan Kutz. "Fourier and Wavelet Transforms". In: *Data-Driven Science and Engineering: Machine Learning, Dynamical Systems, and Control*. Cambridge University Press, 2019, 47–83. DOI: 10.1017/9781108380690.003.

[19] Martin Buhmann and Arieh Iserles. "Stability of the discretized pantograph differential equation". In: *Mathematics of Computation* 60.202 (1993), pp. 575–589.

[20] Musa Cakir, Derya Arslan, et al. "The Adomian decomposition method and the differential transform method for numerical solution of multi-pantograph delay differential equations". In: *Applied Mathematics* 6.08 (2015), p. 1332.

[21] Alberto Calderón. "Intermediate spaces and interpolation, the complex method". In: *Studia Mathematica* 24.2 (1964), pp. 113–190.

[22] Michele Caputo and Mauro Fabrizio. "A new definition of fractional derivative without singular kernel". In: *Progr. Fract. Differ. Appl* 1.2 (2015), pp. 1–13.

[23] Mourad Chamekh, Tarig M. Elzaki, and Nabiha Brik. "Semi-analytical solution for some proportional delay differential equations". In: *SN Applied Sciences* 1.2 (2019), p. 148.

[24] CF Chen and CH Hsiao. "Haar wavelet method for solving lumped and distributed-parameter systems". In: *IEE Proceedings-Control Theory and Applications* 144.1 (1997), pp. 87–94.

[25] Xumei Chen and Linjun Wang. "The variational iteration method for solving a neutral functional-differential equation with proportional delays". In: *Computers & Mathematics with Applications* 59.8 (2010), pp. 2696–2702.

[26] C. K. Chui. *An introduction to wavelets*. Boston: Academic Press, 1992.

[27] Kenneth L Cooke. "Differential—difference equations". In: *International Symposium on Nonlinear Differential Equations and Nonlinear Mechanics*. Elsevier. 2012, p. 155.

[28] Ingrid Daubechies. *Ten lectures on wavelets*. SIAM, 1992.

[29] Sara Davaeifar and Jalil Rashidinia. "Solution of a system of delay differential equations of multi pantograph type". In: *Journal of Taibah University for Science* 11.6 (2017), pp. 1141–1157.

[30] Lokenath Debnath. "Recent applications of fractional calculus to science and engineering". In: *International Journal of Mathematics and Mathematical Sciences* 2003.54 (2003), pp. 3413–3442.

[31] Lokenath Debnath and Firdous Ahmad Shah. *Wavelet transforms and their applications*. Springer, 2002.

[32] Kai Diethelm. *The analysis of fractional differential equations: An application-oriented exposition using differential operators of Caputo type*. Springer Science & Business Media, 2010.

[33] EH Doha et al. "A new Jacobi rational–Gauss collocation method for numerical solution of generalized pantograph equations". In: *Applied Numerical Mathematics* 77 (2014), pp. 43–54.

[34] R. D. Driver. *Ordinary and delay differential equations*. New York: Springer-Verlag, 1977.

[35] Rodney David Driver. *Ordinary and delay differential equations*. Vol. 20. Springer Science & Business Media, 2012.

[36] Leslie Fox et al. "On a functional differential equation". In: *IMA Journal of Applied Mathematics* 8.3 (1971), pp. 271–307.

[37] Roberto Garrappa. "Numerical solution of fractional differential equations: A survey and a software tutorial". In: *Mathematics* 6.2 (2018), p. 16.

[38] Fazhan Geng, Yingzhen Lin, and Minggen Cui. "A piecewise variational iteration method for Riccati differential equations". In: *Computers & Mathematics with Applications* 58 (2009), pp. 2518–2522.

[39] Fateme Ghomanjani and Mohammad Hadi Farahi. "The Bezier control points method for solving delay differential equation". In: *Intelligent Control and Automation* 3.2 (2012), pp. 188–196.

[40] Fateme Ghomanjani and Esmaile Khorram. "Approximate solution for quadratic Riccati differential equation". In: *Journal of Taibah university for science* 11.2 (2017), pp. 246–250.

[41] Fateme Ghomanjani and Stanford Shateyi. "Solving a Quadratic Riccati Differential Equation, Multi-Pantograph Delay Differential Equations, and Optimal Control Systems with Pantograph Delays". In: *Axioms* 9.3 (2020), p. 82.

[42] Mikhail A Grekov. "Mathematical models of boundary value problems in nanomechanics". In: *AIP Conference Proceedings*. Vol. 1863. 1. AIP Publishing LLC. 2017, p. 170006.

[43] Alexander Grossmann and Jean Morlet. "Decomposition of Hardy functions into square integrable wavelets of constant shape". In: *SIAM journal on mathematical analysis* 15.4 (1984), pp. 723–736.

[44] Andrei Halanay and Carmen Anca Safta. "A critical case for stability of equilibria of delay differential equations and the study of a model for an electrohydraulic servomechanism". In: *Systems & Control Letters* 142 (2020), p. 104722.

[45] Jack K Hale. *Theory of functional differential equations*. Vol. 3. Springer Science & Business Media, 2012.

[46] G Hariharan. "Solving finite length beam equation by the Haar wavelet method". In: *Int. J. Comput. Appl* 9.1 (2010), pp. 0975–8887.

[47] V Hlaváček, M Marek, and M Kubíček. "Modelling of chemical reactors—X Multiple solutions of enthalpy and mass balances for a catalytic reaction within a porous catalyst particle". In: *Chemical Engineering Science* 23.9 (1968), pp. 1083–1097.

[48] Tamas Insperger, John Milton, and Gabor Stepan. “Semidiscretization for time-delayed neural balance control”. In: *Siam Journal on Applied Dynamical Systems* 14.3 (2015), pp. 1258–1277.

[49] Arieh Iserles and Yunkang Liu. “On neutral functional–differential equations with proportional delays”. In: *Journal of Mathematical Analysis and Applications* 207.1 (1997), pp. 73–95.

[50] Mohammad Izadi and HM Srivastava. “An efficient approximation technique applied to a non-linear Lane–Emden pantograph delay differential model”. In: *Applied Mathematics and Computation* 401 (2021), p. 126123.

[51] H Jafari, M Mahmoudi, and MH Noori Skandari. “A new numerical method to solve pantograph delay differential equations with convergence analysis”. In: *Advances in Difference Equations* 2021.1 (2021), pp. 1–12.

[52] Gerald Kaiser and Lonnie H Hudgins. *A friendly guide to wavelets*. Vol. 300. Springer, 1994.

[53] F Karakoç and H Bereketoğlu. “Solutions of delay differential equations by using differential transform method”. In: *International Journal of Computer Mathematics* 86.5 (2009), pp. 914–923.

[54] Eleni Karatza and Vangelis Karalis. “Delay differential equations for the description of Irbesartan pharmacokinetics: A population approach to model absorption complexities leading to dual peaks”. In: *European Journal of Pharmaceutical Sciences* 153 (2020), p. 105498.

[55] Anatoliĭ Kilbas. *Theory and applications of fractional differential equations*.

[56] Yang Kuang. *Delay differential equations*. University of California Press, 2012.

[57] Sunil Kumar et al. “A study of fractional Lotka-Volterra population model using Haar wavelet and Adams-Bashforth-Moulton methods”. In: *Mathematical Methods in the Applied Sciences* 43.8 (2020), pp. 5564–5578.

[58] Stefan Langer and RC Swanson. "On boundary-value problems for RANS equations and two-equation turbulence models". In: *Journal of Scientific Computing* 85.1 (2020), pp. 1–33.

[59] Irena Lasiecka and Roberto Triggiani. *Differential and algebraic Riccati equations with application to boundary/point control problems: continuous theory and approximation theory*. Vol. 164. Springer, 1991.

[60] Ülo Lepik and Helle Hein. *Haar Wavelets: With Applications*. Springer Science & Business Media, 2014.

[61] D Li and MZ Liu. "Runge–Kutta methods for the multi-pantograph delay equation". In: *Applied mathematics and computation* 163.1 (2005), pp. 383–395.

[62] Mengmeng Li and JinRong Wang. "Representation of solution of a Riemann–Liouville fractional differential equation with pure delay". In: *Applied Mathematics Letters* 85 (2018), pp. 118–124.

[63] Dianchen Lu et al. "Approximate Solution of Multi-Pantograph Equations With Variable Coefficients via Collocation Method Based on Hermite Polynomials". In: *Communications in Mathematics and Applications* 9.4 (2018), pp. 601–614.

[64] Xueqin Lv and Yue Gao. "The RKHSM for solving neutral functional–differential equations with proportional delays". In: *Mathematical Methods in the Applied Sciences* 36.6 (2013), pp. 642–649.

[65] Richard L Magin. "Fractional calculus models of complex dynamics in biological tissues". In: *Computers & Mathematics with Applications* 59.5 (2010), pp. 1586–1593.

[66] Francesco Mainardi. *Fractional calculus and waves in linear viscoelasticity: an introduction to mathematical models*. World Scientific, 2010.

[67] J Majak et al. "Convergence theorem for the Haar wavelet based discretization method". In: *Composite Structures* 126 (2015), pp. 227–232.

[68] J Majak et al. "On the accuracy of the Haar wavelet discretization method". In: *Composites Part B: Engineering* 80 (2015), pp. 321–327.

[69] GV Malinin et al. "Mathematical model, the solution of boundary value problems for alloys with shape memory effect by analytical, numerical-analytical and numerical methods". In: *IOP Conference Series: Materials Science and Engineering*. Vol. 441. 1. IOP Publishing. 2018, p. 012031.

[70] Stephane G Mallat. "A theory for multiresolution signal decomposition: the wavelet representation". In: *IEEE transactions on pattern analysis and machine intelligence* 11.7 (1989), pp. 674–693.

[71] HR Marzban and M Razzaghi. "Rationalized Haar approach for nonlinear constrained optimal control problems". In: *Applied Mathematical Modelling* 34.1 (2010), pp. 174–183.

[72] Mark M Meerschaert. "Fractional calculus, anomalous diffusion, and probability". In: *Fractional dynamics: recent advances* (2012), pp. 265–284.

[73] Liu Meng et al. "Haar wavelet transform and variational iteration method for fractional option pricing models". In: *Mathematical Methods in the Applied Sciences* (2022).

[74] Martin J Mohlenkamp and María Cristina Pereyra. *Wavelets, their friends, and what they can do for you*. Vol. 8. European Mathematical Society, 2008.

[75] Supriya Mukherjee and Banamali Roy. "Solution of Riccati equation with variable co-efficient by differential transform method". In: *International journal of nonlinear science* 14.2 (2012), pp. 251–256.

[76] Thomas Müller et al. "Estimation of delay times in biological systems". In: *Annals of biomedical engineering* 31.11 (2003), pp. 1423–1439.

[77] P Muthukumar and B Ganesh Priya. "Numerical solution of fractional delay differential equation by shifted Jacobi polynomials". In: *International Journal of Computer Mathematics* 94.3 (2017), pp. 471–492.

[78] Sim Borisovich Norkin et al. *Introduction to the theory and application of differential equations with deviating arguments.* Academic Press, 1973.

[79] John Richard Ockendon and Alan B Tayler. “The dynamics of a current collection system for an electric locomotive”. In: *Proceedings of the Royal Society of London. A. Mathematical and Physical Sciences* 322.1551 (1971), pp. 447–468.

[80] Shin'ichi Oishi. “Numerical inclusion of exact periodic solutions for time delay Duffing equation”. In: *Journal of Computational and Applied Mathematics* 372 (2020), p. 112620.

[81] Keith B Oldham. “Fractional differential equations in electrochemistry”. In: *Advances in Engineering software* 41.1 (2010), pp. 9–12.

[82] Ömer Oruç, Alaattin Esen, and Fatih Bulut. “A Haar wavelet approximation for two-dimensional time fractional reaction–subdiffusion equation”. In: *Engineering with Computers* 35.1 (2019), pp. 75–86.

[83] Shagun Panghal and Manoj Kumar. “Neural network method: delay and system of delay differential equations”. In: *Engineering with Computers* (2021), pp. 1–10.

[84] A Patra and S Saha Ray. “Numerical simulation based on Haar wavelet operational method to solve neutron point kinetics equation involving sinusoidal and pulse reactivity”. In: *Annals of Nuclear Energy* 73 (2014), pp. 408–412.

[85] Igor Podlubny. *Fractional differential equations: an introduction to fractional derivatives, fractional differential equations, to methods of their solution and some of their applications.* Elsevier, 1998.

[86] Ahmed G Radwan and Khaled N Salama. “Fractional-order RC and RL circuits”. In: *Circuits, Systems, and Signal Processing* 31.6 (2012), pp. 1901–1915.

[87] Santanu Saha Ray and Arun Kumar Gupta. *Wavelet methods for solving partial differential equations and fractional differential equations*. CRC Press, 2018.

[88] Akmal Raza and Arshad Khan. "Haar wavelet series solution for solving neutral delay differential equations". In: *Journal of King Saud University-Science* 31.4 (2019), pp. 1070–1076.

[89] Akmal Raza et al. "Solution of singularly perturbed differential difference equations and convection delayed dominated diffusion equations using Haar wavelet". In: *Mathematical Sciences* 15.2 (2021), pp. 123–136.

[90] William Thomas Reid and William Thomas Reid. *Riccati differential equations*. Vol. 86. Academic Press, 1972.

[91] Jacobo Riccati. "Animadversiones in aequationes differentiales secundi gradus". In: *Actorum Eruditorum Supplementa* 8.1724 (1724), pp. 66–73.

[92] Fathalla A Rihan. *Delay differential equations and applications to biology*. Springer, 2021.

[93] Abbas Saadatmandi and Mehdi Dehghan. "Variational iteration method for solving a generalized pantograph equation". In: *Computers & Mathematics with Applications* 58.11-12 (2009), pp. 2190–2196.

[94] Mehmet Giyas Sakar, Ali Akgül, and Dumitru Baleanu. "On solutions of fractional Riccati differential equations". In: *Advances in Difference Equations* 2017.1 (2017), pp. 1–10.

[95] Stefan G Samko and Bertram Ross. "Integration and differentiation to a variable fractional order". In: *Integral transforms and special functions* 1.4 (1993), pp. 277–300.

[96] S Sedaghat, Y Ordokhani, and Mehdi Dehghan. "Numerical solution of the delay differential equations of pantograph type via Chebyshev polynomials". In: *Communications in Nonlinear Science and Numerical Simulation* 17.12 (2012), pp. 4815–4830.

[97] Firdous A Shah, R Abass, and Lokenath Debnath. “Numerical solution of fractional differential equations using Haar wavelet operational matrix method”. In: *International Journal of Applied and Computational Mathematics* 3.3 (2017), pp. 2423–2445.

[98] Kamal Shah et al. “Haar wavelet collocation approach for the solution of fractional order COVID-19 model using Caputo derivative”. In: *Alexandria Engineering Journal* 59.5 (2020), pp. 3221–3231.

[99] Fatemeh Shakeri and Mehdi Dehghan. “Application of the decomposition method of Adomian for solving the pantograph equation of order m”. In: *Zeitschrift für Naturforschung A* 65.5 (2010), pp. 453–460.

[100] Fatemeh Shakeri and Mehdi Dehghan. “Solution of delay differential equations via a homotopy perturbation method”. In: *Mathematical and computer Modelling* 48.3-4 (2008), pp. 486–498.

[101] Hal L Smith. *An introduction to delay differential equations with applications to the life sciences*. Vol. 57. Springer New York, 2011.

[102] Hari M Srivastava, Firdous A Shah, and Mohd Irfan. “Generalized wavelet quasilinearization method for solving population growth model of fractional order”. In: *Mathematical Methods in the Applied Sciences* 43.15 (2020), pp. 8753–8762.

[103] E Tohidi, AH Bhrawy, and Kh Erfani. “A collocation method based on Bernoulli operational matrix for numerical solution of generalized pantograph equation”. In: *Applied Mathematical Modelling* 37.6 (2013), pp. 4283–4294.

[104] Duarte Valério, José Tenreiro Machado, and Virginia Kiryakova. “Some pioneers of the applications of fractional calculus”. In: *Fractional Calculus and Applied Analysis* 17.2 (2014), pp. 552–578.

[105] David F Walnut. *An introduction to wavelet analysis*. Springer Science & Business Media, 2002.

[106] Wan-Sheng Wang and Shou-Fu Li. "On the one-leg θ-methods for solving nonlinear neutral functional differential equations". In: *Applied Mathematics and Computation* 193.1 (2007), pp. 285–301.

[107] Wansheng Wang, Tingting Qin, and Shoufu Li. "Stability of one-leg θ-methods for nonlinear neutral differential equations with proportional delay". In: *Applied Mathematics and Computation* 213.1 (2009), pp. 177–183.

[108] Wansheng Wang, Yuan Zhang, and Shoufu Li. "Stability of continuous Runge–Kutta-type methods for nonlinear neutral delay-differential equations". In: *Applied Mathematical Modelling* 33.8 (2009), pp. 3319–3329.

[109] Lorna RM Wilson, Nicholas C Cryer, and Eamon Haughey. "Simulation of the effect of rainfall on farm-level cocoa yield using a delayed differential equation model". In: *Scientia horticulturae* 253 (2019), pp. 371–375.

[110] Changjin Xu, Peiluan Li, and Shuai Yuan. "New findings on exponential convergence of a Nicholson's blowflies model with proportional delay". In: *Advances in Difference Equations* 2019.1 (2019), pp. 1–7.

[111] Song Xueli et al. "Global asymptotic stability of CNNs with impulses and multi-proportional delays". In: *Mathematical Methods in the Applied Sciences* 39.4 (2016), pp. 722–733.

[112] Salih Yalçinbaş, Müge Aynigül, and Mehmet Sezer. "A collocation method using Hermite polynomials for approximate solution of pantograph equations". In: *Journal of the Franklin Institute* 348.6 (2011), pp. 1128–1139.

[113] Changqing Yang. "Modified Chebyshev collocation method for pantograph-type differential equations". In: *Applied Numerical Mathematics* 134 (2018), pp. 132–144.

[114] Beyhan Yilmaz. "A new type electromagnetic curves in optical fiber and rotation of the polarization plane using fractional calculus". In: *Optik* 247 (2021), p. 168026.

[115] Şuayip Yüzbaşi, Niyazi Şahin, and Mehmet Sezer. "A Bessel collocation method for numerical solution of generalized pantograph equations". In: *Numerical Methods for Partial Differential Equations* 28.4 (2012), pp. 1105–1123.

[116] Şuayip Yüzbaşı and Mehmet Sezer. "An exponential approximation for solutions of generalized pantograph-delay differential equations". In: *Applied Mathematical Modelling* 37.22 (2013), pp. 9160–9173.